

# Gromov-Wassertein-like Distances in the Gaussian Mixture Models Space

Antoine Salmona<sup>1</sup>, Julie Delon<sup>2</sup>, Agnès Desolneux<sup>1</sup>.

<sup>1</sup> ENS Paris-Saclay, CNRS, Centre Borelli UMR 9010

<sup>2</sup> Université de Paris, CNRS, MAP5 UMR 8145 and Institut Universitaire de France

October 18, 2023

## Abstract

In this paper, we introduce two Gromov-Wasserstein-type distances on the set of Gaussian mixture models. The first one takes the form of a Gromov-Wasserstein distance between two discrete distributions on the space of Gaussian measures. This distance can be used as an alternative to Gromov-Wasserstein for applications which only require to evaluate how far the distributions are from each other but does not allow to derive directly an optimal transportation plan between clouds of points. To design a way to define such a transportation plan, we introduce another distance between measures living in incomparable spaces that turns out to be closely related to Gromov-Wasserstein. When restricting the set of admissible transportation couplings to be themselves Gaussian mixture models in this latter, this defines another distance between Gaussian mixture models that can be used as another alternative to Gromov-Wasserstein and which allows to derive an optimal assignment between points. Finally, we design a transportation plan associated with the first distance by analogy with the second, and we illustrate their practical uses on medium-to-large scale problems such as shape matching and hyperspectral image color transfer.

**Keywords**— optimal transport, Wasserstein distance, Gromov-Wasserstein distance, Gaussian mixture models

## 1 Introduction

The goal of optimal transport (OT) theory is to design meaningful ways to compare probability distributions. It provides very useful mathematical tools for diverse imaging sciences and machine learning tasks including generative modeling (Arjovsky et al., 2017; Genevay et al., 2018; Tolstikhin et al., 2018), domain adaptation (Courty et al., 2016), image processing (Rabin et al., 2012, 2014), and embedding learning (Courty et al., 2018; Xu et al., 2018). For two probability distributions  $\mu$  and  $\nu$ , respectively on two Polish (i.e complete, separable, metrizable) spaces  $\mathcal{X}$  and  $\mathcal{Y}$  and given a lower semi-continuous function  $c : \mathcal{X} \times \mathcal{Y} \rightarrow \mathbb{R}_+$  called *cost*, optimal transport in its most classic form, aims at solving the following optimization problem,

$$\inf_{\pi \in \Pi(\mu, \nu)} \int_{\mathcal{X} \times \mathcal{Y}} c(x, y) d\pi(x, y), \quad (1)$$

where  $\Pi(\mu, \nu)$  is the set of measures on  $\mathcal{X} \times \mathcal{Y}$  with marginals  $\mu$  and  $\nu$ . When  $\mathcal{Y}$  is equal to  $\mathcal{X}$ , the choice of cost  $c_p(x, y) = d_{\mathcal{X}}(x, y)^p$ , with  $p \geq 1$  and  $d_{\mathcal{X}}$  being the metric of the space  $\mathcal{X}$ , induces a distance between probability distributions with finite  $p$ -th moments called the Wasserstein distance  $W_p$ . In the discrete setting, Problem (1) becomes

$$\inf_{\omega \in \Pi(a, b)} \sum_{k, l} C_{k, l} \omega_{k, l},$$

where  $a = (a_1, \dots, a_m)^T$  and  $b = (b_1, \dots, b_n)^T$  are respectively in the  $\mathbb{R}^m$  and  $\mathbb{R}^n$  simplexes  $\Delta_m$  and  $\Delta_n$ <sup>1</sup>,  $\Pi(a, b) = \{\omega \in \Delta_{m \times n} : \omega \mathbb{1}_n = a \text{ and } \omega^T \mathbb{1}_m = b\}$  and  $C$  is a non-negative matrix of size  $m \times n$  also called cost.

<sup>1</sup>The simplex  $\Delta_m$  is the subset of  $\mathbb{R}^m$  of  $x = (x_1, \dots, x_m)^T$  such that for all  $k \leq m$ ,  $x_k \geq 0$ , and  $\sum_{k=1}^m x_k = 1$ .

One weakness of this classical optimal transport approach lies in the fact that it implicitly assumes that the spaces  $\mathcal{X}$  and  $\mathcal{Y}$  are *comparable*, i.e. that there exists a relevant cost function  $c : \mathcal{X} \times \mathcal{Y} \rightarrow \mathbb{R}_+$  to compare them. Yet, this assumption is not always verified. For instance, if  $\mathcal{X} = \mathbb{R}^d$  and  $\mathcal{Y} = \mathbb{R}^{d'}$  with  $d \neq d'$ , the definition of a meaningful cost function  $c : \mathbb{R}^d \times \mathbb{R}^{d'} \rightarrow \mathbb{R}_+$  is not straightforward. Furthermore, some applications such as shape matching require having an OT distance that is invariant to important families of transformations, such as translations or rotations or more generally to *isometries*<sup>2</sup>. Even if the two distributions involved in these applications do live in the same ground space, it is not straightforward to design a cost function such that the resulting OT distance will be invariant to these families of transformations. To overcome those limitations, several non-convex variants of Problem (1) have been proposed (Cohen and Guibas, 1999; Pele and Taskar, 2013; Alvarez-Melis et al., 2019; Cai and Lim, 2022). The most commonly used among them is perhaps the Gromov-Wasserstein (GW) distance (Mémoli, 2011) which has recently received high interest thanks to the flexibility this approach offers. Indeed, it only requires modeling topological aspects of the distributions within each domain to compare them without having to specify first a subset of invariances nor to design a relevant cost function between the spaces the distributions lie on. This approach has been applied to shape matching (Mémoli, 2009) or more generally to correspondence problems (Solomon et al., 2016), word embedding (Alvarez-Melis and Jaakkola, 2018), graph classification (Vayer et al., 2019a), graph prediction (Brogat-Motte et al., 2022), and generative modeling (Bunne et al., 2019).

Optimal transport is known to be computationally challenging. Between discrete distributions, its computation involves solving a linear program that rapidly becomes costly as soon as the number of points is moderately large. Between two sets of  $n$  points, its computation is done in  $O(n^3 \log(n))$  (Seguy et al., 2017), which compromises its usability for settings with more than a few tens of thousand of points. To lighten OT computational cost, a large number of works have developed efficient computational tools in order to solve OT problems. In particular, Cuturi (2013) proposes to solve an entropic regularized OT problem using the Sinkhorn-Knopp algorithm (Sinkhorn and Knopp, 1967), reducing the cost of the problem to  $O(n^2)$ . Over the last past years, a large body of works have focused on speeding up the Sinkhorn-Knopp algorithm, building mostly on diverse low-rank approximations (Solomon et al., 2015; Altschuler et al., 2018, 2019; Forrow et al., 2019; Scetbon and Cuturi, 2020; Scetbon et al., 2021). These approaches have helped to reduce the computational cost of the problem from cubic (for the non-regularized problem) to linear complexity. Another type of commonly used solvers are building on sliced mechanisms (Rabin et al., 2012; Kolouri et al., 2019) that leverage the fact that the OT problem between one-dimensional distributions can be solved using a simple sorting algorithm. These solvers roughly consist in computing infinitely many linear projections of the high-dimensional distributions to one-dimensional distributions and then computing the average of the Wasserstein distances between these one-dimensional representations. Alternatively, Delon and Desolneux (2020) have proposed an OT distance not relying on direct comparison of histograms of points. First, a *Gaussian mixture model* (GMM) is fitted on each distribution, then the two obtained GMMs are compared using a restricted version of the  $W_2$  distance where the admissible transportation couplings  $\pi$  must themselves be GMMs. This OT problem has an equivalent formulation, that had already been proposed by Chen et al. (2018), that allows to solve it by merely calculating  $W_2$  distances between pairwise Gaussian components, which can be done analytically, and then solving a small-scale discrete OT problem. The main benefit of this latter approach is that the complexity of the composite OT problem does not depend on the dimension nor on the number of points but only on the number of components in the GMMs, implying that the computational cost of this approach comes almost entirely from the fitting of the GMMs. Although this method probably doesn't compete with the fastest recent refinements of the Sinkhorn-Knopp algorithm in terms of pure computational cost, it provides a relatively scalable and computationally effective OT distance that is particularly suited when there already exists a kind of clustering structure in the data. This approach has been used for texture synthesis (Leclaire et al., 2022), evaluating generative models (Luzi et al., 2023), or Gaussian Mixture reduction (Zhang and Chen, 2020).

Computationally speaking, the Gromov-Wasserstein problem is known to be much more costly to solve than the classic linear OT problem. Indeed, solving numerically the non-regularized GW problem involves solving a classic OT problem at each iteration. As for linear OT, entropic-regularized solvers have also been proposed (Peyré et al., 2016; Solomon et al., 2016) and involve in that case solving a regularized linear OT problem at each iteration. Recently, Scetbon et al. (2022) have shown that the low-rank approximations used to speed-up the Sinkhorn-Knopp algorithm were particularly suited for the regularized GW problem, resulting in a much more computationally efficient solver. Alternatively, other works have proposed efficient solvers by reducing the size of the GW problem, either through

<sup>2</sup>We say that  $\phi : \mathcal{X} \rightarrow \mathcal{Y}$  is an isometry if for all  $(x, x') \in \mathcal{X}^2$ ,  $d_{\mathcal{Y}}(\phi(x), \phi(x')) = d_{\mathcal{X}}(x, x')$ .

quantization of input measures (Chowdhury et al., 2021), or by recursive clustering approaches (Xu et al., 2019; Blumberg et al., 2020). Specifically to the Euclidean setting, Vayer et al. (2019b) has introduced a solver building on a sliced mechanism, and leveraging the observation that the GW problem seems most of the time easy to solve between one-dimensional distributions. In this work, we aim to construct an OT distance between GMMs that is invariant to isometries and that stays relevant between GMMs of different dimensions, in order to design a relatively efficient and scalable solver for Gromov-Wasserstein related problems, especially when there already exists a kind of clustering structure in the data.

**Contributions of the paper.** In this paper, we introduce two Gromov-Wasserstein type OT distances between GMMs. More precisely, we introduce in Section 3 a natural Gromov version of the distance introduced by Chen et al. (2018) and Delon and Desolneux (2020), that we call  $MGW_2$  for *Mixture Gromov Wasserstein*. This distance can be used for applications which only require to evaluate how far the distributions are from each other, without having to identify correspondences between points. However, this formulation does not allow to derive directly an optimal transportation plan between the points. To design a way to define such an optimal transportation plan, we define in Section 4 another distance that we call  $EW_2$  for *Embedded Wasserstein*. This latter turns out to be closely related to the Gromov-Wasserstein distance and to coincides with the OT distance introduced by Alvarez-Melis et al. (2019) as well as with the distance between metric measure spaces introduced by Sturm (2006). We show that when restricting the admissible transportation couplings  $\pi$  to be themselves GMMs, this distance can be used as another alternative to Gromov-Wasserstein, not as computationally effective as  $MGW_2$  but that allows to derive directly an optimal transportation plan between the points. We also define a transportation plan for  $MGW_2$  by analogy with  $EW_2$ . Finally, in Section 5, we illustrate the practical use of our distances on medium-to-large scale problems such as shape matching and hyperspectral image color transfer. All the proofs are postponed to the appendix.

## Notations

We define in the following some of the notations that will be used in the paper.

- $\langle x, x' \rangle_d$  stands for the Euclidean inner-product in  $\mathbb{R}^d$  between  $x$  and  $x'$ . We will denote  $\langle x, x' \rangle$  when there is no ambiguity about the dimension.
- $\|x\|_{\mathbb{R}^d}$  stands for the Euclidean norm of  $x \in \mathbb{R}^d$ . We will denote  $\|x\|$  when there is no ambiguity about the dimension.
- the notation  $\text{tr}(M)$  denotes the trace of a matrix  $M$ .
- $\|M\|_{\mathcal{F}}$  stands for the Frobenius norm of a matrix  $M$ , i.e.  $\|M\|_{\mathcal{F}} = \sqrt{\text{tr}(M^T M)}$ .
- $\|M\|_*$  stands for the nuclear norm of a matrix  $M$ , i.e.  $\|M\|_* = \text{tr}((M^T M)^{\frac{1}{2}})$ .
- the notation  $\sigma(M)$  denotes the vector of singular values of the matrix  $M$ .
- $\text{Id}_d$  is the identity matrix of size  $d \times d$ .
- $\tilde{\text{Id}}_d$  stands for any matrix of size  $d \times d$  of the form  $\text{diag}((\pm 1)_{1 \leq i \leq d})$
- Suppose  $d \geq d'$ . For any matrix  $M$  of size  $d \times d$ , we denote  $M^{(d')}$  the submatrix of size  $d' \times d'$  containing the  $d'$  first rows and the  $d'$  first columns of  $A$ .
- Let  $r \leq d$  and  $s \leq d'$ . For any matrix  $M$  of size  $r \times s$ , we denote  $M^{[d, d']}$  the matrix of size of the form  $\begin{pmatrix} M & 0 \\ 0 & 0 \end{pmatrix}$ . When  $d = d'$ , we will denote  $M^{[d]}$ .
- For any  $x \in \mathbb{R}^d$ ,  $\text{diag}(x)$  denotes the matrix of size  $d \times d$  with diagonal vector  $x$ .
- We denote  $\mathbb{S}^d$  the set of symmetric matrices of size  $d \times d$ ,  $\mathbb{S}_+^d$  the set of symmetric positive semi-definite matrices, and  $\mathbb{S}_{++}^d$  the set of symmetric positive definite matrices.
- $\mathbb{1}_{d', d} = (1)_{\substack{1 \leq i \leq d' \\ 1 \leq j \leq d}}$  denotes the matrix of ones with  $d'$  rows and  $d$  columns.
- The notation  $X \sim \mu$  means that  $X$  is a random variable with probability distribution  $\mu$ .

- If  $\mu$  is a positive measure on  $\mathcal{X}$  and  $\phi : \mathcal{X} \rightarrow \mathcal{Y}$  is a mapping  $\phi_{\#}\mu$  stands for the push-forward measure of  $\mu$  by  $T$ , i.e. the measure on  $\mathcal{Y}$  such that for any measurable set  $A$  of  $\mathcal{Y}$ ,  $\phi_{\#}\mu(A) = \mu(\phi^{-1}(A))$ .
- If  $\mu$  is a positive measure on  $\mathcal{X}$ ,  $\text{supp}(\mu)$  denotes its support, i.e. the subset of  $\mathcal{X}$  defined as  $\text{supp}(\mu) = \{x \in \mathcal{X} \mid \text{there exists } N_x \text{ open such that } x \in N_x \text{ and } \mu(N_x) > 0\}$ .
- If  $X$  and  $Y$  are random vectors on  $\mathbb{R}^d$  and  $\mathbb{R}^{d'}$ , we denote  $\text{Cov}(X, Y)$  the matrix of size  $d \times d'$  of the form  $\mathbb{E}[(X - \mathbb{E}[X])(Y - \mathbb{E}[Y])^T]$ .
- For any positive measure  $\mu$ , we denote  $\bar{\mu}$  its associated centered measure, i.e. the measure such that if  $X \sim \mu$ , we have  $X - \mathbb{E}_{X \sim \mu}[X] \sim \bar{\mu}$ .
- For any  $m \in \mathbb{R}^d$  and any  $\Sigma \in \mathbb{S}_+^d$ , we denote  $N(m, \Sigma)$  the Gaussian measure of mean  $m$  and covariance matrix  $\Sigma$ .
- For  $x \in \mathcal{X}$ ,  $\delta_x$  denotes the Dirac distribution at  $x$ .

## 2 Background : Mixture-Wasserstein and Gromov-Wasserstein-type distances

We recall in this section the definitions and some important properties of the different OT distances used throughout the paper. For any Polish space  $\mathcal{X}$ , we write  $\mathcal{P}(\mathcal{X})$  the set probability measures on  $\mathcal{X}$ . For  $d \geq 1$  and  $p \geq 1$ , the Wasserstein space  $\mathcal{W}_p(\mathbb{R}^d)$  is defined as the set of probability measures  $\mu$  on  $\mathbb{R}^d$  with finite moment of order  $p$ , i.e. such that

$$\int_{\mathbb{R}^m} \|x\|^p d\mu(x) < +\infty,$$

with  $\|\cdot\|$  being the Euclidean norm on  $\mathbb{R}^d$ .

### 2.1 Mixture-Wasserstein distance between GMMs

We present here the distance introduced in [Delon and Desolneux \(2020\)](#), as well as various results of this latter paper. We denote  $GMM_K(\mathbb{R}^d)$  the set of Gaussian mixtures on  $\mathbb{R}^d$  with less than  $K$  components, i.e. the set of measures in  $\mathcal{P}(\mathbb{R}^d)$  which can be written

$$\mu = \sum_{k=1}^{K'} a_k \mu_k,$$

where  $K' \leq K$ ,  $a = (a_1, \dots, a_{K'})^T$  is in  $\Delta_{K'}$ , and  $\{\mu_k\}_k$  is a family of pairwise distinct Gaussian distributions, each of mean  $m_k \in \mathbb{R}^d$  and covariance matrix  $\Sigma_k \in \mathbb{S}_+^d$ . Again, to avoid degeneracy issues where locations with no mass are accounted for, we will assume that the elements of  $a$  are all positive. The set of all finite Gaussian mixture distributions on  $\mathbb{R}^d$  is then written

$$GMM_{\infty}(\mathbb{R}^d) = \bigcup_{K \geq 0} GMM_K(\mathbb{R}^d).$$

Note that the condition that the Gaussian components are pairwise distinct ensures the identifiability of the elements of  $GMM_{\infty}(\mathbb{R}^d)$  ([Yakowitz and Spragins, 1968](#)), in the sense that two GMMs  $\mu = \sum_k^K a_k \mu_k$  and  $\nu = \sum_l^L b_l \nu_l$  are equal if and only if  $K = L$ , and we can reorder the indices such that for all  $k$ ,  $a_k = b_k$  and  $\mu_k = \nu_k$ . It can be shown that  $GMM_{\infty}(\mathbb{R}^d)$  is dense in  $\mathcal{W}_p(\mathbb{R}^d)$  for the metric  $W_p$ , meaning that any measure in  $\mathcal{W}_p(\mathbb{R}^d)$  can be approximated with any precision for the distance  $W_p$  by a finite Gaussian mixture distribution. Let  $\mu \in GMM_K(\mathbb{R}^d)$  and  $\nu \in GMM_L(\mathbb{R}^d)$ . The Mixture-Wasserstein distance of order 2 is defined as

$$MW_2(\mu, \nu) = \left( \inf_{\pi \in \Pi(\mu, \nu) \cap GMM_{\infty}(\mathbb{R}^{2d})} \int_{\mathbb{R}^d \times \mathbb{R}^d} \|x - y\|^2 d\pi(x, y) \right)^{\frac{1}{2}}. \quad (MW_2)$$

As for  $W_2$  with  $\mathcal{W}_2(\mathbb{R}^d)$ ,  $MW_2$  defines a metric on  $GMM_{\infty}(\mathbb{R}^d)$ . In general, the transportation plan solution of the  $W_2$  problem is not a Gaussian mixture, thus by restricting the set of admissible couplings, we most of the time have  $MW_2(\mu, \nu) > W_2(\mu, \nu)$ . It can be shown that the difference between  $MW_2(\mu, \nu)$

and  $W_2(\mu, \nu)$  is upper-bounded by a term that only depends on the weights and the covariances matrices of the components of the two mixtures. Finally,  $MW_2$  can be written in an equivalent form, which had already been introduced in [Chen et al. \(2018\)](#): if  $\mu = \sum_k^K a_k \mu_k$  and  $\nu = \sum_l^L b_l \nu_l$ , then

$$MW_2^2(\mu, \nu) = \inf_{\omega \in \Pi(a,b)} \sum_{k,l} \omega_{k,l} W_2^2(\mu_k, \nu_l), \quad (2)$$

where  $a = (a_1, \dots, a_K)^T$ ,  $b = (b_1, \dots, b_L)^T$ . From a computational point of view, this latter formulation reduces the problem to a simple small-scale discrete optimal transport problem since the  $W_2$  distance between Gaussian distributions has a closed form: indeed, recall that if  $\mu_k = \mathcal{N}(m_k, \Sigma_k)$  and  $\nu_l = \mathcal{N}(m_l, \Sigma_l)$ , then

$$W_2^2(\mu_k, \nu_l) = \|m_k - m_l\|^2 + \text{tr} \left( \Sigma_k + \Sigma_l - 2 \left( \Sigma_k^{\frac{1}{2}} \Sigma_l \Sigma_k^{\frac{1}{2}} \right)^{\frac{1}{2}} \right).$$

## 2.2 Gromov-Wasserstein distance

The Gromov-Wasserstein problem ([Mémoli, 2011](#)) can be defined as the following: given two Polish spaces  $\mathcal{X}$  and  $\mathcal{Y}$ , two measurable functions  $c_{\mathcal{X}} : \mathcal{X} \times \mathcal{X} \rightarrow \mathbb{R}$  and  $c_{\mathcal{Y}} : \mathcal{Y} \times \mathcal{Y} \rightarrow \mathbb{R}$ , and two probability measures  $\mu \in \mathcal{P}(\mathcal{X})$  and  $\nu \in \mathcal{P}(\mathcal{Y})$  with  $p \geq 1$ , it aims at finding

$$GW_p(c_{\mathcal{X}}, c_{\mathcal{Y}}, \mu, \nu) = \left( \inf_{\pi \in \Pi(\mu, \nu)} \int_{\mathcal{X} \times \mathcal{Y}} \int_{\mathcal{X} \times \mathcal{Y}} |c_{\mathcal{X}}(x, x') - c_{\mathcal{Y}}(y, y')|^p d\pi(x, y) d\pi(x', y') \right)^{\frac{1}{p}}. \quad (GW_p)$$

The fundamental metric properties of  $GW_p$  have been studied in depth in ([Mémoli, 2011](#); [Sturm, 2012](#); [Chowdhury and Mémoli, 2019](#)). When  $c_{\mathcal{X}}$  and  $c_{\mathcal{Y}}$  are powers of the metrics of the base spaces  $\mathcal{X}$  and  $\mathcal{Y}$ ,  $GW_p$  induces a metric over the space of *metric measure spaces* (i.e. the triplets  $(\mathcal{X}, d_{\mathcal{X}}, \mu)$ ) quotiented by the *strong isomorphisms* ([Sturm, 2012](#)), where one say that two metric measures spaces  $(\mathcal{X}, d_{\mathcal{X}}, \mu)$  and  $(\mathcal{Y}, d_{\mathcal{Y}}, \nu)$  are strongly isomorphic if there exists an isometric bijection  $\phi : \text{supp}(\mu) \rightarrow \text{supp}(\nu)$  that transports  $\mu$  into  $\nu$ . When  $c_{\mathcal{X}}$  and  $c_{\mathcal{Y}}$  are not powers of the metrics of the base spaces,  $GW_p$  still defines a metric, but this time over the space of *network measure spaces* (i.e. the triplets  $(\mathcal{X}, c_{\mathcal{X}}, \mu)$ ), quotiented by the *weak isomorphisms* ([Chowdhury and Mémoli, 2019](#)), which are spaces isomorphic for the costs  $c_{\mathcal{X}}$  and  $c_{\mathcal{Y}}$  relatively to a third space, see ([Chowdhury and Mémoli, 2019](#)) for details. Note that in both cases, the metric property of  $GW_p$  strictly holds only when it takes finite values, and so it is natural to restrict it to the following space

$$\mathbb{M}_p = \{(\mathcal{X}, c_{\mathcal{X}}, \mu) : \int_{\mathcal{X} \times \mathcal{X}} c_{\mathcal{X}}^p(x, x') d\mu(x) d\mu(x') < +\infty\}.$$

Finally, in the discrete setting, given  $a = (a_1, \dots, a_m)^T$  and  $b = (b_1, \dots, b_n)^T$  being respectively in  $\Delta_m$  and  $\Delta_n$ , and given two non-negative cost matrices  $C^x$  and  $C^y$  of respective size  $m \times m$  and  $n \times n$ , the Gromov-Wasserstein distance can be written as

$$GW_p(C^x, C^y, \alpha, \beta) = \inf_{\omega \in \Pi(a,b)} \sum_{i,j,k,l} |C_{i,k}^x - C_{j,l}^y|^p \omega_{i,j} \omega_{k,l}.$$

## 2.3 Other invariant distances

In the Euclidean setting, [Alvarez-Melis et al. \(2019\)](#) have introduced another family of invariant OT distances which can also be used to compare distributions on spaces of different dimensions. Initially, [Alvarez-Melis et al. \(2019\)](#) have introduced this OT distance in the setting where  $\mu$  and  $\nu$  are both living in the same Euclidean space  $\mathbb{R}^d$ . Yet, it generalizes well to settings where  $\mu$  and  $\nu$  are living in spaces of different dimensions. Between two measures  $\mu$  and  $\nu$  on  $\mathbb{R}^d$ , this reads as

$$IW_2(\mathcal{H}, \mu, \nu) = \left( \inf_{\pi \in \Pi(\mu, \nu)} \inf_{h \in \mathcal{H}} \int_{\mathbb{R}^d \times \mathbb{R}^d} \|x - h(y)\|^2 d\pi(x, y) \right)^{\frac{1}{2}}, \quad (IW_2)$$

where  $\mathcal{H}$  is a class of mappings from  $\mathbb{R}^{d'}$  to  $\mathbb{R}^d$  encoding the invariance. This is a *non-convex* optimization problem in  $\pi$  and  $h$  that becomes convex in  $\pi$  if  $h$  is fixed and becomes also convex in  $h$  if  $\pi$  is fixed and  $\mathcal{H}$  is a convex set. When  $d$  is equal to  $d'$  and both measures are centered, [Alvarez-Melis et al. \(2019\)](#) have notably shown that when  $\nu$  is such that  $\mathbb{E}_{Y \sim \nu}[Y Y^T] = \text{Id}_d$  and when  $\mathcal{H} = \mathcal{H}_1 := \{P \in \mathbb{R}^{d \times d} : \|P\|_{\mathcal{F}} \leq \sqrt{d}\}$ ,

Problem  $(IW_2)$  is equivalent to the Gromov-Wasserstein problem  $(GW_p)$  of order 2 with inner-product costs. Indeed, it can be shown that both problems are equivalent in that case to

$$\sup_{\pi \in \Pi(\mu, \nu)} \left\| \int_{\mathbb{R}^d \times \mathbb{R}^d} xy^T d\pi(x, y) \right\|_{\mathcal{F}}, \quad (\mathcal{F}\text{-COV})$$

where for any matrix  $A$  of size  $d \times d$ ,  $\|A\|_{\mathcal{F}}$  denotes the Frobenius norm, i.e.  $\sqrt{\text{tr}(A^T A)}$ . Another interesting case is when  $\mathcal{H} = \mathcal{H}_2 := \mathcal{O}(\mathbb{R}^d) := \{P \in \mathbb{R}^{d \times d} : P^T P = \text{Id}_d\}$  is the set of orthogonal matrices of size  $d \times d$ . In that case, Problem  $(IW_2)$  is equivalent to

$$\sup_{\pi \in \Pi(\mu, \nu)} \left\| \int_{\mathbb{R}^d \times \mathbb{R}^d} xy^T d\pi(x, y) \right\|_*, \quad (*\text{-COV})$$

where for any matrix  $A$  of size  $d \times d$ ,  $\|A\|_*$  is the nuclear norm of  $A$ , i.e.  $\|A\|_* = \text{tr}((A^T A)^{\frac{1}{2}})$ . Note that both Problems  $(\mathcal{F}\text{-COV})$  and  $(*\text{-COV})$  are *non-convex*. These results have been shown by [Alvarez-Melis et al. \(2019\)](#) in the case where  $\mu$  and  $\nu$  are discrete but can easily be extended to continuous distributions. Observe that problem  $(*\text{-COV})$  consists in maximizing the sum of the singular values of the cross-covariance matrix  $\int xy^T d\pi(x, y)$ , whereas the Problem  $(\mathcal{F}\text{-COV})$  consists in maximizing the sum of the squared singular values of the cross-covariance matrix. In general, these two problems are not equivalent despite being structurally similar, as the example of Figure 1 illustrates it.

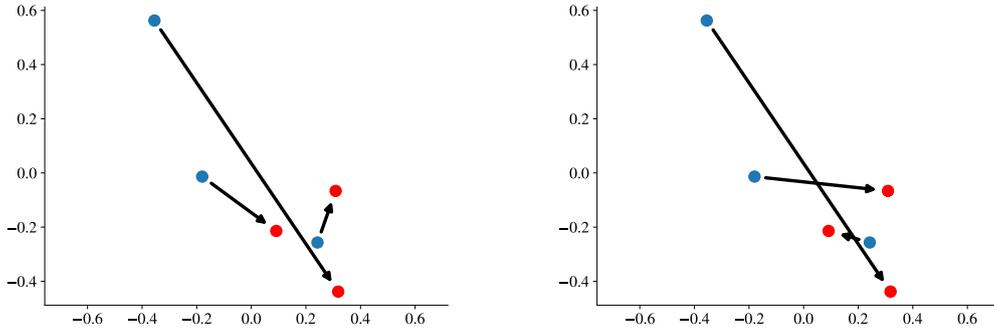


Figure 1: Transport plans between two discrete centered distributions on  $\mathbb{R}^2$  composed of three points. Left: optimal coupling given by the maximization of Problem  $(\mathcal{F}\text{-COV})$ . Right: optimal coupling given by the maximization of Problem  $(*\text{-COV})$ .

### 3 Gromov-Wasserstein distance between mixture of Gaussians

In this section, we define a Gromov-Wasserstein type distance between Gaussian mixture distributions. This distance is a natural "Gromovization" of Problem (2). Indeed, as it has already been observed in the literature ([Chen et al., 2018](#); [Lambert et al., 2022](#)), any Gaussian mixture in dimension  $d$  can be identified with a probability distribution on  $\mathbb{R}^d \times \mathbb{S}_+^d$ , i.e. the product space of means and covariance matrices. Equivalently, a finite Gaussian mixture can be seen as a discrete probability distribution on the space of Gaussian distributions  $\mathcal{N}(\mathbb{R}^d)^3$ , which has been proven to be a complete metric space when endowed with  $W_2$  ([Takatsu, 2010](#)) and is furthermore separable since it is a subspace of  $\mathcal{W}_2(\mathbb{R}^d)$  which is itself a separable metric space when endowed with  $W_2$  ([Bolley, 2008](#)). Since the theory of optimal transport still applies on measures over non-Euclidean spaces ([Villani, 2008](#)), it follows that Problem (2) can formally be thought as a simple OT problem between two discrete measures in  $\mathcal{P}(\mathcal{N}(\mathbb{R}^d))$ . Thus, one can define directly its Gromov version.

**Definition 1.** Let  $\mu = \sum_k a_k \mu_k$  and  $\nu = \sum_l b_l \nu_l$  be two Gaussian mixtures respectively on  $\mathbb{R}^d$  and  $\mathbb{R}^{d'}$ , we define

$$MGW_2^2(\mu, \nu) = \inf_{\omega \in \Pi(a, b)} \sum_{i, j, k, l} |W_2^2(\mu_i, \mu_k) - W_2^2(\nu_j, \nu_l)|^2 \omega_{i, j} \omega_{k, l}. \quad (MGW_2)$$

<sup>3</sup> $\mathcal{N}(\mathbb{R}^d)$  includes the degenerate Gaussian distributions, as for instance the Dirac distributions.

Unlike  $MW_2$ , there is no straightforward equivalent formulation of this latter problem. In particular, it is not clear whether Problem ( $MGW_2$ ) is equivalent or not to the continuous GW problem between  $\mu$  and  $\nu$  - seen as continuous measures on  $\mathbb{R}^d$  and  $\mathbb{R}^{d'}$  - where the set of admissible couplings is restricted to Gaussian mixture distributions. In the rest of the chapter, we distinguish the distribution  $\tilde{\mu} \in \mathcal{P}(\mathcal{N}(\mathbb{R}^d))$  from its associated GMM  $\mu \in GMM_\infty(\mathbb{R}^d)$ . Thanks to the identifiability property of the set of finite Gaussian mixture, we have that each  $\mu \in GMM_\infty(\mathbb{R}^d)$  is associated with a unique discrete distribution  $\tilde{\mu} \in \mathcal{P}(\mathcal{N}(\mathbb{R}^d))$  and  $MGW_2$  between  $\mu$  and  $\nu$  coincides with  $GW_2$  with squared  $W_2$  as cost functions between the associated measures  $\tilde{\mu}$  and  $\tilde{\nu}$ . More generally, one can define for any metric measure space of the form  $(\mathcal{N}(\mathbb{R}^d), W_2^2, \tilde{\mu})$  and  $(\mathcal{N}(\mathbb{R}^{d'}), W_2^2, \tilde{\nu})$ , the following continuous GW problem,

$$\inf_{\pi \in \Pi(\tilde{\mu}, \tilde{\nu})} \int_{\mathcal{N}(\mathbb{R}^d) \times \mathcal{N}(\mathbb{R}^{d'})} \int_{\mathcal{N}(\mathbb{R}^d) \times \mathcal{N}(\mathbb{R}^{d'})} |W_2^2(\gamma, \gamma') - W_2^2(\zeta, \zeta')|^2 d\pi(\gamma, \zeta) d\pi(\gamma', \zeta'),$$

where  $\tilde{\mu}$  and  $\tilde{\nu}$  can be possibly thought as infinite mixture of Gaussians. However, there is in general no identifiability property for infinite Gaussian mixture and so for a given GMM  $\mu$  on  $\mathbb{R}^d$ , they might be more than one associated measure  $\tilde{\mu}$  on  $\mathcal{N}(\mathbb{R}^d)$ . For instance, the standard Normal distribution  $N(0, 1)$  can naturally be identified in  $\mathcal{P}(\mathcal{N}(\mathbb{R}))$  with the Dirac distribution at  $N(0, 1)$ , but also with the Normal distribution  $N(0, 1/2)$  over the parametrized line  $\{N(\theta, 1/2) \in \mathcal{N}(\mathbb{R}) : \theta \in \mathbb{R}\}$ , or with  $N(0, 1)$  over the parametrized line  $\{\delta_\theta \in \mathcal{N}(\mathbb{R}) : \theta \in \mathbb{R}\}$ .

### 3.1 Metric properties

Here we study the metric property of  $MGW_2$  that mainly arises from the Gromov-Wasserstein structure of Problem ( $MGW_2$ ). Indeed, the following result is a direct consequence of the theory developed by [Sturm \(2012\)](#).

**Theorem 2.** *In the following,  $\mu = \sum_k a_k \mu_k$  and  $\nu = \sum_l b_l \nu_l$  are two GMMs respectively in  $GMM_K(\mathbb{R}^d)$  and  $GMM_L(\mathbb{R}^{d'})$ .*

- (i)  $MGW_2$  is non-negative and symmetric.
- (ii)  $MGW_2$  satisfies the triangle inequality, i.e. for any  $\xi \in GMM_S(\mathbb{R}^{d''})$ ,

$$MGW_2(\mu, \nu) \leq MGW_2(\mu, \xi) + MGW_2(\xi, \nu).$$

- (iii)  $MGW_2(\mu, \nu) = 0$  if and only if there exists a bijection  $\phi : \{\mu_k\}_k \rightarrow \{\nu_l\}_l$  such that  $\nu = \sum_k a_k \phi(\mu_k)$  and  $\phi$  is an isometry for  $W_2$ , i.e. for all  $k$  and  $i$  smaller than  $K$ ,  $W_2(\phi(\mu_k), \phi(\mu_i)) = W_2(\mu_k, \mu_i)$ .

*Sketch of proof.* The proof of this results mainly consists in applying the theory of [Sturm \(2012\)](#), using the facts that  $\mathcal{N}(\mathbb{R}^d)$  is complete ([Takatsu, 2010](#)), separable ([Bolley, 2008](#)), and metrizable with the Wasserstein distance.  $\square$

$MGW_2$  defines thus a pseudometric on the set of all finite Gaussian mixtures of arbitrary dimensions, i.e. the set,

$$GMM_\infty = \bigsqcup_{d \geq 1} GMM_\infty(\mathbb{R}^d),$$

that is invariant to the mappings  $\phi$  that transform a finite Gaussian mixture  $\sum_{k=1}^K a_k \mu_k$  into another finite Gaussian mixture of the form  $\sum_{k=1}^K a_k \nu_k$  such that for all  $k$  and  $i$  smaller than  $K$ ,  $W_2(\nu_k, \nu_i) = W_2(\mu_k, \mu_i)$ . A question that arises is: are all these mappings  $\phi$  associated with mappings  $T$  that are isometries for the Euclidean norm and such that  $T_\#$  coincides with  $\phi$ ? We can already state the following converse result.

**Proposition 3.** *Let  $d \geq d'$ , and let  $T : \mathbb{R}^{d'} \rightarrow \mathbb{R}^d$  be a mapping that is an isometry for the Euclidean norm. Then the mapping  $\phi_T : GMM_\infty(\mathbb{R}^{d'}) \rightarrow \mathcal{P}(\mathbb{R}^d)$  defined as  $\phi_T(\mu) = T_\# \mu$  for all  $\mu \in GMM_\infty(\mathbb{R}^{d'})$ , is such that for any  $\mu$  of the form  $\sum_{k=1}^K a_k \mu_k$ ,  $\phi_T(\mu)$  is in  $GMM_\infty(\mathbb{R}^d)$  and is of the form  $\sum_{k=1}^K a_k \nu_k$ , with  $\{\nu_k\}_{k=1}^K$  being such that, for all  $k$  and  $i$  smaller than  $K$ ,  $W_2(\nu_k, \nu_i) = W_2(\mu_k, \mu_i)$  and so  $MGW_2(\mu, T_\# \mu) = 0$ .*

*Sketch of proof.* The proof of this result mainly consists in showing that for any  $\mu \in GMM_\infty(\mathbb{R}^{d'})$ ,  $\phi_T(\mu)$  is in  $GMM_\infty(\mathbb{R}^d)$  because  $T$  is necessarily affine, as a direct consequence of the Mazur-Ulam theorem ([Mazur and Ulam, 1932](#)) which implies that any isometry from  $\mathbb{R}^{d'}$  to  $\mathbb{R}^d$  (endowed with the Euclidean norm) is necessarily affine.  $\square$

Hence, if  $T : \mathbb{R}^{d'} \rightarrow \mathbb{R}^d$  is an isometry for the Euclidean norm, then  $MGW_2$  is invariant to the mapping  $\phi_T : GMM_\infty(\mathbb{R}^{d'}) \rightarrow GMM_\infty(\mathbb{R}^d)$  such that for all  $\mu \in GMM_\infty(\mathbb{R}^{d'})$ ,  $\phi(\mu) = T\#\mu$ . Yet, in general, there exist mappings  $\phi : \mathcal{W}_2(\mathbb{R}^{d'}) \rightarrow \mathcal{W}_2(\mathbb{R}^d)$  that are isometries for  $W_2$  and that are not induced by any mapping  $T : \mathbb{R}^{d'} \rightarrow \mathbb{R}^d$  that is an isometry for the Euclidean norm. This has been proven by Kloeckner (2010) in the general case when considering isometries defined all over  $\mathcal{W}_2(\mathbb{R}^d)$  but remains true when restricting to isometries defined over subspaces of  $\mathcal{N}(\mathbb{R}^d)$  as the following example suggests: let  $\mathcal{N}_{++}(\mathbb{R})$  be the set of one-dimensional Gaussian distributions with strictly positive mean. Let  $\phi : \mathcal{N}_{++}(\mathbb{R}) \rightarrow \mathcal{N}_{++}(\mathbb{R})$  be the mapping that swaps the mean and the standard deviation, i.e. such that for any  $\gamma = N(m_\gamma, \sigma_\gamma^2)$  with  $m_\gamma > 0$  and  $\sigma_\gamma > 0$ ,  $\phi(\gamma) = N(\sigma_\gamma, m_\gamma^2)$ . Then  $\phi$  is an isometry for  $W_2$ . Observe indeed that for  $\gamma$  and  $\zeta$  in  $\mathcal{N}_{++}(\mathbb{R})$ , we have

$$W_2(\phi(\gamma), \phi(\zeta)) = (\sigma_\gamma - \sigma_\zeta)^2 + (m_\gamma - m_\zeta)^2 = W_2(\gamma, \zeta).$$

Thus  $\phi$  is an isometry for  $W_2$ , yet  $\phi$  is not induced by any isometry of  $\mathbb{R}$ . Hence there exist mappings from  $GMM_\infty(\mathbb{R}^{d'})$  to  $GMM_\infty(\mathbb{R}^d)$  that satisfy the conditions above but which are not induced by isometries for the Euclidean norm from  $\mathbb{R}^{d'}$  to  $\mathbb{R}^d$ .

### 3.2 $MGW_2$ in practice

**Using  $MGW_2$  on discrete data distributions.** Most applications of optimal transport involve discrete data that can be thought as samples drawn from underlying distributions, which are not GMMs in general. In those applications, we aim to evaluate an OT distance between two distributions of the form  $\hat{\mu} = (1/M) \sum_i \delta_{x_i}$  and  $\hat{\nu} = (1/N) \sum_j \delta_{y_j}$  where  $\{x_i\}_i$  and  $\{y_j\}_j$  are families of respectively  $M$  and  $N$  vectors of  $\mathbb{R}^d$  and  $\mathbb{R}^{d'}$ . Though  $\hat{\mu}$  and  $\hat{\nu}$  can be thought as mixtures of degenerate Gaussian distributions, evaluating directly  $MGW_2(\hat{\mu}, \hat{\nu})$  is not particularly interesting since we have in that case  $MGW_2(\hat{\mu}, \hat{\nu}) = GW_2(\|\cdot\|^2, \|\cdot\|^2, \hat{\mu}, \hat{\nu})$ . However, we can design a pseudometric  $MGW_{K,2}$  between  $\hat{\mu}$  and  $\hat{\nu}$  by fitting two GMMs  $\mu$  and  $\nu$  with  $K$  components on  $\hat{\mu}$  and  $\hat{\nu}$  and then setting  $MGW_{K,2}(\hat{\mu}, \hat{\nu}) = MGW_2(\mu, \nu)$ . The approximation of  $\hat{\mu}$  and  $\hat{\nu}$  by  $\mu$  and  $\nu$  can be done by maximizing the log-likelihood of the GMMs with the EM algorithm (Dempster et al., 1977). Note that if  $K$  is chosen too small, the approximations  $\hat{\mu}$  and  $\hat{\nu}$  will be of bad quality and we are likely to observe undesirable behaviors, as for instance having  $MGW_{K,2}(\hat{\mu}, \hat{\nu}) = 0$  despite  $\hat{\mu}$  and  $\hat{\nu}$  not being equal up to an isometry. Thus, the choice of  $K$  must be a compromise between the quality of the approximation given by the GMM and the computational cost. To illustrate the practical use of  $MGW_2$  on a simple toy example, we draw 150 samples from the spiral dataset provided in the scikit-learn toolbox<sup>4</sup> (Pedregosa et al., 2011) and we apply rotations with various angles on this dataset. We then fit independently GMMs with 20 components on the initial and the target rotated datasets and we compute  $MGW_2$  between the two obtained GMMs. We also compute  $GW_2$  with inner-product as cost functions,  $MW_2$  using also 20 Gaussian components and  $W_2$ . The results can be found in Figure 2. As expected,  $MGW_2$  is rotation-invariant as  $GW_2$  which is not the case of  $MW_2$  and  $W_2$ .

**Difficulty of designing a transportation plan.** The  $MGW_2$  problem can be used on discrete data to provide an optimal coupling between the Gaussian components of the two Gaussian mixtures  $\mu$  and  $\nu$  that approximate the discrete data distributions  $\hat{\mu}$  and  $\hat{\nu}$ . However, some applications require an optimal coupling between the points that compose  $\hat{\mu}$  and  $\hat{\nu}$ . It is not straightforward to design such a transportation plan associated with the plan that minimizes the  $MGW_2$  problem. More precisely, for two GMMs  $\mu = \sum_k a_k \mu_k$  and  $\nu = \sum_l b_l \nu_l$ , the discrete  $MW_2$  problem between the associated distributions  $\tilde{\mu} \in \mathcal{P}(\mathcal{N}(\mathbb{R}^d))$  and  $\tilde{\nu} \in \mathcal{P}(\mathcal{N}(\mathbb{R}^d))$  is equivalent to restricting the set of coupling to be GMMs in the continuous  $W_2$  problem between  $\mu$  and  $\nu$ . Thus, there exists a direct relationship between the optimal couplings  $\omega^*$  and  $\pi^*$  associated with these two latter problems. Indeed, when the  $\mu_k$  are all non-degenerate distributions, we have for any  $x, y \in \mathbb{R}^d$ ,

$$\pi^*(x, y) = \sum_{k,l} \omega_{k,l}^* p_{\mu_k}(x) \delta_{y=T_{W_2}^{k,l}(x)}, \quad (3)$$

where for  $\mu_k = N(m_k, \Sigma_k)$ ,  $p_{\mu_k}(x) = (2\pi)^{-\frac{m}{2}} |\Sigma_k|^{-\frac{1}{2}} \exp[-\frac{1}{2}(x - m_k)^T \Sigma_k^{-1} (x - m_k)]$  is the density of  $\mu_k$  in  $x$ , and  $T_{W_2}^{k,l}$  is the optimal affine transportation map between  $\mu_k$  and  $\nu_l = N(m_l, \Sigma_l)$  associated with  $W_2$ , i.e. for all  $x \in \mathbb{R}^d$ ,

$$T_{W_2}^{k,l}(x) = m_l + \Sigma_k^{-\frac{1}{2}} (\Sigma_k^{\frac{1}{2}} \Sigma_l \Sigma_k^{\frac{1}{2}})^{\frac{1}{2}} \Sigma_k^{-\frac{1}{2}} (x - m_k).$$

<sup>4</sup>The package is accessible here: <https://scikit-learn.org/stable/>.

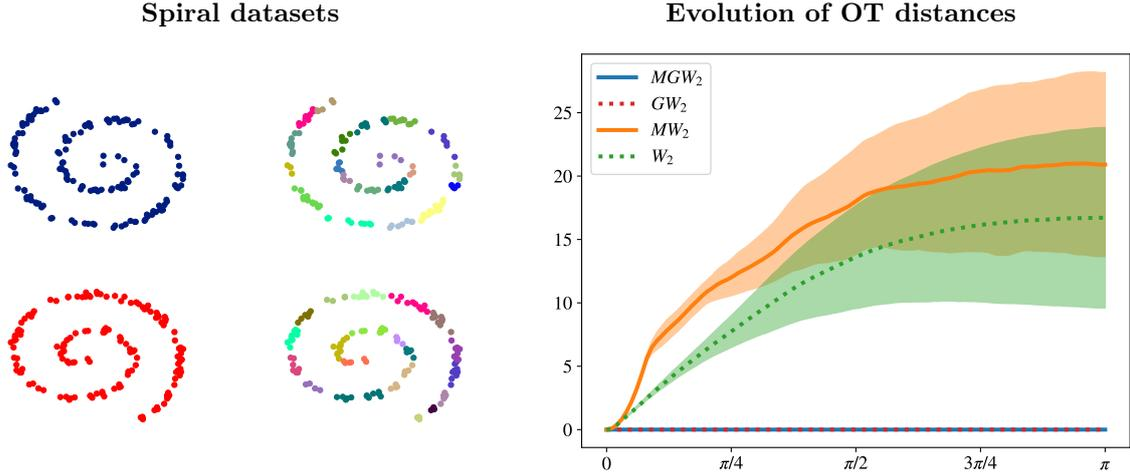


Figure 2: Left first column: spiral datasets (in blue and red) composed of 150 points of  $\mathbb{R}^2$ . The red dataset corresponds to points sampled from the distribution of the blue dataset rotated from  $\pi$ . Left second column: The two corresponding learned GMMs with 20 components via EM algorithm (each color corresponds to a Gaussian component of the GMMs). Right: evolution of  $MGW_2$ ,  $GW_2$ ,  $MW_2$ , and  $W_2$  between the initial distribution (in blue) and the rotated ones in function of the angle of rotation. Experiments are averaged over 10 runs and the colored bands correspond to  $\pm$  the standard deviation. This experiment is inspired from Vayer et al. (2019b).

However, in the case of  $MGW_2$ , there doesn't exist to the best of our knowledge, any equivalent continuous formulation of the problem and so there is formally no such plan  $\pi^*$  associated with the discrete optimal coupling  $\omega^*$  that minimizes the  $MGW_2$  problem. Yet, supposing without any loss of generality that  $d \geq d'$ , and that  $\nu \in GMM_L(\mathbb{R}^{d'})$ , one could still define by analogy a plan  $\pi$  relatively to  $\omega^*$  using (3) and replacing  $T_{W_2}$  by suited transportation maps between Gaussian components. A naive approach would be to simply replace  $T_{W_2}$  by the affine transportation map  $T_{GGW_2}$  associated with the Gaussian plan that minimizes Problem ( $GW_p$ ) with squared Euclidean distance costs restricted to Gaussian couplings, that we have exhibited in Salmona et al. (2021):

$$T_{GGW_2}^{k,l}(x) = m_l + P_l \left( \tilde{\text{Id}}_{d'} D_l^{\frac{1}{2}} D_k^{(d')^{-\frac{1}{2}}} \right)^{[d',d]} P_k^T (x - m_k),$$

where  $(P_k, D_k)$  and  $(P_l, D_l)$  are the respective diagonalizations of  $\Sigma_k (= P_k D_k P_k^T)$  and  $\Sigma_l (= P_l D_l P_l^T)$  that sort the eigenvalues in non-increasing order, where  $\tilde{\text{Id}}_{d'}$  is any matrix of the form  $\text{diag}((\pm 1)_{i \leq d'})$ , where  $D_k^{(d')}$  denotes the submatrix of size  $d' \times d'$  containing the  $d'$  first rows and the  $d'$  first columns of  $D_k$ , and where for any matrix  $A$  of size  $r \times s$  with  $r \leq d'$  and  $s \leq d$ , we denote  $A^{[d',d]}$  the matrix of size  $d' \times d$  of the form

$$A^{[d',d]} = \begin{pmatrix} A & 0 \\ 0 & 0 \end{pmatrix}.$$

Yet this approach implies that each Gaussian component is transported independently of the others and so offers too many degrees of freedom. Observe indeed that  $T_{GGW_2}$  is defined up to  $\tilde{\text{Id}}_{d'}$  that can be any matrix of the form  $\text{diag}((\pm 1)_{i \leq d'})$ , implying that we have  $2^{d'}$  possibilities for each Gaussian component. For each component, since we want that points that are close to each other but associated with different Gaussian components remain close when transported, we need to determine, relatively to all the other components, which of the  $2^{d'}$  possibilities is the correct one. To illustrate this problem, we show in Figure 3 a 2-dimensional example where we derive two different transport maps using  $T_{GGW_2}$  but each time with a different  $\tilde{\text{Id}}_2$ . If the transport on the middle of Figure 3 preserves the global structure of the distribution since two points that are close to each other but associated with different Gaussian components remain close when transported, this is not the case of the transport on the right.

Therefore, in order to design a transport plan  $\pi_{MGW_2}$  associated with the  $MGW_2$  problem, it is in general necessary to determine for each pair of indices  $k, l$ , which  $\tilde{\text{Id}}_{d'}$  preserves, relatively to the others, the global structure of the GMM, which becomes a difficult combinatorial problem in itself as soon as the dimension  $d'$  is large. Alternatively, a less tedious solution to design such plan would be to derive

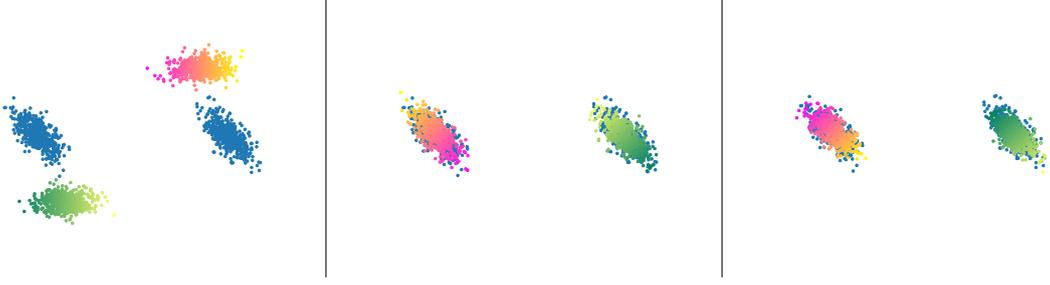


Figure 3: Left: two discrete distributions  $\hat{\mu}$  (in gradient of colors) and  $\hat{\nu}$  (in blue) that have been drawn from two GMMs. The colors have been added to  $\hat{\mu}$  in order to visualize the couplings between  $\hat{\mu}$  and  $\hat{\nu}$ . Middle: transport of  $\hat{\mu}$  obtained by plugging the discrete plan that minimizes  $MGW_2$  in (3), then using  $T_{GGW_2}$  with  $\tilde{\text{Id}}_2 = \text{Id}_2$  for all components to transport the points. Right: transport of  $\hat{\mu}$  obtained the same way as previously, but with another  $\tilde{\text{Id}}_2$ .

explicitly the isometric transformation that has been implicitly applied to one of the two measures when solving the  $MGW_2$  problem. This is the idea behind the embedded Wasserstein distance that we introduce in the following section.

## 4 Embedded Wasserstein distance

In this section, we define an alternative distance to Gromov-Wasserstein also invariant to isometries which explicitly the isometric transformation applied to one of the measure when computing the distance.

**Definition 4.** Let  $\mu \in \mathcal{P}(\mathbb{R}^d)$  and  $\nu \in \mathcal{P}(\mathbb{R}^{d'})$ . For  $r \geq 1$  and  $s \geq 1$ , let us denote  $\text{Isom}_s(\mathbb{R}^r)$  the set of all isometries - for the Euclidean norm - from  $\mathbb{R}^s$  to  $\mathbb{R}^r$ . We define

$$EW_2(\mu, \nu) = \inf \left\{ \inf_{\phi \in \text{Isom}_{d'}(\mathbb{R}^d)} W_2(\mu, \phi \# \nu), \inf_{\psi \in \text{Isom}_d(\mathbb{R}^{d'})} W_2(\psi \# \mu, \nu) \right\}, \quad (EW_2)$$

with the convention that the infimum over an empty set is equal to  $+\infty$ .

Observe that if  $d > d'$ , the set  $\text{Isom}_d(\mathbb{R}^{d'})$  is empty and so  $EW_2(\mu, \nu) = \inf_{\phi \in \text{Isom}_{d'}(\mathbb{R}^d)} W_2(\mu, \phi \# \nu)$ . In contrast, if  $d < d'$ ,  $\text{Isom}_{d'}(\mathbb{R}^d)$  is empty and so  $EW_2(\mu, \nu) = \inf_{\psi \in \text{Isom}_d(\mathbb{R}^{d'})} W_2(\psi \# \mu, \nu)$ . When  $d = d'$ , the two infimums are equivalent. In all what follows, we will suppose without any loss of generality that  $d \geq d'$ . More generally, one can define, given two - not necessarily Euclidean - Polish spaces  $\mathcal{X}$  and  $\mathcal{Y}$  each endowed with respective distances  $d_{\mathcal{X}}$  and  $d_{\mathcal{Y}}$ , and given two measures  $\mu \in \mathcal{P}(\mathcal{X})$  and  $\nu \in \mathcal{P}(\mathcal{Y})$ , the following OT distance

$$EW_p(\mu, \nu) = \inf \left\{ \inf_{\phi \in \text{Isom}_{\mathcal{Y}}(\mathcal{X})} W_p(\mu, \phi \# \nu), \inf_{\psi \in \text{Isom}_{\mathcal{X}}(\mathcal{Y})} W_p(\psi \# \mu, \nu) \right\}, \quad (EW_p)$$

where  $p \geq 1$  and  $\text{Isom}_{\mathcal{Y}}(\mathcal{X})$  (respectively  $\text{Isom}_{\mathcal{X}}(\mathcal{Y})$ ) is the set of all isometries from  $\mathcal{Y}$  to  $\mathcal{X}$  (respectively from  $\mathcal{X}$  to  $\mathcal{Y}$ ), i.e. such that  $d_{\mathcal{X}}(\phi(y), \phi(y')) = d_{\mathcal{Y}}(y, y')$  for  $y, y' \in \mathcal{Y}$ , and  $W_p$  is the Wasserstein distance of order  $p$  on  $\mathcal{P}(\mathcal{X})$ . However there might be cases where both set  $\text{Isom}_{\mathcal{Y}}(\mathcal{X})$  and  $\text{Isom}_{\mathcal{X}}(\mathcal{Y})$  are empty. In that case, by convention  $EW_p(\mu, \nu) = +\infty$ .

### 4.1 Equivalent formulations

First we show that when  $d \geq d'$ ,  $EW_2$  is equivalent to the OT distance introduced by Alvarez-Melis et al. (2019) described in Section 2.3 for a particular choice of transformation space  $\mathcal{H}$ . In all what follows, we denote  $\mathbb{V}_{d'}(\mathbb{R}^d)$  the *Stiefel manifold* (James, 1976), i.e. the set of rectangular orthogonal matrices of size  $d \times d'$  such that  $P^T P = \text{Id}_{d'}$ . We show the following result.

**Proposition 5.** Let  $\mu \in \mathcal{W}_2(\mathbb{R}^d)$  and  $\nu \in \mathcal{W}_2(\mathbb{R}^{d'})$  and let suppose without any loss of generality  $d \geq d'$ . Then,

$$EW_2^2(\mu, \nu) = \inf_{\pi \in \Pi(\mu, \nu)} \inf_{P \in \mathbb{V}_{d'}(\mathbb{R}^d), b \in \mathbb{R}^d} \int_{\mathbb{R}^d \times \mathbb{R}^{d'}} \|x - Py - b\|^2 d\pi(x, y). \quad (4)$$

*Sketch of proof.* This is principally a consequence of the Mazur-Ulam theorem (Mazur and Ulam, 1932) which implies that any isometry from  $\mathbb{R}^{d'}$  to  $\mathbb{R}^d$  (endowed with the Euclidean norm) is necessarily affine.  $\square$

Note that it is easy to show from Proposition 5 that the infimum in  $(EW_2)$  is always achieved, see Appendix C for details. Now we can derive an equivalent formulation of the  $EW_2$  problem. For any measure  $\mu \in \mathcal{W}_2(\mathbb{R}^d)$ , let us denote  $\bar{\mu}$  its associated centered measure, i.e. the measure such that if  $X \sim \mu$ , then  $X - \mathbb{E}_{X \sim \mu}[X] \sim \bar{\mu}$ .

**Proposition 6.** *Let  $\mu \in \mathcal{W}_2(\mathbb{R}^d)$  and  $\nu \in \mathcal{W}_2(\mathbb{R}^{d'})$  and let suppose  $d \geq d'$ . Problem  $(EW_2)$  is equivalent to*

$$\sup_{\pi \in \Pi(\bar{\mu}, \bar{\nu})} \sup_{P \in \mathbb{V}_{d'}(\mathbb{R}^d)} \text{tr}(P^T K_\pi), \quad (5)$$

where  $\bar{\mu}$  and  $\bar{\nu}$  denotes the centered measures associated with  $\mu$  and  $\nu$  and  $K_\pi = \int_{\mathbb{R}^d \times \mathbb{R}^{d'}} xy^T d\pi(x, y)$ . Furthermore, solving this latter problem in  $P$  for a fixed  $\pi$ , (5) reduces to

$$\sup_{\pi \in \Pi(\bar{\mu}, \bar{\nu})} \left\| \int_{\mathbb{R}^d \times \mathbb{R}^{d'}} xy^T d\pi(x, y) \right\|_* , \quad (6)$$

and this is achieved at

$$P_\pi^* = U_\pi \text{Id}_{d'}^{[d, d']} V_\pi^T ,$$

where  $U_\pi \in \mathbb{O}(\mathbb{R}^d)$  and  $V_\pi \in \mathbb{O}(\mathbb{R}^{d'})$  are the left and right orthogonal matrices associated with the Singular Value Decomposition (SVD) of  $K_\pi$ .

*Sketch of proof.* The equivalence between Problems (4) and (5) can be established with straightforward computation. The equivalence between Problems (5) and (6) can then be proved directly using (Alvarez-Melis et al., 2019, lemma 4.2). For the sake of completeness, we offer an alternative proof of this latter equivalence based on Lagrangian analysis.  $\square$

Observe that  $P_\pi^*$  is the projection of  $K_\pi$  on the Stiefel manifold  $\mathbb{V}_{d'}(\mathbb{R}^d)$  since  $\text{tr}(P^T K_\pi)$  is the Frobenius inner-product between  $P$  and  $K_\pi$  and so maximizing the inner-product is equivalent to minimizing the distance between  $K_\pi$  and  $P$  since  $\|P\|_{\mathcal{F}}$  is necessarily equal to  $d'$ . Using Propositions 5 and 6, one can show that  $EW_2$  also coincides with the OT distance between metric measure spaces introduced by Sturm (2006), that reads as,

$$D((\mathcal{X}, d_{\mathcal{X}}, \mu), (\mathcal{Y}, d_{\mathcal{Y}}, \nu)) = \inf_{\mathcal{Z}, \psi, \phi} W_2(\psi_{\#}\mu, \phi_{\#}\nu),$$

where  $(\mathcal{X}, d_{\mathcal{X}}, \mu)$  and  $(\mathcal{Y}, d_{\mathcal{Y}}, \nu)$  are two metric measure spaces as defined in Section 2.2,  $\mathcal{Z}$  is a third Polish space, and  $\psi : \mathcal{X} \rightarrow \mathcal{Z}$  and  $\phi : \mathcal{Y} \rightarrow \mathcal{Z}$  are two isometric mappings. Indeed, we show the following result.

**Proposition 7.** *Let  $\mu \in \mathcal{W}_2(\mathbb{R}^d)$  and  $\nu \in \mathcal{W}_2(\mathbb{R}^{d'})$  with  $d$  not necessarily greater than  $d'$ . Let  $r \geq \max\{d, d'\}$  and let  $\psi \in \text{Isom}_d(\mathbb{R}^r)$ . Then,  $EW_2(\mu, \nu) = EW_2(\psi_{\#}\mu, \nu)$ .*

*Sketch of proof.* The proof of this result consists mainly in observing that transforming the measures with an isometric mapping does not affect the singular values of the cross-covariance matrix  $\int xy^T d\pi(x, y)$ .  $\square$

Note that it is straightforward using Proposition 7 to show that  $EW_2$  defines a pseudometric on  $\bigsqcup_{k \geq 1} \mathcal{W}_2(\mathbb{R}^k)$  that is invariant to isometries for the Euclidean norm, see Appendix C for details. Finally, to complete this section, we emphasize that  $EW_2$  is different of the distance proposed in Cai and Lim (2022), that we call here  $PW_2$  for Projection Wasserstein discrepancy. Between two measures  $\mu \in \mathcal{P}(\mathbb{R}^d)$  and  $\nu \in \mathcal{P}(\mathbb{R}^{d'})$ , and supposing that  $d \geq d'$ , they define

$$PW_2(\mu, \nu) = \inf_{\phi \in \Gamma_d(\mathbb{R}^{d'})} W_2(\phi_{\#}\mu, \nu), \quad (PW_2)$$

where  $\Gamma_d(\mathbb{R}^{d'})$  is the set of affine mappings  $\phi$  from  $\mathbb{R}^d$  to  $\mathbb{R}^{d'}$  such that for all  $x \in \mathbb{R}^d$ ,  $\phi(y) = P^T(x - b)$  where  $b \in \mathbb{R}^d$  and  $P \in \mathbb{V}_{d'}(\mathbb{R}^d)$ . Observe that in that case  $\phi$  is not an isometry since it is not injective. As a result, the term only depending of the marginal  $\mu$  in the development of the square of the distance

will now depends on  $P$  and thus one can show - see Appendix D for details - that Problem ( $PW_2$ ) is equivalent to the following problem

$$\inf_{\pi \in \Pi(\bar{\mu}, \bar{\nu})} \inf_{P \in \mathbb{V}_{d'}(\mathbb{R}^d)} \left( \text{tr}(P^T \Sigma_x P) - 2\text{tr}(P^T K_\pi) \right), \quad (7)$$

where  $\Sigma_x = \int_{\mathbb{R}^d \times \mathbb{R}^d} xx^T d\bar{\mu}(x)$ ,  $K_\pi = \int_{\mathbb{R}^d \times \mathbb{R}^{d'}} xy^T d\pi(x, y)$ . Observe that Problem (7) can be interpreted as a regularization in  $P$  of Problem (5). It can also be interpreted as a  $W_2$  problem between  $\nu$  and a measure  $\mu'$  which has a different second-order moment than  $\mu$ . More details about the difference between  $PW_2$  and  $EW_2$ , especially between Gaussian distributions, can be found in Appendix D.

## 4.2 Link with Gromov-Wasserstein

Before studying  $EW_2$  between Gaussian mixture models, we exhibits here two particular cases where the Problem ( $EW_2$ ) shares close connections with the Gromov-Wasserstein problem ( $GW_p$ ) of order 2 with inner-product costs between the centered measures  $\bar{\mu}$  and  $\bar{\nu}$ , i.e.

$$GW_2^2(\langle \cdot, \cdot \rangle_d, \langle \cdot, \cdot \rangle_{d'}, \bar{\mu}, \bar{\nu}) = \inf_{\pi \in \Pi(\bar{\mu}, \bar{\nu})} \int_{\mathbb{R}^d \times \mathbb{R}^{d'}} \int_{\mathbb{R}^d \times \mathbb{R}^{d'}} (\langle x, x' \rangle_d - \langle y, y' \rangle_{d'})^2 d\pi(x, y) \pi(x', y'). \quad (GW_2\text{-IP})$$

These cases are when one of the two distributions is 1D and when both distributions are Gaussian.

**Univariate case.** When  $\nu$  is a one-dimensional distribution on  $\mathbb{R}$ , the  $EW_2$  problem is equivalent to the  $GW_2$  problem with inner-products as cost functions. Indeed, since  $K_\pi = \int_{\mathbb{R}^d \times \mathbb{R}} xy^T d\pi(x, y)$  is of size  $d \times 1$ , it has a unique singular value  $\lambda_\pi > 0$ , and so one can observe that Problems ( $\mathcal{F}\text{-COV}$ ) and ( $\ast\text{-COV}$ ), i.e.

$$\sup_{\pi \in \Pi(\bar{\mu}, \bar{\nu})} \|K_\pi\|_{\mathcal{F}} \quad \text{and} \quad \sup_{\pi \in \Pi(\bar{\mu}, \bar{\nu})} \|K_\pi\|_{\ast},$$

that are respectively equivalent to Problems ( $GW_2\text{-IP}$ ) and ( $EW_2$ ), can both be rewritten

$$\sup_{\pi \in \Pi(\bar{\mu}, \bar{\nu})} \lambda_\pi,$$

implying thus that the two problems are equivalent. Observe that this allows to recover almost directly the result of (Vayer, 2020, Theorem 4.2.4) that states that the GW problem with inner-product costs between two centered one-dimensional distributions  $\mu \in \mathcal{W}_2(\mathbb{R})$  and  $\nu \in \mathcal{W}_2(\mathbb{R})$  such that  $\mu$  is absolutely continuous with respect of the Lebesgue measure that are respectively of the form  $(\text{Id}_{\mathbb{R}}, T_{\text{GW}}^\uparrow) \# \mu$  and  $(\text{Id}_{\mathbb{R}}, T_{\text{GW}}^\downarrow) \# \mu$  where  $T_{\text{GW}}^\uparrow = F_\nu^{-1} \circ F_\mu^\uparrow$  and  $T_{\text{GW}}^\downarrow = F_\nu^{-1} \circ F_\mu^\downarrow$  with  $F_\nu^{-1}$  being the generalized quantile function associated with  $\nu$  and  $F_\mu^\uparrow$  and  $F_\mu^\downarrow$  are respectively the *cumulative* and *anti-cumulative* distribution function associated with  $\mu$ , i.e for all  $x \in \mathbb{R}$ ,

$$F_\mu^\uparrow(x) = \mu((-\infty, x]) \quad \text{and} \quad F_\mu^\downarrow(x) = \mu([-x, +\infty)).$$

Interestingly, this result doesn't hold anymore in the case the costs functions in the GW problem are the squared Euclidean distances instead of the inner-product. Indeed, in the case where are discrete distributions, Beinert et al. (2022) have exhibited a counter-example. A procedure to exhibit other counter-examples has been proposed in Dumont et al. (2022).

**Gaussian distributions.** When  $\mu = N(m_0, \Sigma_0)$  with  $m_0 \in \mathbb{R}^d$  and  $\Sigma_0 \in \mathbb{S}_{++}^d$  and  $\nu = N(m_1, \Sigma_1)$  with  $m_1 \in \mathbb{R}^{d'}$  and  $\Sigma_1 \in \mathbb{S}_{++}^{d'}$ , one can show - see Appendix C.2 for details - that Problems ( $GW_2\text{-IP}$ ) and ( $EW_2$ ) share some common solutions which are of the ones exhibited in Salmona et al. (2021), i.e. with  $\pi$  of the form  $(\text{Id}_d, T)$ , with  $T$  affine such that for all  $x \in \mathbb{R}^d$ ,

$$T(x) = m_1 + P_1 \left( \tilde{\text{Id}}_{d'} D_1^{\frac{1}{2}} D_0^{(d')^{-\frac{1}{2}}} \right)^{[d', d]} P_0^T (x - m_0),$$

where  $(P_0, D_0)$  and  $(P_1, D_1)$  are the respective diagonalizations of  $\Sigma_0 (= P_0 D_0 P_0^T)$  and  $\Sigma_1 (= P_1 D_1 P_1^T)$  that sort the eigenvalues in non-increasing order and  $\tilde{\text{Id}}_{d'}$  is any matrix of the form  $\text{diag}((\pm 1)_{1 \leq i \leq d'})$ . Note that it is not clear if the two problems are strictly equivalent or only share some solutions, since we are unable to prove that the solutions of the GW problem with inner-product costs exhibited in Salmona et al. (2021) are the only solutions of the problem. Thus, there might exist solutions of Problem ( $GW_2\text{-IP}$ ) which are not of the form above and which are not solution of Problem ( $EW_2$ ).

### 4.3 Embedded Wasserstein distance between GMMs

Similarly to [Delon and Desolneux \(2020\)](#), one can define an OT distance derived from  $EW_2$  when  $\mu$  and  $\nu$  are GMMs by restricting the set of admissible couplings to be themselves GMMs.

**Definition 8.** Let  $\mu \in GMM_K(\mathbb{R}^d)$  and  $\nu \in GMM_L(\mathbb{R}^{d'})$  and suppose that  $d \geq d'$ . We define

$$MEW_2(\mu, \nu) = \inf \left\{ \inf_{\phi \in \text{Isom}_{d'}(\mathbb{R}^d)} MW_2(\mu, \phi_{\#}\nu), \inf_{\psi \in \text{Isom}_d(\mathbb{R}^{d'})} MW_2(\psi_{\#}\mu, \nu) \right\}. \quad (8)$$

As before, one can reformulate this latter problem by observing that the isomorphic mappings for the Euclidean norm are necessarily of the form  $Px + b$  with  $P \in \mathbb{V}_{d'}(\mathbb{R}^d)$  and  $b \in \mathbb{R}^d$ . Similarly to  $EW_2$ , one can show that the infimum in  $\phi$  is always achieved and that  $MEW_2$  satisfies all the properties of a pseudometric on  $\mathcal{GMM}_{\infty}$ . Supposing without any loss of generality that  $d \geq d'$  and using the equivalent discrete formulation (2) of the  $MW_2$  problem, we get that for  $\mu = \sum_k a_k \mu_k$  and  $\nu = \sum_l b_l \nu_l$ , the problem is equivalent to

$$\inf_{P \in \mathbb{V}_{d'}(\mathbb{R}^d)} \inf_{\omega \in \Pi(a, b)} \sum_{k, l} \omega_{k, l} W_2^2(\mu'_k, P_{\#}\nu'_l), \quad (MEW_2)$$

where for any  $k \leq K$  and  $l \leq L$ ,  $\mu'_k$  and  $\nu'_l$  are the Gaussian components respectively associated to the centered GMMs  $\bar{\mu}$  and  $\bar{\nu}$ . Note that  $\mu'_k$  and  $\nu'_l$  are not necessarily themselves centered.

#### 4.3.1 Numerical solver

This time, it is not possible to derive analytically the closed form of the optimal  $P^*$  for Problem ( $MEW_2$ ). However, one can still solve the problem numerically using an alternate minimization scheme. Indeed, Problem ( $MEW_2$ ) is not convex in  $P$  and  $\omega$ , but is convex in  $\omega$  if  $P$  is fixed and is furthermore a simple small-scale discrete OT problem in that case, which motivates the use of an alternating optimization scheme for solving this problem. However, Problem ( $MEW_2$ ) is not convex in  $P$  for a fixed  $\omega$  because the feasible set, i.e. the Stiefel manifold  $\mathbb{V}_{d'}(\mathbb{R}^d)$ , is not convex. For a fixed  $\omega$ , the minimization in  $P$  can be done by projected gradient descent ([Calamai and Moré, 1987](#)), i.e. for a given iterate  $P^{\{i\}}$  and a given  $\omega$ , the next iterate  $P^{\{i+1\}}$  is given by

$$P^{\{i+1\}} = \kappa_{\mathbb{V}_{d'}(\mathbb{R}^d)} \left( P^{\{i\}} - \eta \frac{\partial J_{\omega}(P^{\{i\}})}{\partial P} \right),$$

where  $\kappa_{\mathbb{V}_{d'}(\mathbb{R}^d)}$  is the projection mapping on the Stiefel manifold, where  $\eta > 0$  and where for all matrices  $P$  of size  $d' \times d$ ,  $J_{\omega}(P) = \sum_{k, l} \omega_{k, l} W_2^2(\mu'_k, P_{\#}\nu'_l)$ . As we have seen above in [Proposition 6](#), for all  $P$  of size  $d' \times d$ , the projection  $\kappa_{\mathbb{V}_{d'}(\mathbb{R}^d)}$  can be written

$$\kappa_{\mathbb{V}_{d'}(\mathbb{R}^d)}(P) = U_P \text{Id}_{d'}^{[d, d']} V_P^T,$$

where  $U_P \in \mathbb{O}(\mathbb{R}^d)$  and  $V_P \in \mathbb{O}(\mathbb{R}^{d'})$  are respectively the left and right orthogonal matrices associated with the SVD of  $P$ . In a nutshell, this yields to [Algorithm 1](#).

---

#### Algorithm 1 Mixture embedded Wasserstein solver

---

**Require:**  $\mu = \sum_k a_k \mu_k$ ,  $\nu = \sum_l b_l \nu_l$ ,  $P^{\{0\}} \in \mathbb{V}_{d'}(\mathbb{R}^d)$ ,  $\eta > 0$ .

- 1: **while** not converged **do**
  - 2:    $[C]_{k, l} \leftarrow W_2^2(\mu_k, \nu_l)$  for  $k = 1, \dots, K$ ;  $l = 1, \dots, L$
  - 3:    $\omega^{\{i\}} \leftarrow \text{SOLVE-OT}(a, b, C)$  ▷ Solve a classic OT problem.
  - 4:   **while** not converged **do** ▷ Do projected gradient descent on  $P$ .
  - 5:      $A \leftarrow P^{\{i-1\}} - \eta \partial J_{\omega^{\{i\}}}(P^{\{i-1\}}) / \partial P$
  - 6:      $U, \Sigma, V^T \leftarrow \text{SVD}(A)$
  - 7:      $P^{\{i\}} \leftarrow U \text{Id}_{d'}^{[d, d']} V^T$
  - 8:   **end while**
  - 9: **end while**
  - 10: **return**  $\omega, P$
- 

When  $\mu$  and  $\nu$  are only composed of non-degenerate Gaussian components, one can compute  $\partial J_{\omega}(P) / \partial P$  either by using automatic differentiation ([Baydin et al., 2018](#)) or by using the following technical result, whose proof is postponed to [Appendix B](#).

**Lemma 9.** *Let for any  $k \leq K$ ,  $\mu_k = N(m_{0k}, \Sigma_{0k})$  with  $m_{0k} \in \mathbb{R}^d$  and  $\Sigma_{0k} \in \mathbb{S}_{++}^d$  and for any  $l \leq L$ ,  $\nu_l = N(m_{1l}, \Sigma_{1l})$  with  $m_{1l} \in \mathbb{R}^{d'}$  and  $\Sigma_{1l} \in \mathbb{S}_{++}^{d'}$ . For any  $\omega$  in the  $K \times L$  simplex, let  $J_\omega : \mathbb{R}^{d \times d'} \rightarrow \mathbb{R}$  be the functional defined, for all matrix  $P$  of size  $d \times d'$ , by*

$$J_\omega(P) = \sum_{k,l} \omega_{k,l} W_2^2(\mu_k, P_{\#} \nu_l).$$

Then for any full-rank matrix  $P$  of size  $d \times d'$ , we have

$$\frac{\partial J_\omega(P)}{\partial P} = 2 \sum_{k,l} \omega_{k,l} \left[ P m_{1l} m_{1l}^T - m_{0k} m_{0k}^T - \Sigma_{0k} P \Sigma_{1l}^{-\frac{1}{2}} (\Sigma_{1l}^{-\frac{1}{2}} P^T \Sigma_{0k} P \Sigma_{1l}^{-\frac{1}{2}})^{-\frac{1}{2}} \Sigma_{1l}^{-\frac{1}{2}} \right].$$

**Initialization procedure.** Since the problem is non-convex, the solution to which Algorithm 1 converges strongly depends on the initialization of  $P$ . It is therefore crucial to design a good initialization procedure. To do so, we propose to use the *annealing* scheme introduced by Alvarez-Melis et al. (2019). More precisely, we propose to set the initial  $P$  as the solution of the following iterative procedure. First we solve an entropic-regularized  $W_2$  problem between the two discrete measures  $\mu^\circ = \sum_k a_k \delta_{m_{0k}}$  and  $\nu^\circ = \sum_l b_l \delta_{m_{1l}}$  with a large value of regularization  $\varepsilon_0$  in order to obtain a coupling  $\omega^{\{1\}}$ . Then we set

$$P^{\{1\}} = \kappa_{\mathbb{V}_{d'}(\mathbb{R}^d)} \left( \sum_{k,l} \omega_{k,l}^{\{1\}} m_{0k} m_{1l}^T \right).$$

We then solve another entropic-regularized  $W_2$  problem, this time between  $\mu^\circ$  and  $P_{\#}^{\{1\}} \nu^\circ$ , using a smaller value of regularization  $\varepsilon_1 = \alpha \times \varepsilon_0$  with  $\alpha \in (0, 1)$ . We obtain thus a new coupling  $\omega^{\{2\}}$  and we can then derive  $P^{\{2\}}$  as previously. We repeat this procedure  $N_{it}$  times until the regularization term  $\varepsilon_{N_{it}}$  becomes small enough. This boils down to Algorithm 2.

---

**Algorithm 2** Annealed initialization procedure for mixture embedded Wasserstein

---

**Require:**  $a, b, \{m_{0k}\}_k^K, \{m_{1l}\}_l^L, \varepsilon_0 > 0, \alpha \in (0, 1), P^{\{0\}} = \text{Id}_{d'}^{[d,d']}$

- 1: **for**  $i = 1, \dots, N_{it}$  **do**
  - 2:    $[C]_{k,l} \leftarrow \|m_{0k} - P^{\{i-1\}} m_{1l}\|^2$
  - 3:    $\omega^{\{i\}} \leftarrow \varepsilon\text{-OT}(a, b, C, \varepsilon_{i-1})$  ▷ Solve a regularized OT problem.
  - 4:    $A \leftarrow \sum_{k,l} \omega_{k,l}^{\{i\}} m_{0k} m_{1l}^T$
  - 5:    $U, \Sigma, V^T \leftarrow \text{SVD}(A)$
  - 6:    $P^{\{i\}} = U \text{Id}_{d'}^{[d,d']} V^T$
  - 7:    $\varepsilon_i \leftarrow \alpha \varepsilon_{i-1}$  ▷ Annealing scheme.
  - 8: **end for**
  - 9: **return**  $P$
- 

In practice, we set in all our experiments  $\alpha = 0.95$  and  $\varepsilon_0 = 1$  as in Alvarez-Melis et al. (2019). Furthermore we observed that in most cases, setting  $N_{it} = 10$  was sufficient to obtain a good initialization of  $P$  for Algorithm 1.

### 4.3.2 Transportation plans and transportation maps

Since  $(MEW_2)$  has a continuous equivalent formulation (8), one can derive from any optimal solution  $(\omega^*, P^*)$  of the former, an optimal solution  $(\pi^*, \phi^*)$  of the latter. More precisely, we have on the one hand for all  $y \in \mathbb{R}^{d'}$ ,  $\phi^*(y) = P^* y + b^*$ , where  $b^* = \mathbb{E}_{X \sim \mu}[X] - P^* \mathbb{E}_{Y \sim \nu}[Y]$ , and on the other hand for all  $(x, y) \in \mathbb{R}^d \times \mathbb{R}^{d'}$ ,

$$\pi^*(x, y) = \sum_{k,l} \omega_{k,l}^* p_{\mu_k}(x) \delta_{y = \psi^* \circ T_{W_2}^{k,l}(x)}, \quad (9)$$

where  $T_{W_2}^{k,l}(x)$  is the optimal  $W_2$  transport map between  $\mu'_k$  and  $P_{\#}^* \nu'_l$  and  $\psi^* : \mathbb{R}^d \rightarrow \mathbb{R}^{d'}$  is defined for all  $x \in \mathbb{R}^d$  as  $\psi^*(x) = P^{*T}(x - b^*)$ . As in Delon and Desolneux (2020), it is possible to define a unique assignment of each  $x$  by setting for all  $x \in \mathbb{R}^d$ ,

$$T_{\text{mean}}(x) = \mathbb{E}_{(X,Y) \sim \pi^*}[Y|X=x] = \frac{\sum_{k,l} \omega_{k,l}^* p_{\mu_k}(x) \psi^* \circ T_{W_2}^{k,l}(x)}{\sum_k a_k p_{\mu_k}(x)}.$$

Note that  $T_{\text{mean}}$  is not a Monge map since  $\pi^*$  is not of the form  $(\text{Id}_d, T)_{\#}\mu$ . In particular,  $T_{\text{mean}\#\mu}$  is not equal to  $\nu$  and  $T_{\text{mean}\#\mu}$  is not necessarily the gradient of a convex function. Another possible way to define an assignment proposed by [Delon and Desolneux \(2020\)](#) is to define it as a random assignment for a fixed  $x$ , i.e.

$$T_{\text{rand}}(x) = \psi^* \circ T_{W_2}^{k,l}(x) \quad \text{with probability} \quad p_{k,l}(x) = \frac{\omega_{k,l}^* p_{\mu_k}(x)}{\sum_i a_i p_{\mu_i}(x)}.$$

Hence, when using  $MEW_2$  to obtain an assignment between two sets  $\{x_i\}_i^M$  and  $\{y_j\}_j^N$  of respectively  $M$  and  $N$  vectors of  $\mathbb{R}^d$  and  $\mathbb{R}^{d'}$ , one can compute either  $T_{\text{mean}}(x)$  or  $T_{\text{rand}}(x)$  for each  $x_i$ , and then determine for each  $x_i$  which  $y_j$  is the closest of  $T_{\text{mean}}(x_i)$  - or  $T_{\text{rand}}(x_i)$  - using a nearest-neighbor algorithm ([Fix and Hodges, 1951](#)).

### 4.3.3 Improving the $MGW_2$ method

Inspired by the  $MEW_2$  method presented above, we propose in this section to improve the  $MGW_2$  method by: (i) proposing an annealed scheme similarly to [Algorithm 2](#) in order to reduce the chances of converging to sub-optimal local minima, (ii) designing a transportation plan for  $MGW_2$  similarly to [\(9\)](#).

**Annealing scheme.** Since Problem [\( \$MGW\_2\$ \)](#) is non-convex, we are only guaranteed to converge towards a local minimum when solving it with a classic non-regularized GW solver ([Peyré et al., 2016](#)). Furthermore, the convergence towards a particular minimum depends strongly on the initialization of the coupling  $\omega$ . Since the discrete GW problem in  $MGW_2$  is of very small scale and so not costly in itself, we propose, by analogy with  $MEW_2$ , to use a similar annealing scheme as in [Algorithm 2](#) to reduce the chance of converging to a sub-optimal local minimum. More precisely, this gives the following algorithm.

---

#### Algorithm 3 Annealed mixture Gromov-Wasserstein solver

---

**Require:**  $\mu = \sum_k a_k \mu_k$ ,  $\nu = \sum_l b_l \nu_l$ ,  $\alpha \in (0, 1)$ ,  $\varepsilon_0$ ,  $\omega^{\{0\}} = ab^T$

- 1:  $[C^x]_{k,i} \leftarrow W_2^2(\mu_k, \mu_i)$  for  $k = 1, \dots, K$ ,  $i = 1, \dots, K$
- 2:  $[C^y]_{l,j} \leftarrow W_2^2(\nu_l, \nu_j)$  for  $l = 1, \dots, L$ ,  $j = 1, \dots, L$
- 3: **for**  $n = 1, \dots, N_{it}$  **do**
- 4:      $\omega^{\{n\}} \leftarrow \varepsilon$ -GW( $a, b, C^x, C^y, \varepsilon_{n-1}, \omega^{\{n-1\}}$ ) ▷ Solve a regularized GW problem.
- 5:      $\varepsilon_n \leftarrow \alpha \varepsilon_{n-1}$  ▷ Annealing scheme.
- 6: **end for**
- 7: **return** SOLVE-GW( $a, b, C^x, C^y, \omega^{\{N_{it}\}}$ ) ▷ Solve the non-regularized GW problem.

---

As previously, we set in our experiments  $\alpha = 0.95$  and  $\varepsilon_0 = 1$  as in [Alvarez-Melis et al. \(2019\)](#) and we observed that, in toy cases where we know what the global minimum is, that  $N_{it} = 10$  seemed to be a sufficient number of iterations to prevent the algorithm from converging towards a sub-optimal minimum.

**Designing a transportation plan.** Still by analogy with  $MEW_2$ , one can design a transportation plan for  $MGW_2$  by defining a matrix  $P_{MGW_2} \in \mathbb{V}_{d'}(\mathbb{R}^d)$  and a vector  $b_{MGW_2} \in \mathbb{R}^d$ , and then replacing  $T_{W_2} \circ \psi^*$  in [\(9\)](#) by  $T_{W_2} \circ \psi_{MGW_2}$ , where for all  $x \in \mathbb{R}^d$ ,  $\psi_{MGW_2}(x) = P_{MGW_2}^T(x - b_{MGW_2})$ . Given two GMMs  $\mu = \sum_k a_k \mu_k$  and  $\nu = \sum_l b_l \nu_l$  respectively in  $GMM_K(\mathbb{R}^d)$  and  $GMM_L(\mathbb{R}^{d'})$  and given the optimal discrete plan  $\omega^*$  solution of Problem [\( \$MGW\_2\$ \)](#), one can define the matrix  $P_{MGW_2}$  as the solution of the following problem

$$\inf_{P \in \mathbb{V}_{d'}(\mathbb{R}^d)} \sum_{k,l} \omega_{k,l}^* W_2^2(\mu'_k, P_{\#}\nu'_l), \quad (10)$$

where  $\mu'_k$  and  $\nu'_l$  are the Gaussian component of the centered GMMs  $\bar{\mu}$  and  $\bar{\nu}$ , then we can set  $b_{MGW_2} = \mathbb{E}_{X \sim \mu}[X] - P_{MGW_2} \mathbb{E}_{Y \sim \nu}[Y]$ . As above, this problem can be solved numerically by performing a projected gradient descent on  $P$ , using either automatic differentiation or [Lemma 9](#). This is also a non-convex optimization problem since  $\mathbb{V}_{d'}(\mathbb{R}^d)$  is non-convex and so the solution given by the projected gradient descent depends on the initialization. We propose thus to initialize with the projection on the Stiefel manifold of the discrete cross-covariance matrix between the means of the Gaussian components, i.e.

$$P_{MGW_2}^{\{0\}} = \kappa_{\mathbb{V}_{d'}(\mathbb{R}^d)} \left( \sum_{k,l} \omega_{k,l}^* m_{0k} m_{1l}^T \right).$$

Finally, using  $P_{MGW_2}$  one can define a continuous plan  $\pi_{MGW_2}$  associated with the discrete optimal plan  $\omega^*$  solution of the  $MGW_2$  problem similarly to (9). We can therefore use  $MGW_2$  to transport distributions, using as previously either  $T_{\text{mean}}$  or  $T_{\text{rand}}$ . We can also, as for  $MEW_2$ , use  $MGW_2$  to obtain an assignment between two sets of points.

## 5 Experiments

In what follows, we use  $MGW_2$  and  $MEW_2$  to solve Gromov-Wasserstein related tasks on various datasets. More precisely, we apply first the two methods on simple toy low-dimensional GMMs. Then, we show that both methods can be used to solve relatively efficiently GW related tasks on real datasets in large scale settings involving sometimes several tens of thousands of points. We apply thus our methods to two shape matching problems, then to color transfer on hyperspectral images. In all our experiments, we use the numerical solvers provided by the Python Optimal Transport (POT) package<sup>5</sup> (Flamary et al., 2021) that implements solvers for the non-regularized and regularized classic OT and GW problems.

### 5.1 Low dimensional GMMs

In Figure 4, we use again the example of Figure 3 and we derive an optimal transport plan for the  $MGW_2$  problem as described in Section 4.3.3. We also show the plan obtained by solving the  $EW_2$  problem. One can see that with both solutions, the global structure of the distribution is preserved in the sense that points that are close to each other but in two different Gaussian components have been sent to points that are also close to each other but in different Gaussian components.

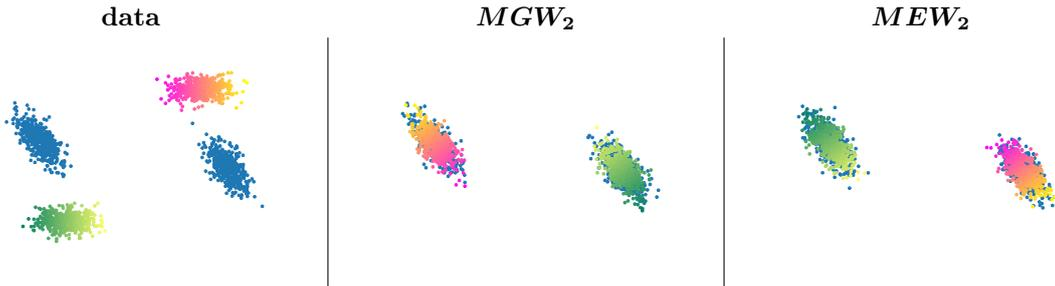


Figure 4: Left: two discrete distributions  $\hat{\mu}$  (in gradient of colors) and  $\hat{\nu}$  (in blue) that have been drawn from two GMMs. The colors have been added to  $\hat{\mu}$  in order to visualize the couplings between  $\hat{\mu}$  and  $\hat{\nu}$ . Middle: transport of  $\hat{\mu}$  obtained by solving the  $MGW_2$  problem, then deriving  $P_{MGW_2} \in \mathbb{V}_2(\mathbb{R}^2)$  by solving Problem (10). Right: transport of  $\hat{\mu}$  obtained by solving the  $MEW_2$  problem.

### 5.2 Application to shape matching

We apply now our methods on two shape matching problems. The first one consists in reproducing an experiment originally conducted in Rustamov et al. (2013) and presented in Solomon et al. (2016) with the use of entropic-regularized GW, that aims to recover the cyclical nature of a horse’s gallop. The second problem consists in drawing correspondences between human shaped meshes from the SHREC’19 dataset<sup>6</sup> (Melzi et al., 2019) in the sense that we aim to assign a hand with a hand, a foot with a foot, etc. Note that the goal of these experiments is not to obtain state-of-the-art results in shape-matching, but rather to demonstrate the usability of our methods in moderate-to-large scale settings.

**Galoping horse sequence.** Here we reproduce the experiment of the galloping horse, that has been originally conducted in Rustamov et al. (2013) and presented in Solomon et al. (2016) with the use of entropic-regularized GW. The goal of this experiment is to compute a matrix of pairwise distances between the 45 meshes representing a galloping horse, and then to conduct a Multi-Dimensional Scaling (MDS) (Borg and Groenen, 2005) - which roughly can be thought as a generalization of PCA - of the pairwise distances in order to plot each mesh as a 2-dimensional point. The results can be found in Figure 5. As in Solomon et al. (2016), the cyclical nature of the motion is recovered in both cases when  $MGW_2$  or  $MEW_2$

<sup>5</sup>The package is accessible here: <https://pythonot.github.io/>.

<sup>6</sup>The SHREC’19 dataset is accessible here: <http://profs.scienze.univr.it/marin/shrec19/>

is used to compare the meshes. Each mesh is composed of approximately 9000 vertices and the average time to compute one distance when using the POT implementation of the entropic-regularized GW solver is around 30 minutes which makes the computation of the full pairwise distance matrix impractical, as mentioned in Solomon et al. (2016). In contrast, when using our methods with GMMs with  $K = 20$  components, it took us only approximately 10 minutes to compute the full distance matrix using  $MGW_2$ , and around one hour using  $MEW_2$ , these times including the fitting of all the GMMs.

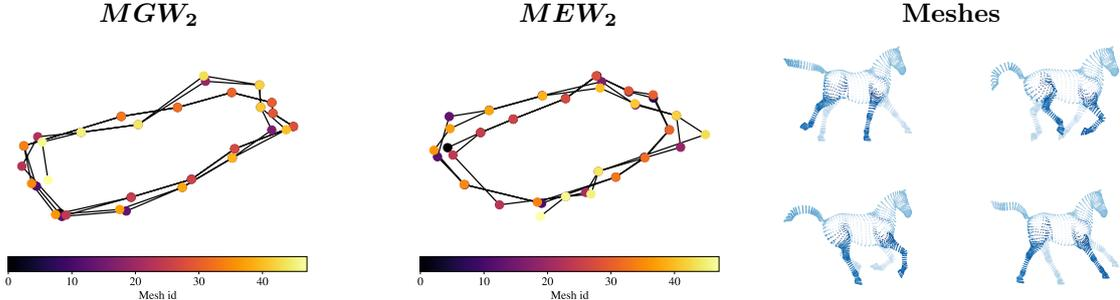


Figure 5: MDS on the galloping horse animation using the  $MGW_2$  distance (left), and the  $MEW_2$  distance (middle). Each point corresponds to a given mesh and the meshes are colored in function of their number in the sequence. The computation of both distances have been done by first fitting GMMs with 20 components on each mesh independently.

**Local minima.** To highlight the importance of using an annealing scheme when deriving  $MGW_2$  or  $MEW_2$ , we have reconducted the previous experiment but this time without the annealing schemes described in Algorithm 3 and Algorithm 2. In Figure 6, we plot the evolutions of the values of  $MGW_2^2$  and  $MEW_2^2$  between one given fixed mesh and all the others. In both cases, the annealing scheme seems to be useful to prevent the solver to converge towards sub-optimal minima. However, if the  $MGW_2$  solver seems to often converge to the same optimum regardless the use of the annealing scheme, this is not the case of  $MEW_2$  which, without the annealing initialization procedure (Algorithm 2), converges most of the time to a sub-optimal minimum, so much that the periodical aspect doesn't even appear in that case. Beside to highlight the importance of using a good initialization, this experiment also emphasizes the fact that when solving a GW problem with classic non-regularized or entropic solvers from Peyré et al. (2016), we are not at all guaranteed to converge towards a global minimum and, more critically, we have in general no ways to know if the solution we converged to is actually optimal or sub-optimal.

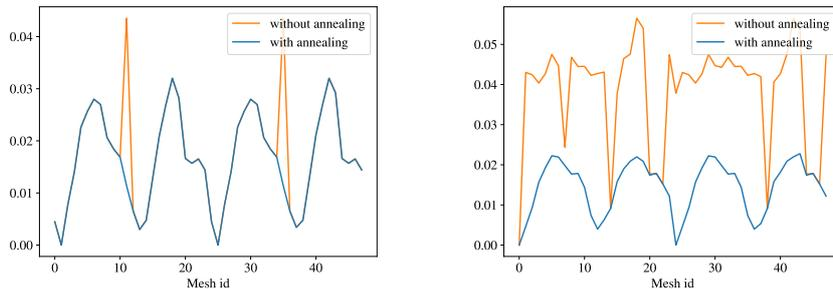


Figure 6: Left: Evolution of  $MGW_2^2$  between the second mesh and all the others, using an annealing scheme (Algorithm 3) in blue, and without the annealing scheme in orange. Right: Evolution of  $MEW_2^2$  between the first mesh and all the others, with the annealing initialization procedure (Algorithm 2) in blue, and without in orange. The computation of both distances have been done by first fitting GMMs with 20 components on each mesh independently.

**Matching human shaped meshes.** To demonstrate the usability of our methods in larger scale settings, we use the SHREC'19 dataset that contains human shaped meshes that can sometimes be composed of more than 300000 vertices. Our goal is to draw correspondences between the shapes using

only the information of the vertices (the dataset also includes edges). To do so, we first fit independently GMMs with 20 components on each mesh and we derive directly couplings at the scale of the Gaussian components that represents the different parts of the bodies. In such large scale settings, the main bottleneck of the methods in terms of computational time is clearly the fitting of the GMMs that can take at worst 2 minutes for the meshes composed of the highest number of vertices. The results are displayed on Figure 7. Observe that in most cases, both methods seem to be able to match correctly the colored parts. Yet in the last row,  $MEW_2$  matches a leg at the left in red to an arm at the right. This probably implies that the method has been trapped in a local minimum despite the annealing initialization procedure. Finally, note that we presented here cases where the methods performed relatively well, but there are cases where  $MGW_2$  or  $MEW_2$  fail to find correct correspondences and exhibit behaviors similar to  $MEW_2$  in the last row, which suggests that the methods converge sometimes to sub-optimal minima despite the annealing schemes.

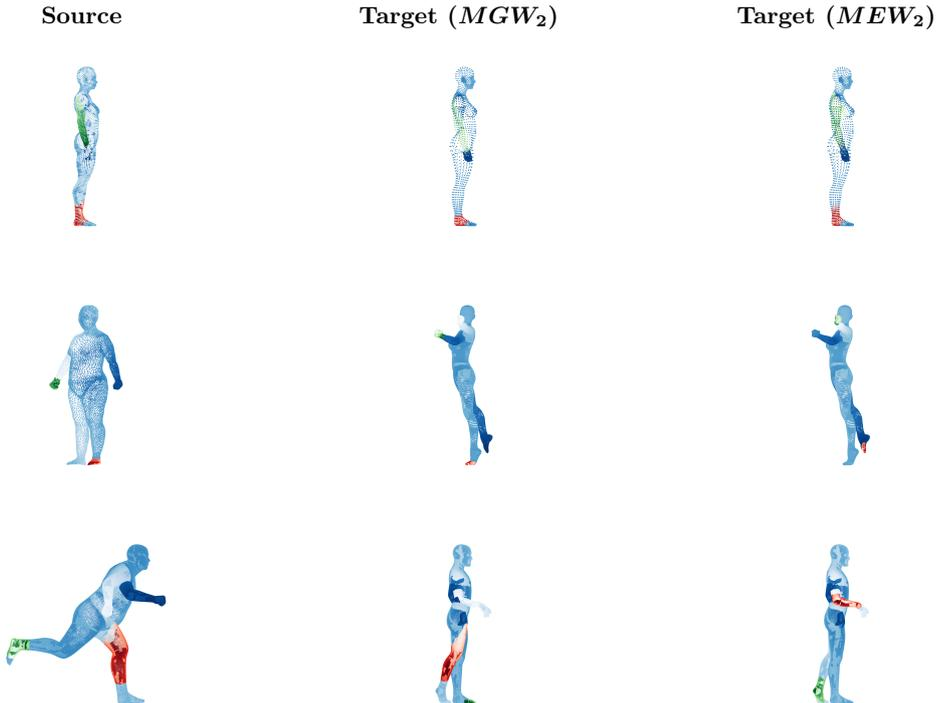


Figure 7: Shape matching between human-shaped meshes using  $MGW_2$  (middle) and  $MEW_2$  (right). Each shape on the left column is matched with the shapes on the same row. GMMs with 20 components have been fitted independently on each shape and the points colored in green and red correspond to Gaussian components that are matched together when solving  $MGW_2$  or  $MEW_2$ . From left to right and top to bottom, the meshes are composed respectively of 84912, 30300, 75000, 273624, 360678, and 360357 vertices.

### 5.3 Application to hyperspectral image color transfer

The goal here is to reproduce the experiment of color transfer conducted in [Delon and Desolneux \(2020\)](#), but this time using a hyperspectral image, i.e an image with more than 3 color channels. More precisely, we aim to create an RGB image from an hyperspectral image  $u$  using the colors of another RGB image  $v$ . To do so, we consider images as empirical distributions in the color spaces and we solve a Gromov-Wasserstein problem between the distributions  $\hat{\mu} = \frac{1}{M} \sum_k \delta_{u_k}$  and  $\hat{\nu} = \frac{1}{N} \sum_l \delta_{v_l}$ , where  $M$  and  $N$  are the number of pixels in respectively the hyperspectral image and the RGB image we use as color palette, and  $\{u_k\}_k^M$  and  $\{v_l\}_l^N$  are the values at each pixel, i.e for here all  $l$ ,  $v_l \in \mathbb{R}^3$  and for all  $k$ ,  $u_k \in \mathbb{R}^d$  with  $d > 3$ . We thus fit two GMMs  $\mu$  and  $\nu$  and respectively  $\hat{\mu}$  and  $\hat{\nu}$  and we use  $MGW_2$  or  $MEW_2$  to derive a mapping  $T_{\text{mean}} : \mathbb{R}^d \rightarrow \mathbb{R}^3$ , as described in Section 4.3.2. We apply this process to a hyperspectral image of  $512 \times 512$  pixels with 15 channels that are displayed in Figure 8 top left. We use as color palettes two paintings by Gauguin and Renoir, displayed in Figure 8 top right, that are respectively *Manhana no atua*

(top) and *Le déjeuner des canotiers* (bottom). These two images are composed of  $1024 \times 768$  pixels. The resulting images  $T_{\text{mean}}(u)$  are displayed in Figure 8 bottom (Gauguin at the left and Renoir at the right). For this experiment, we observed that setting the number of Gaussian components to  $K = 15$  was a good compromise between capturing the complexity of the color distributions and obtaining a relatively regular mapping  $T_{\text{mean}}$ . This experiment shows that  $MGW_2$  and  $MEW_2$  can be used in large scale settings: observe indeed that the color distributions  $\hat{\mu}$  and  $\hat{\nu}$  are composed respectively of approximately 300000 and 800000 points, which makes the problem intractable with entropic-GW solvers such as [Peyré et al. \(2016\)](#) or [Solomon et al. \(2016\)](#). Furthermore, note also that  $d = 15$  is already a relatively high dimension in the context of Gromov-Wasserstein. In term of computation time, the fitting of the GMM for the hyperspectral image takes approximately 15 minutes against one minute for the GMM for the RGB image. The projected gradient descent becomes rather slow in that setting, which makes it preferable to few updates of  $P$  at each step of Algorithm 1 for the computation of  $MEW_2$ . Finally, for both methods, it takes around 20 minutes to compute the whole RGB image  $T_{\text{mean}}(u)$ .

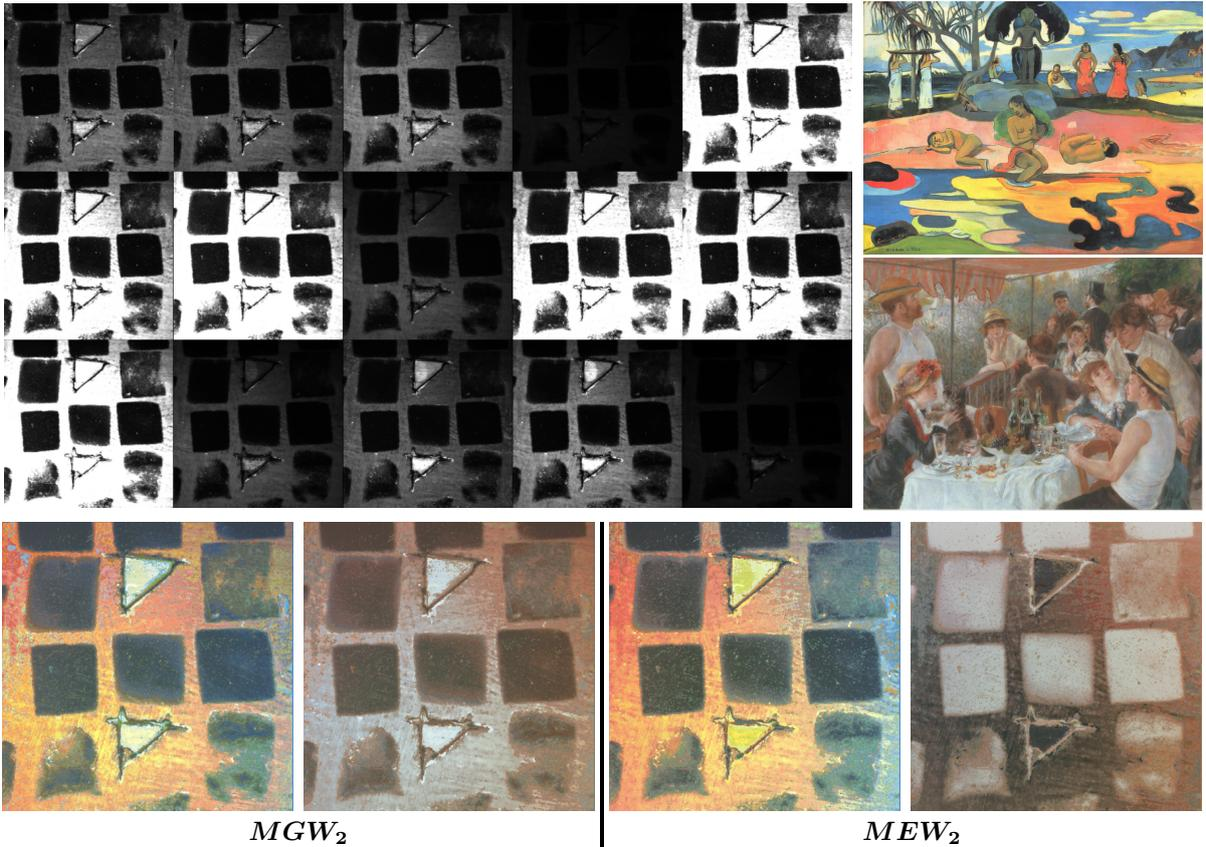


Figure 8: Color transfers between a hyperspectral image with 15 channels (top left) and two paintings by Gauguin and Renoir (top right, top to bottom). Bottom line: the obtained RGB images using  $MGW_2$  and  $MEW_2$ . For this experiment, we used GMMs with 15 components. Image taken by Francesca Ramacciotti (Alma Mater Studiorum - University of Bologna) and Laure Cazals (supported by the European Commission in the framework of the GoGreen project (GA no. 101060768)).

## 6 Discussion

In this chapter, we have introduced two new OT distances on the set of Gaussian mixture models,  $MGW_2$  and  $MEW_2$ , and we have shown that they both can be used to solve relatively efficiently Gromov-Wasserstein related problems on Euclidean spaces, especially in moderate-to-large scale settings involving several tens of thousands of points. These OT distances are also by design particularly suited to settings where there already exists a kind of clustering structure in the data. This being said, if  $MEW_2$  remains an efficient alternative to the entropic GW solvers proposed by [Peyré et al. \(2016\)](#) and [Solomon et al.](#)

(2016), we observed that the method was actually slower and perhaps harder to tune than  $MGW_2$  for roughly the same quality of results, and so we believe that  $MGW_2$  is a better choice in practice. This latter distance is part of the families of Gromov-Wasserstein type OT distances that reduce the size of the GW problem by quantization (Chowdhury et al., 2021) or by clustering (Xu et al., 2019; Blumberg et al., 2020). To the best of our knowledge, however, no such methods specific to the Euclidean case had already been proposed in the literature.  $MGW_2$  could also be easily extended to other type of mixtures as soon as we have an identifiability property between the mixtures and the probability distributions on the space of the distributions that compose the mixtures. If in the Euclidean setting GMMs seem to be versatile enough to represent large classes of concrete and applied problems, an interesting extension on our work could be to consider mixture of distributions on non-Euclidean spaces.

Computationally speaking, the main bottleneck of the method probably comes from the fitting of the GMMs with the Expectation-Maximization (EM) algorithm (Dempster et al., 1977) which can become relatively costly in large scale settings or as soon as the dimension increases. If the EM algorithm remains invariably the classical algorithm for learning GMMs, some recent approaches (Hosseini and Sra, 2020; Sembach et al., 2022; Pasande et al., 2022) have proposed alternative algorithms that seems to outperform it. These approaches are based on Riemannian stochastic optimization, leveraging the rich Riemannian structure of the set of positive definite matrices. Another interesting alternative that has been shown to outperform the EM algorithm has been proposed by (Kolouri et al., 2018) and is based on the minimization of the sliced-Wasserstein distance. Integrating this in our method could result thus in an approach fully-based on optimal transport.

Another possible limitation of our work lies in the fact that the  $MGW_2$  solver converges sometimes to sub-optimal local minima. If the annealed procedure introduced in Section 4.3.3 seems to reduce this issue, we generally have no guarantee that the solution we have converged to is optimal. This is not specific to our method and comes from the gradient descent structure of the classic GW solvers. Still, when solving the GW problem between GMMs rather than solving it directly between the points, it is likely that we increase the probability of converging towards a sub-optimal local minimum because we inevitably introduce symmetries by simplifying the problem and so we probably increase in the mean time the number of local minima in the GW objective. In the Euclidean setting, the recent work of Ryner et al. (2023) proposes an algorithm for solving the GW problem that is guaranteed to converge toward a global minimum, leveraging the low-rank structure of the cost matrices when the cost functions are the squared Euclidean distances. A future perspective of work could be therefore to study if a similar idea could be applied for solving the  $MGW_2$  problem.

## References

- Altschuler, J., Bach, F., Rudi, A., and Niles-Weed, J. (2019). Massively scalable Sinkhorn distances via the Nyström method. *Advances in neural information processing systems*, 32.
- Altschuler, J., Bach, F., Rudi, A., and Weed, J. (2018). Approximating the quadratic transportation metric in near-linear time. *arXiv preprint arXiv:1810.10046*.
- Alvarez-Melis, D. and Jaakkola, T. (2018). Gromov–Wasserstein alignment of word embedding spaces. In *Proceedings of the 2018 Conference on Empirical Methods in Natural Language Processing*, pages 1881–1890.
- Alvarez-Melis, D., Jegelka, S., and Jaakkola, T. S. (2019). Towards optimal transport with global invariances. In *The 22nd International Conference on Artificial Intelligence and Statistics*, pages 1870–1879. PMLR.
- Arjovsky, M., Chintala, S., and Bottou, L. (2017). Wasserstein generative adversarial networks. In *International Conference on Machine Learning*, pages 214–223. PMLR.
- Baker, J. (1971). Isometries in normed spaces. *The American Mathematical Monthly*, 78(6):655–658.
- Baydin, A. G., Pearlmutter, B. A., Radul, A. A., and Siskind, J. M. (2018). Automatic differentiation in machine learning: a survey. *Journal of Machine Learning Research*, 18:1–43.
- Beinert, R., Heiss, C., and Steidl, G. (2022). On assignment problems related to Gromov–Wasserstein distances on the real line. *arXiv preprint arXiv:2205.09006*.

- Blumberg, A. J., Carriere, M., Mandell, M. A., Rabadan, R., and Villar, S. (2020). MREC: a fast and versatile framework for aligning and matching point clouds with applications to single cell molecular data. *stat*, 1050:20.
- Bolley, F. (2008). Separability and completeness for the Wasserstein distance. *Lecture Notes in Mathematics-Springer-Verlag*, 1934:371.
- Borg, I. and Groenen, P. J. (2005). *Modern multidimensional scaling: theory and applications*. Springer Science & Business Media.
- Brogat-Motte, L., Flamary, R., Brouard, C., Rousu, J., and d’Alché Buc, F. (2022). Learning to predict graphs with fused Gromov–Wasserstein barycenters. In *International Conference on Machine Learning*, pages 2321–2335. PMLR.
- Bunne, C., Alvarez-Melis, D., Krause, A., and Jegelka, S. (2019). Learning generative models across incomparable spaces. In *International conference on machine learning*, pages 851–861. PMLR.
- Cai, Y. and Lim, L.-H. (2022). Distances between probability distributions of different dimensions. *IEEE Transactions on Information Theory*, 68(6):4020–4031.
- Calamai, P. H. and Moré, J. J. (1987). Projected gradient methods for linearly constrained problems. *Mathematical programming*, 39(1):93–116.
- Chen, Y., Georgiou, T. T., and Tannenbaum, A. (2018). Optimal transport for Gaussian mixture models. *IEEE Access*, 7:6269–6278.
- Chowdhury, S. and Mémoli, F. (2019). The Gromov–Wasserstein distance between networks and stable network invariants. *Information and Inference: A Journal of the IMA*, 8(4):757–787.
- Chowdhury, S., Miller, D., and Needham, T. (2021). Quantized Gromov–Wasserstein. In *Machine Learning and Knowledge Discovery in Databases. Research Track: European Conference, ECML PKDD 2021, Bilbao, Spain, September 13–17, 2021, Proceedings, Part III 21*, pages 811–827. Springer.
- Cohen, S. and Guibasm, L. (1999). The Earth mover’s distance under transformation sets. In *Proceedings of the Seventh IEEE International Conference on Computer Vision*, volume 2, pages 1076–1083. IEEE.
- Courant, R. (1920). Über die eigenwerte bei den differentialgleichungen der mathematischen physik. *Mathematische Zeitschrift*, 7(1-4):1–57.
- Courty, N., Flamary, R., and Ducoffe, M. (2018). Learning Wasserstein embeddings. In *ICLR 2018-6th International Conference on Learning Representations*, pages 1–13.
- Courty, N., Flamary, R., Tuia, D., and Rakotomamonjy, A. (2016). Optimal transport for domain adaptation. In *Transactions on Pattern Analysis and Machine Intelligence*, volume 39, pages 1853–1865. IEEE.
- Cuturi, M. (2013). Sinkhorn distances: lightspeed computation of optimal transport. *Advances in neural information processing systems*, 26.
- Delon, J. and Desolneux, A. (2020). A Wasserstein-type distance in the space of Gaussian mixture models. *SIAM Journal on Imaging Sciences*, 13(2):936–970.
- Delon, J., Gozlan, N., and Saint-Dizier, A. (2022). Generalized Wasserstein barycenters between probability measures living on different subspaces. *Annals of Applied Probability*.
- Dempster, A. P., Laird, N. M., and Rubin, D. B. (1977). Maximum likelihood from incomplete data via the EM algorithm. *Journal of the royal statistical society: series B (methodological)*, 39(1):1–22.
- Dumont, T., Lacombe, T., and Vialard, F.-X. (2022). On the existence of Monge maps for the Gromov–Wasserstein problem.
- Fischer, E. (1905). Über quadratische formen mit reellen koeffizienten. *Monatshefte für Mathematik und Physik*, 16:234–249.
- Fix, E. and Hodges, J. (1951). Discriminatory analysis: nonparametric discrimination: consistency properties. report. 4. *T. USAF School of Aviation Medicine*.

- Flamary, R., Courty, N., Gramfort, A., Alaya, M. Z., Boisbunon, A., Chambon, S., Chapel, L., Corenflos, A., Fatras, K., Fournier, N., et al. (2021). POT: Python Optimal Transport. *The Journal of Machine Learning Research*, 22(1):3571–3578.
- Forrow, A., Hütter, J.-C., Nitzan, M., Rigollet, P., Schiebinger, G., and Weed, J. (2019). Statistical optimal transport via factored couplings. In *The 22nd International Conference on Artificial Intelligence and Statistics*, pages 2454–2465. PMLR.
- Genevay, A., Peyre, G., and Cuturi, M. (2018). Learning generative models with Sinkhorn divergences. In *International Conference on Artificial Intelligence and Statistics*, volume 84, pages 1608–1617. PMLR.
- Givens, C. R., Shortt, R. M., et al. (1984). A class of Wasserstein metrics for probability distributions. In *Michigan Mathematical Journal*, volume 31, pages 231–240. the University of Michigan.
- Hosseini, R. and Sra, S. (2020). An alternative to EM for Gaussian mixture models: batch and stochastic Riemannian optimization. *Mathematical programming*, 181(1):187–223.
- James, I. M. (1976). *The topology of Stiefel manifolds*, volume 24. Cambridge University Press.
- Kloeckner, B. (2010). A geometric study of Wasserstein spaces: Euclidean spaces. *Annali della Scuola Normale Superiore di Pisa-Classe di Scienze*, 9(2):297–323.
- Kolouri, S., Nadjahi, K., Simsekli, U., Badeau, R., and Rohde, G. (2019). Generalized sliced Wasserstein distances. *Advances in neural information processing systems*, 32.
- Kolouri, S., Rohde, G. K., and Hoffmann, H. (2018). Sliced Wasserstein distance for learning Gaussian mixture models. In *Proceedings of the IEEE Conference on Computer Vision and Pattern Recognition*, pages 3427–3436.
- Lambert, M., Chewi, S., Bach, F., Bonnabel, S., and Rigollet, P. (2022). Variational inference via Wasserstein gradient flows. In *Advances in Neural Information Processing Systems*.
- Leclaire, A., Delon, J., and Desolneux, A. (2022). Optimal transport between GMMs for texture synthesis.
- Luzi, L., Marrero, C. O., Wynar, N., Baraniuk, R. G., and Henry, M. J. (2023). Evaluating generative networks using Gaussian mixtures of image features. In *Proceedings of the IEEE/CVF Winter Conference on Applications of Computer Vision*, pages 279–288.
- Magnus, J. R. and Neudecker, H. (2019). *Matrix differential calculus with applications in statistics and econometrics*. John Wiley & Sons.
- Mazur, S. and Ulam, S. (1932). Sur les transformations isométriques d’espaces vectoriels normés. *CR Acad. Sci. Paris*, 194(946-948):116.
- Melzi, S., Marin, R., Rodolà, E., Castellani, U., Ren, J., Poulencard, A., Wonka, P., and Ovsjanikov, M. (2019). SHREC 2019: matching humans with different connectivity. In *Eurographics Workshop on 3D Object Retrieval*, volume 7, page 3. The Eurographics Association.
- Mémoli, F. (2009). Spectral Gromov–Wasserstein distances for shape matching. In *2009 IEEE 12th International Conference on Computer Vision Workshops, ICCV Workshops*, pages 256–263. IEEE.
- Mémoli, F. (2011). Gromov–Wasserstein distances and the metric approach to object matching. In *Foundations of Computational Mathematics*, volume 11, pages 417–487. Springer.
- Pasande, M., Hosseini, R., and Araabi, B. N. (2022). Stochastic first-order learning for large-scale flexibly tied Gaussian mixture model. *arXiv preprint arXiv:2212.05402*.
- Pedregosa, F., Varoquaux, G., Gramfort, A., Michel, V., Thirion, B., Grisel, O., Blondel, M., Prettenhofer, P., Weiss, R., Dubourg, V., et al. (2011). Scikit-learn: machine learning in python. *the Journal of machine Learning research*, 12:2825–2830.
- Pele, O. and Taskar, B. (2013). The tangent Earth mover’s distance. In *Geometric Science of Information: First International Conference, GSI 2013, Paris, France, August 28-30, 2013. Proceedings*, pages 397–404. Springer.

- Petersen, K. B., Pedersen, M. S., et al. (2008). The matrix cookbook. *Technical University of Denmark*, 7(15):510.
- Peyré, G., Cuturi, M., and Solomon, J. (2016). Gromov–Wasserstein averaging of kernel and distance matrices. In *International conference on machine learning*, pages 2664–2672. PMLR.
- Rabin, J., Ferradans, S., and Papadakis, N. (2014). Adaptive color transfer with relaxed optimal transport. In *2014 IEEE international conference on image processing (ICIP)*, pages 4852–4856. IEEE.
- Rabin, J., Peyré, G., Delon, J., and Bernot, M. (2012). Wasserstein barycenter and its application to texture mixing. In *Scale Space and Variational Methods in Computer Vision: Third International Conference, SSVN 2011, Ein-Gedi, Israel, May 29–June 2, 2011, Revised Selected Papers 3*, pages 435–446. Springer.
- Rustamov, R. M., Ovsjanikov, M., Azencot, O., Ben-Chen, M., Chazal, F., and Guibas, L. (2013). Map-based exploration of intrinsic shape differences and variability. *ACM Transactions on Graphics (TOG)*, 32(4):1–12.
- Ryner, M., Kronqvist, J., and Karlsson, J. (2023). Globally solving the Gromov–Wasserstein problem for point clouds in low dimensional euclidean spaces. *arXiv preprint arXiv:2307.09057*.
- Salmona, A., Delon, J., and Desolneux, A. (2021). Gromov–Wasserstein distances between Gaussian distributions. *Journal of Applied Probability*, 59(4).
- Scetbon, M. and Cuturi, M. (2020). Linear time Sinkhorn divergences using positive features. *Advances in Neural Information Processing Systems*, 33:13468–13480.
- Scetbon, M., Cuturi, M., and Peyré, G. (2021). Low-rank Sinkhorn factorization. In *International Conference on Machine Learning*, pages 9344–9354. PMLR.
- Scetbon, M., Peyré, G., and Cuturi, M. (2022). Linear-time Gromov–Wasserstein distances using low rank couplings and costs. In *International Conference on Machine Learning*, pages 19347–19365. PMLR.
- Seguy, V., Damodaran, B. B., Flamary, R., Courty, N., Rolet, A., and Blondel, M. (2017). Large-scale optimal transport and mapping estimation. *arXiv preprint arXiv:1711.02283*.
- Sembach, L., Burgard, J. P., and Schulz, V. (2022). A Riemannian Newton trust-region method for fitting Gaussian mixture models. *Statistics and Computing*, 32(1):8.
- Sinkhorn, R. and Knopp, P. (1967). Concerning nonnegative matrices and doubly stochastic matrices. *Pacific Journal of Mathematics*, 21(2):343–348.
- Solomon, J., De Goes, F., Peyré, G., Cuturi, M., Butscher, A., Nguyen, A., Du, T., and Guibas, L. (2015). Convolutional Wasserstein distances: efficient optimal transportation on geometric domains. *ACM Transactions on Graphics (ToG)*, 34(4):1–11.
- Solomon, J., Peyré, G., Kim, V. G., and Sra, S. (2016). Entropic metric alignment for correspondence problems. *ACM Transactions on Graphics (ToG)*, 35(4):1–13.
- Sturm, K.-T. (2006). On the geometry of metric measure spaces. i. *Acta Math*, 196:65–131.
- Sturm, K.-T. (2012). The space of spaces: curvature bounds and gradient flows on the space of metric measure spaces. *arXiv preprint arXiv:1208.0434*.
- Takatsu, A. (2010). On Wasserstein geometry of Gaussian measures. In *Probabilistic approach to geometry*, pages 463–472. Mathematical Society of Japan.
- Tolstikhin, I., Bousquet, O., Gelly, S., and Schölkopf, B. (2018). Wasserstein auto-encoders. In *6th International Conference on Learning Representations (ICLR 2018)*. OpenReview. net.
- Vayer, T. (2020). *A contribution to Optimal Transport on incomparable spaces*. PhD thesis, Lorient.
- Vayer, T., Courty, N., Tavenard, R., and Flamary, R. (2019a). Optimal transport for structured data with application on graphs. In *International Conference on Machine Learning*, pages 6275–6284. PMLR.

- Vayer, T., Flamary, R., Courty, N., Tavenard, R., and Chapel, L. (2019b). Sliced Gromov–Wasserstein. *Advances in Neural Information Processing Systems*, 32.
- Villani, C. (2008). *Optimal transport: old and new*, volume 338. Springer Science & Business Media.
- Xu, H., Luo, D., and Carin, L. (2019). Scalable Gromov–Wasserstein learning for graph partitioning and matching. *Advances in neural information processing systems*, 32.
- Xu, H., Wang, W., Liu, W., and Carin, L. (2018). Distilled Wasserstein learning for word embedding and topic modeling. *Advances in Neural Information Processing Systems*, 31.
- Yakowitz, S. J. and Spragins, J. D. (1968). On the identifiability of finite mixtures. *The Annals of Mathematical Statistics*, 39(1):209–214.
- Zhang, Q. and Chen, J. (2020). A unified framework for Gaussian mixture reduction with composite transportation distance. *arXiv preprint arXiv:2002.08410*.

## Organization of the supplementary

The supplementary is organized as follows. First, in Appendix A, we show five technical results that will be used throughout the proofs of the paper. In Appendix B, we give the full proofs of the technical results of the paper. In Appendix C, we give more details on the metric properties of  $EW_2$  and on the behavior of this latter distance on Gaussian distributions. Finally, in Appendix D, we give more details on the OT distance introduced by Cai and Lim (2022) that we call here projection Wasserstein discrepancy.

## A Technical lemmas

Before turning to the proofs of the theoretical results, we state here five technical lemmas that will be used throughout the proofs of the results of the paper.

### A.1 A property of couplings between measures living in different dimensions

First we start by recalling the following result by Delon et al. (2022).

**Lemma A1 (Delon et al., 2022).** *Let  $\mu \in \mathcal{W}_2(\mathbb{R}^d)$  and  $\nu \in \mathcal{W}_2(\mathbb{R}^{d'})$  with  $d$  not necessarily greater than  $d'$ , and let  $T : \mathbb{R}^{d'} \rightarrow \mathbb{R}^d$  be a measurable map. Then  $\pi' \in \Pi(\mu, T_{\#}\nu)$  if and only if there is some  $\pi \in \Pi(\mu, \nu)$  such that  $\pi' = (\text{Id}_d, T)_{\#}\pi$ . In particular, if there exist  $a, b \geq 0$  such that  $\|T(y)\| \leq a + b\|y\|$  for all  $y \in \mathbb{R}^{d'}$ , then*

$$\inf_{\pi \in \Pi(\mu, \nu)} \int_{\mathbb{R}^d \times \mathbb{R}^{d'}} \|x - T(y)\|^2 d\pi(x, y) = \inf_{\pi \in \Pi(\mu, T_{\#}\nu)} \int_{\mathbb{R}^d \times \mathbb{R}^d} \|x - z\|^2 d\pi(x, z).$$

### A.2 Isometries in Euclidean spaces

We show the following result, that states that any isometry  $T : \mathbb{R}^{d'} \rightarrow \mathbb{R}^d$  for the Euclidean norms is affine and of the form, for all  $y \in \mathbb{R}^{d'}$ ,  $T(y) = Py + b$ , where  $b \in \mathbb{R}^d$  and  $P$  is in the Stiefel manifold  $\mathbb{V}_{d'}(\mathbb{R}^d)$  as defined in Section 4.1.

**Lemma A2.** *Suppose  $d \geq d'$ . Then  $\phi : \mathbb{R}^{d'} \rightarrow \mathbb{R}^d$  is an isometry for the Euclidean norm if and only if there exists  $P \in \mathbb{V}_{d'}(\mathbb{R}^d)$  and  $b \in \mathbb{R}^d$  such that for all  $y \in \mathbb{R}^{d'}$ ,  $\phi$  is of the form*

$$\phi(y) = Py + b.$$

*Proof.* First observe that for  $P \in \mathbb{V}_{d'}(\mathbb{R}^d)$  and  $b \in \mathbb{R}^d$ ,  $y \mapsto Py + b$  is an isometry since we have, for any  $y$  and  $y'$  in  $\mathbb{R}^{d'}$

$$\|Py + b - Py' - b\|^2 = \|P(y - y')\|^2 = (y - y')^T P^T P (y - y') = (y - y')^T (y - y') = \|y - y'\|^2.$$

The converse is a consequence of the Mazur–Ulam theorem (Mazur and Ulam, 1932) that states - in the version of Baker (1971) - that an isometry from a real normed space to a *strictly convex* normed space, i.e. a normed space where the unit ball is a strictly convex set, is necessarily affine. Since it is easy to show

that the unit ball  $\{x \in \mathbb{R}^d : \|x\| \leq 1\}$  is a strictly convex set, we get that for all  $x \in \mathbb{R}^d$ ,  $\phi$  is of the form  $y \mapsto Py + b$  with  $P$  being a matrix of size  $d \times d'$ , and  $b \in \mathbb{R}^d$ . Moreover we have for all  $y, y' \in \mathbb{R}^{d'}$

$$\|\phi(y) - \phi(y')\|^2 = \|Py - Py'\|^2 = \|P(y - y')\|^2 = (y - y')^T P^T P (y - y').$$

Since  $\phi$  is an isometry, it follows that  $\|y - y'\|^2 = (y - y')^T P^T P (y - y')$  and so  $P^T P = \text{Id}_{d'}$ , which concludes the proof.  $\square$

### A.3 Centering of measures

Finally, we show the following result.

**Lemma A3.** *Let  $\mu \in \mathcal{W}_2(\mathbb{R}^d)$  and  $\nu \in \mathcal{W}_2(\mathbb{R}^{d'})$  with  $d$  not necessarily greater than  $d'$ . Let  $\bar{\mu}$  and  $\bar{\nu}$  denote the centered measures associated to  $\mu$  and  $\nu$  and let  $\mathfrak{P}$  be any subset of matrices of size  $d \times d'$ . Then,*

$$\inf_{\pi \in \Pi(\mu, \nu)} \inf_{P \in \mathfrak{P}, b \in \mathbb{R}^d} \int_{\mathbb{R}^d \times \mathbb{R}^{d'}} \|x - Py - b\|^2 d\pi(x, y) = \inf_{\pi \in \Pi(\bar{\mu}, \bar{\nu})} \inf_{P \in \mathfrak{P}} \int_{\mathbb{R}^d \times \mathbb{R}^{d'}} \|x - Py\|^2 d\pi(x, y).$$

*Proof.* Denoting  $m_0 = \mathbb{E}_{X \sim \mu}[X]$ ,  $m_1 = \mathbb{E}_{Y \sim \nu}[Y]$ ,  $\tilde{x} = x - m_0$ , and  $\tilde{y} = y - m_1$ , we have for any  $\pi \in \Pi(\mu, \nu)$ ,

$$\begin{aligned} \int_{\mathbb{R}^d \times \mathbb{R}^{d'}} \|x - Py - b\|^2 d\pi(x, y) &= \int_{\mathbb{R}^d \times \mathbb{R}^{d'}} \|\tilde{x} - P\tilde{y} - b + m_0 - Pm_1\|^2 d\pi(x, y) \\ &= \|m_0 - b - Pm_1\|^2 + \int_{\mathbb{R}^d \times \mathbb{R}^{d'}} \|\tilde{x} - P\tilde{y}\|^2 d\pi(x, y), \end{aligned}$$

since  $\int \langle \tilde{x} - P\tilde{y}, m_0 - b - Pm_1 \rangle d\pi(x, y) = 0$ . Thus it follows,

$$\begin{aligned} \inf_{\pi \in \Pi(\mu, \nu)} \inf_{P \in \mathfrak{P}, b \in \mathbb{R}^d} \int_{\mathbb{R}^d \times \mathbb{R}^{d'}} \|x - Py - b\|^2 d\pi(x, y) \\ = \inf_{P \in \mathfrak{P}} \left( \inf_{b \in \mathbb{R}^d} \|m_0 - Pm_1 - b\|^2 + \inf_{\pi \in \Pi(\bar{\mu}, \bar{\nu})} \int_{\mathbb{R}^d \times \mathbb{R}^{d'}} \|x - Py\|^2 d\pi(x, y) \right). \end{aligned}$$

Observe now that for any  $P \in \mathfrak{P}$ ,  $\|m_0 - Pm_1 - b\|^2 = 0$  if  $b = m_0 - Pm_1$ , which concludes the proof.  $\square$

### A.4 Some properties of symmetric matrices

Here we state two technical results on symmetric matrices that will be useful during the proofs of the results on Gaussian distributions.

**Lemma A4.** *Let  $A \in \mathbb{S}^d$ . We denote  $\lambda_1$  and  $\lambda_d$  its largest and smallest eigenvalues. For all  $x \in \mathbb{R}^d$  such that  $\|x\| = 1$ , we have*

(i)  *$x$  is an eigenvector of  $A$  associated to  $\lambda_1$  if and only if  $x^T Ax = \lambda_1$ .*

(ii)  *$x$  is an eigenvector of  $A$  associated to  $\lambda_d$  if and only if  $x^T Ax = \lambda_d$ .*

*Proof.* Let  $x \in \mathbb{R}^d$  such  $\|x\| = 1$ . Since  $A$  is symmetric, there exists  $O \in \mathbb{O}(\mathbb{R}^d)$  and  $\Lambda = \text{diag}((\lambda_k)_{1 \leq k \leq d})$  such that  $x^T Ax = x^T O \Lambda O^T x$ . Denoting  $z$  the vector  $O^T x$ , we get thus

$$x^T Ax = z^T \Lambda z = \sum_{k=1}^d \lambda_k z_k^2.$$

Hence it follows that

$$\lambda_d \|z\|^2 \leq x^T Ax \leq \lambda_1 \|z\|^2,$$

with equality if and only if  $z$  is an eigenvector associated with  $\lambda_1$  or  $\lambda_d$ .  $\square$

**Lemma A5.** *Suppose that  $d \geq d'$ . Let  $\Sigma$  be a positive semi-definite (PSD) matrix of size  $d + d'$  of the form*

$$\Sigma = \begin{pmatrix} \Sigma_0 & K \\ K^T & \Sigma_1 \end{pmatrix},$$

with  $\Sigma_0 \in \mathbb{S}_{++}^d$ ,  $\Sigma_1 \in \mathbb{S}_+^{d'}$  and  $K$  being a rectangular matrix of size  $d \times d'$ . Let  $S = \Sigma_1 - K^T \Sigma_0^{-1} K$  be the Schur complement of  $\Sigma$ . Then there exists  $r \leq d'$  and  $B_r \in \mathbb{V}_r(\mathbb{R}^d)$  such that

$$K = \Sigma_0^{\frac{1}{2}} B_r \Lambda_r U_r^T,$$

where  $U_r \in \mathbb{V}_r(\mathbb{R}^{d'})$  and  $\Lambda_r$  is a diagonal positive matrix of size  $r$  such that

$$\Sigma_1 - S = U_r \Lambda_r^2 U_r^T.$$

*Proof.* For a given Schur complement  $S = \Sigma_1 - K^T \Sigma_0^{-1} K$ , we have  $K^T \Sigma_0^{-1} K = \Sigma_1 - S$ . Since  $\Sigma_0 \in \mathbb{S}_{++}^d$ , we can deduce that  $K^T \Sigma_0^{-1} K \in \mathbb{S}_+^{d'}$  and so that  $\Sigma_1 - S \in \mathbb{S}_+^{d'}$ . We note  $r$  the rank of  $K^T \Sigma_0^{-1} K$ . One can observe that

$$r \leq d' \leq d,$$

where the left-hand side inequality follows from the fact that  $\text{rk}(AB) \leq \min\{\text{rk}(A), \text{rk}(B)\}$ . Then,  $\Sigma_1 - S$  can be diagonalized

$$\Sigma_1 - S = K^T \Sigma_0^{-1} K = U \Lambda^2 U^T = U_r \Lambda_r^2 U_r^T, \quad (11)$$

with  $\Lambda^2 = \text{diag}(\lambda_1^2, \dots, \lambda_r^2)^{[d']}$ ,  $\Lambda_r^2 = \text{diag}(\lambda_1^2, \dots, \lambda_r^2)$ , and  $U_r \in \mathbb{V}_r(\mathbb{R}^{d'})$  such that  $U = (U_r \quad U_{d'-r})$ . From (11), we can deduce that

$$(\Sigma_0^{-\frac{1}{2}} K U_r \Lambda_r^{-1})^T \Sigma_0^{-\frac{1}{2}} K U_r \Lambda_r^{-1} = \text{Id}_r,$$

where  $\Lambda_r$  is the unique PSD square-root of  $\Lambda_r^2$ . Let us set  $B_r = \Sigma_0^{-\frac{1}{2}} K U_r \Lambda_r^{-1}$  such that  $B_r \in \mathbb{V}_r(\mathbb{R}^d)$ . It follows that

$$K U_r = \Sigma_0^{\frac{1}{2}} B_r \Lambda_r.$$

Moreover, since  $U_{d-r}^T K^T \Sigma_0^{-1} K U_{d-r} = 0$  and  $\Sigma_0 \in S_d^{++}(\mathbb{R})$ , it follows that  $K U_{d-r} = 0$  and so

$$K = K U U^T = K U_r U_r^T = \Sigma_0^{\frac{1}{2}} B_r \Lambda_r U_r^T,$$

which concludes the proof.  $\square$

## B Proofs of the theoretical results

### B.1 Proof of Theorem 2

*Proof of Theorem 2.* Takatsu (2010) has shown that the space of Gaussian distributions  $\mathcal{N}(\mathbb{R}^d)$  is a complete metric space when endowed with  $W_2$ . Moreover,  $\mathcal{N}(\mathbb{R}^d)$  is separable since it is a subspace of  $\mathcal{W}_2(\mathbb{R}^d)$  which is itself a separable metric space when endowed with  $W_2$  (Bolley, 2008). Thus,  $\mathcal{N}(\mathbb{R}^d)$  is Polish and we can directly apply the Gromov-Wasserstein theory developed in Sturm (2012). Let  $(\mathcal{N}(\mathbb{R}^d), W_2, \tilde{\mu})$  and  $(\mathcal{N}(\mathbb{R}^{d'}), W_2, \tilde{\nu})$  be two metric measure spaces respectively in  $\mathbb{M}_4$ . Let us define

$$D(\tilde{\mu}, \tilde{\nu}) = \inf_{\pi \in \Pi(\tilde{\mu}, \tilde{\nu})} \int_{\mathcal{N}(\mathbb{R}^d) \times \mathcal{N}(\mathbb{R}^{d'})} \int_{\mathcal{N}(\mathbb{R}^d) \times \mathcal{N}(\mathbb{R}^{d'})} |W_2^2(\gamma, \gamma') - W_2^2(\zeta, \zeta')|^2 d\pi(\gamma, \zeta) d\pi(\gamma', \zeta').$$

Applying Sturm (2012, Corollary 9.3), we get that  $D$  defines a metric over the space of metric measure spaces of the form  $(\mathcal{N}(\mathbb{R}^d), W_2, \tilde{\mu})$  quotiented by the strong isomorphisms, and thus we get directly that  $D$  is symmetric, non-negative, satisfies the triangle inequality and  $D(\tilde{\mu}, \tilde{\nu}) = 0$  if and only if there exists a bijection  $\phi : \text{supp}(\tilde{\mu}) \rightarrow \text{supp}(\tilde{\nu})$  such that  $\tilde{\nu} = \phi_{\#} \tilde{\mu}$ , where for any  $\gamma$  and  $\gamma'$  in  $\text{supp}(\tilde{\mu})$ ,  $W_2(\phi(\gamma), \phi(\gamma')) = W_2(\gamma, \gamma')$ . Now observe that if  $\mu = \sum_k a_k \mu_k$  and  $\nu = \sum_l b_l \nu_l$  are respectively in  $GMM_K(\mathbb{R}^d)$  and  $GMM_L(\mathbb{R}^{d'})$  and  $\tilde{\mu} = \sum_k a_k \delta_{\mu_k}$  and  $\tilde{\nu} = \sum_l b_l \delta_{\nu_l}$  are respectively in  $\mathcal{P}(\mathcal{N}(\mathbb{R}^d))$  and  $\mathcal{P}(\mathcal{N}(\mathbb{R}^{d'}))$ , we have

$$\int_{\mathcal{N}(\mathbb{R}^d) \times \mathcal{N}(\mathbb{R}^d)} W_2^4(\gamma, \gamma') d\tilde{\mu}(\gamma) d\tilde{\mu}(\gamma') = \sum_{k,i} a_k a_i W_2^4(\mu_k, \mu_i) < +\infty,$$

and

$$\int_{\mathcal{N}(\mathbb{R}^{d'}) \times \mathcal{N}(\mathbb{R}^{d'})} W_2^4(\zeta, \zeta') d\tilde{\nu}(\zeta) d\tilde{\nu}(\zeta') = \sum_{l,j} b_l b_j W_2^4(\nu_l, \nu_j) < +\infty,$$

so  $(\mathcal{N}(\mathbb{R}^d), W_2, \tilde{\mu})$  and  $(\mathcal{N}(\mathbb{R}^{d'}), W_2, \tilde{\nu})$  are both in  $\mathbb{M}_4$ . Furthermore, we have  $MGW_2(\mu, \nu) = D(\tilde{\mu}, \tilde{\nu})$ . Hence  $MGW_2$  inherits the metric properties of  $D$ , which concludes the proof.  $\square$

## B.2 Proof of Proposition 3

*Proof of Proposition 3.* First recall that the push-forward measure  $T_{\#}\mu$  with  $\mu$  on  $\mathbb{R}^{d'}$  and  $T : \mathbb{R}^{d'} \rightarrow \mathbb{R}^d$  is defined as the measure on  $\mathbb{R}^d$  such that for every Borel set  $A$  of  $\mathbb{R}^d$ ,  $T_{\#}\mu(A) = \mu(T^{-1}(A))$ . Equivalently, for any measurable map  $h : \mathbb{R}^d \rightarrow \mathbb{R}$ , we have

$$\int_{\mathbb{R}^d} h(x) d(T_{\#}\mu)(x) = \int_{\mathbb{R}^{d'}} (h \circ T)(y) d\mu(y).$$

Now observe that for any finite GMM  $\mu$  on  $\mathbb{R}^{d'}$  of the form  $\mu = \sum_k^K a_k \mu_k$ , we have

$$\begin{aligned} \int_{\mathbb{R}^{d'}} (h \circ T)(y) d\mu(y) &= \int_{\mathbb{R}^{d'}} (h \circ T)(y) d\left(\sum_k^K a_k \mu_k(y)\right) \\ &= \sum_k^K a_k \int_{\mathbb{R}^{d'}} (h \circ T)(y) d\mu_k(y) \\ &= \sum_k^K a_k \int_{\mathbb{R}^d} h(x) d(T_{\#}\mu_k)(x) \\ &= \int_{\mathbb{R}^d} h(x) d\left(\sum_k^K a_k (T_{\#}\mu_k)(x)\right), \end{aligned}$$

and so  $T_{\#}\mu$  is of the form  $\sum_k^K a_k (T_{\#}\mu_k)$  with  $T_{\#}\mu_k$  Gaussian since  $T$  is necessarily affine as a consequence of Lemma A2. Thus,  $T_{\#}\mu$  is in  $GMM_{\infty}(\mathbb{R}^d)$ . This proves that  $\phi_T$  takes its values only in  $GMM_{\infty}(\mathbb{R}^d)$  and that  $\phi_T(\sum_{k=1}^K a_k \mu_k)$  is of the form  $\sum_{k=1}^K a_k \nu_k$ . Now observe that, for every  $k$  and  $i$  smaller than  $K$ ,

$$W_2^2(\phi_T(\mu_k), \phi_T(\mu_i)) = \inf_{\pi \in \Pi(T_{\#}\mu_k, T_{\#}\mu_i)} \int_{\mathbb{R}^d \times \mathbb{R}^d} \|x - y\|^2 d\pi(x, y).$$

Using two times successively Lemma A1 using the fact that  $T$  is an isometry and so for any  $y \in \mathbb{R}^{d'}$ ,  $\|T(y)\| = \|y\|$ , it follows

$$\inf_{\pi \in \Pi(T_{\#}\mu_k, T_{\#}\mu_i)} \int_{\mathbb{R}^d \times \mathbb{R}^d} \|x - x'\|^2 d\pi(x, x') = \inf_{\pi \in \Pi(\mu_k, \mu_i)} \int_{\mathbb{R}^{d'} \times \mathbb{R}^{d'}} \|y - y'\|^2 d\pi(y, y') = W_2(\mu_k, \mu_i).$$

Thus,  $MGW_2(\mu, T_{\#}\mu) = 0$  as a direct consequence of Theorem 2, which concludes the proof.  $\square$

## B.3 Proof of Proposition 5

*Proof of Proposition 5.* Since we suppose  $d \geq d'$ , we have

$$EW_2^2(\mu, \nu) = \inf_{\phi \in \text{Isom}_{d'}(\mathbb{R}^d)} W_2^2(\mu, \phi_{\#}\nu).$$

Let  $\phi \in \text{Isom}_{d'}(\mathbb{R}^d)$  for the Euclidean norm. Using Lemma A2, we get that there exists  $P \in \mathbb{V}_{d'}(\mathbb{R}^d)$  and  $b \in \mathbb{R}^d$  such that for all  $y \in \mathbb{R}^{d'}$ ,  $\phi(y) = Py + b$ . Moreover, we have, using Lemma A1,

$$\begin{aligned} EW_2^2(\mu, \nu) &= \inf_{\phi \in \text{Isom}_{d'}(\mathbb{R}^d)} \inf_{\pi \in \Pi(\mu, \phi_{\#}\nu)} \int_{\mathbb{R}^d \times \mathbb{R}^d} \|x - y\|^2 d\pi(x, y) \\ &= \inf_{\phi \in \text{Isom}_{d'}(\mathbb{R}^d)} \inf_{\pi \in \Pi(\mu, \nu)} \int_{\mathbb{R}^{d'} \times \mathbb{R}^d} \|x - \phi(y)\|^2 d\pi(x, y) \\ &= \inf_{\pi \in \Pi(\mu, \nu)} \inf_{P \in \mathbb{V}_{d'}(\mathbb{R}^d), b \in \mathbb{R}^d} \int_{\mathbb{R}^{d'} \times \mathbb{R}^d} \|x - Py - b\|^2 d\pi(x, y), \end{aligned}$$

which concludes the proof.  $\square$

## B.4 Proof of Proposition 6

Before turning to the proof of Proposition 6, we will prove the following lemma.

**Lemma B1.** *Let  $K$  be a matrix of size  $d \times d'$  with Singular Value Decomposition (SVD)  $K = U_K \Sigma_K V_K^T$  and let  $\mathfrak{P}$  be any compact set of matrices of size  $d \times d'$ . Then,*

$$\sup_{P \in \mathfrak{P}} \operatorname{tr}(P^T K) = \max_{P \in \mathfrak{P}} \operatorname{tr}(\Sigma_P^T \Sigma_K),$$

where  $\Sigma_P = \operatorname{diag}^{[d, d']}(\boldsymbol{\sigma}(P))$  with  $\boldsymbol{\sigma}(P) \in \mathbb{R}_+^{d'}$  denoting the vector of singular values of  $P$ . Furthermore it is achieved at  $P$  of the form,

$$P = U_K \Sigma_P V_K^T.$$

*Proof of Lemma B1.* Note that this lemma can be proven with a proof similar to the one of Alvarez-Melis et al. (2019, Lemma 4.2), using the min-max theorem for singular values. Here we offer an alternative proof based on Lagrangian analysis. First observe that the supremum is achieved as a direct consequence of the Weierstrass theorem because  $\mathfrak{P}$  is compact and the mapping  $P \mapsto \operatorname{tr}(P^T K)$  is continuous. For a given  $P \in \mathfrak{P}$ , let  $U_P \Sigma_P V_P^T$  be the SVD of  $P$ . The problem can be rewritten as

$$\max_{P \in \mathfrak{P}} \operatorname{tr}(V_P \Sigma_P^T U_P^T U_K \Sigma_K V_K^T).$$

Now, let us denote  $U = U_P^T U_K$  and  $V = V_P^T V_K$ . Observe that  $U$  is in  $\mathbb{O}(\mathbb{R}^d)$  and  $V$  is in  $\mathbb{O}(\mathbb{R}^{d'})$ . Using the cyclical permutation of the trace operator, the problem becomes

$$\max_{P \in \mathfrak{P}} \operatorname{tr}(\Sigma_P^T U \Sigma_K V^T).$$

Now, for a given fixed  $\Sigma_P$ , we determine which  $U$  and  $V$  maximize  $\operatorname{tr}(\Sigma_P^T U \Sigma_K V^T)$ . This problem reads as

$$\max_{U \in \mathbb{O}(\mathbb{R}^d), V \in \mathbb{O}(\mathbb{R}^{d'})} \operatorname{tr}(\Sigma_P^T U \Sigma_K V^T).$$

The Lagrangian of this problem reads as

$$\mathcal{L}(U, V, C_0, C_1) = -\operatorname{tr}(\Sigma_P^T U \Sigma_K V^T) + \operatorname{tr}(C_0(U^T U - \operatorname{Id}_d)) + \operatorname{tr}(C_1(V^T V - \operatorname{Id}_{d'})),$$

where  $C_0 \in \mathbb{S}^d$  and  $C_1 \in \mathbb{S}^{d'}$  are the Lagrange multipliers respectively associated with the constraints  $U \in \mathbb{O}(\mathbb{R}^d)$  and  $V \in \mathbb{O}(\mathbb{R}^{d'})$ . The first order condition gives

$$\begin{cases} \Sigma_P V \Sigma_K^T = 2U C_0 \\ \Sigma_P^T U \Sigma_K = 2V C_1, \end{cases}$$

or equivalently

$$\begin{cases} U^T \Sigma_P V \Sigma_K^T = 2C_0 \\ \Sigma_P^T U \Sigma_K V^T = 2V C_1 V^T. \end{cases}$$

Since  $C_0$  and  $C_1$  are symmetric matrices (because they are associated with symmetric constraints), we get that both left-hand terms are symmetric. This gives the following conditions

$$\begin{cases} U^T \Sigma_P V \Sigma_K^T = \Sigma_K V^T \Sigma_P^T U \\ \Sigma_P^T U \Sigma_K V^T = V \Sigma_K^T U^T \Sigma_P. \end{cases}$$

Now, observe that when multiplying the first condition at right by  $U^T \Sigma_P$  and multiplying the second condition at left by  $\Sigma_K V^T$ , we get by combining the two conditions

$$\begin{cases} U \Sigma_K V^T \Sigma_P^T \Sigma_P = \Sigma_P \Sigma_P^T U \Sigma_K V^T \\ U^T \Sigma_P V \Sigma_K^T \Sigma_K = \Sigma_K \Sigma_K^T U^T \Sigma_P V^T, \end{cases}$$

or equivalently,

$$\begin{cases} U \Sigma_K V^T D_P = D_P^{[d]} U \Sigma_K V^T \\ U^T \Sigma_P V D_K = D_K^{[d']} U^T \Sigma_P V^T, \end{cases}$$

where  $D_P = \text{diag}(\boldsymbol{\sigma}(P))$  and  $D_K = \text{diag}(\boldsymbol{\sigma}(K))$ . Multiplying the first condition at left by  $V\Sigma_K^T U^T$  and the second condition at right by  $V\Sigma_P^T U$ , this yields to

$$\begin{cases} VD_K V^T D_P = V\Sigma U^T D_P^{[d]} U \Sigma_K V^T \\ D_K^{[d]} U^T D_P^{[d]} U = U^T \Sigma_P V D_K V \Sigma_P^T U. \end{cases}$$

It follows that  $VD_K V^T D_P$  and  $D_K^{[d]} U^T D_P^{[d]} U$  are symmetric matrices and so  $VD_K V^T$  commutes with  $D_P$  and  $U^T D_P^{[d]} U$  commutes with  $D_K^{[d]}$ . Thus we can deduce that  $U$  and  $V$  are permutation matrices. Since the singular values are ordered in non-increasing order, we deduce that the problem is maximized when  $U = \text{Id}_d$  and  $V = \text{Id}_{d'}$ . This implies that  $U_P = U_K$  and  $V_P = V_K$ , which concludes the proof.  $\square$

Note that Lemma B1 is especially useful when the constraint of belonging to the set  $\mathfrak{P}$  can be expressed as a constraint on the singular values. Observe that this is the case of  $\mathbb{V}_{d'}(\mathbb{R}^d)$  since for all  $P \in \mathbb{V}_{d'}(\mathbb{R}^d)$ , we have  $P^T P = \text{Id}_{d'}$  and so an equivalent condition of belonging in  $\mathbb{V}_{d'}(\mathbb{R}^d)$  is that  $\boldsymbol{\sigma}(P) = \mathbb{1}_{d'}$ . Now we are ready to turn to the proof of Proposition 6.

*Proof of Proposition 6.* Using Lemmas A3, Problem (4) can be rewritten

$$\begin{aligned} EW_2^2(\mu, \nu) &= \inf_{P \in \mathbb{V}_{d'}(\mathbb{R}^d)} \inf_{\pi \in \Pi(\bar{\mu}, \bar{\nu})} \int_{\mathbb{R}^d \times \mathbb{R}^{d'}} \|x - Py\|^2 d\pi(x, y) \\ &= \inf_{P \in \mathbb{V}_{d'}(\mathbb{R}^d)} \inf_{\pi \in \Pi(\bar{\mu}, \bar{\nu})} \int_{\mathbb{R}^d \times \mathbb{R}^{d'}} (\|x\|^2 + \|Py\|^2 - 2\langle x, Py \rangle) d\pi(x, y). \end{aligned}$$

Since for all  $P \in \mathbb{V}_{d'}(\mathbb{R}^d)$ ,  $\|Py\|$  doesn't depend on  $P$ , we get that the problem is equivalent to

$$\sup_{P \in \mathbb{V}_{d'}(\mathbb{R}^d)} \sup_{\pi \in \Pi(\bar{\mu}, \bar{\nu})} \int_{\mathbb{R}^d \times \mathbb{R}^{d'}} \langle x, Py \rangle d\pi(x, y).$$

Now observe that for all  $\pi \in \Pi(\bar{\mu}, \bar{\nu})$ ,

$$\int_{\mathbb{R}^d \times \mathbb{R}^{d'}} \langle x, Py \rangle d\pi(x, y) = \int_{\mathbb{R}^d \times \mathbb{R}^{d'}} \text{tr}(xy^T P^T) d\pi(x, y) = \int_{\mathbb{R}^d \times \mathbb{R}^{d'}} \text{tr}(P^T xy^T) d\pi(x, y),$$

where we used the cyclical permutation property of the trace operator. Finally using the linearity of the trace, we get that the problem is equivalent to

$$\sup_{P \in \mathbb{V}_{d'}(\mathbb{R}^d)} \sup_{\pi \in \Pi(\bar{\mu}, \bar{\nu})} \text{tr} \left( P^T \int_{\mathbb{R}^d \times \mathbb{R}^{d'}} xy^T d\pi(x, y) \right),$$

or equivalently,

$$\sup_{P \in \mathbb{V}_{d'}(\mathbb{R}^d)} \sup_{\pi \in \Pi(\bar{\mu}, \bar{\nu})} \left\langle P, \int_{\mathbb{R}^d \times \mathbb{R}^{d'}} xy^T d\pi(x, y) \right\rangle.$$

Now, using Lemma B1 and using the fact that if  $P \in \mathbb{V}_{d'}(\mathbb{R}^d)$ ,  $\boldsymbol{\sigma}(P) = \mathbb{1}_{d'}$ , we get that the problem reduces to

$$\sup_{\pi \in \Pi(\bar{\mu}, \bar{\nu})} \left\| \int_{\mathbb{R}^d \times \mathbb{R}^{d'}} xy^T d\pi(x, y) \right\|_*,$$

and this is achieved for  $P^* = U_\pi \text{Id}_{d'}^{[d, d']} V_\pi^T$ , where  $U_\pi \in \mathbb{O}(\mathbb{R}^d)$  and  $V_\pi \in \mathbb{O}(\mathbb{R}^{d'})$  are respectively the left and right orthogonal matrices of the SVD of  $\int_{\mathbb{R}^d \times \mathbb{R}^{d'}} xy^T d\pi(x, y)$ , which concludes the proof.  $\square$

## B.5 Proof of Proposition 7

*Proof of Proposition 7.* First, using Lemma A2, we get that there exists  $P_1 \in \mathbb{V}_d(\mathbb{R}^r)$  and  $b_1 \in \mathbb{R}^r$  such that for all  $x \in \mathbb{R}^d$ ,  $\psi(x) = P_1 x + b_1$ . Since  $r \geq d'$ , we have, denoting  $\bar{\mu}$ ,  $\bar{\psi}_{\#}\mu$  and  $\bar{\nu}$  the centered measures respectively associated with  $\mu$ ,  $\psi_{\#}\mu$ , and  $\nu$ , and using successively Lemma A3 and Lemma A1,

$$\begin{aligned} EW_2^2(\psi_{\#}\mu, \nu) &= \inf_{\pi \in \Pi(\psi_{\#}\mu, \nu)} \inf_{P \in \mathbb{V}_{d'}(\mathbb{R}^r), b \in \mathbb{R}^r} \int_{\mathbb{R}^r \times \mathbb{R}^{d'}} \|z - Py - b\|^2 d\pi(z, y) \\ &= \inf_{\pi \in \Pi(\psi_{\#}\mu, \bar{\nu})} \inf_{P \in \mathbb{V}_{d'}(\mathbb{R}^r)} \int_{\mathbb{R}^r \times \mathbb{R}^{d'}} \|z - Py\|^2 d\pi(z, y) \end{aligned}$$

$$\begin{aligned}
 &= \inf_{\pi \in \Pi(\bar{\mu}, \bar{\nu})} \inf_{P \in \mathbb{V}_{d'}(\mathbb{R}^r)} \int_{\mathbb{R}^d \times \mathbb{R}^{d'}} \|P_1 x - P y\|^2 d\pi(x, y) \\
 &= \int_{\mathbb{R}^d} \|P_1 x\|^2 d\bar{\mu}(x) + \int_{\mathbb{R}^{d'}} \|P y\|^2 d\bar{\nu}(y) - 2 \sup_{\pi \in \Pi(\bar{\mu}, \bar{\nu})} \sup_{P \in \mathbb{V}_{d'}(\mathbb{R}^r)} \text{tr}(P^T P_1 K_\pi) \\
 &= \int_{\mathbb{R}^d} \|x\|^2 d\bar{\mu}(x) + \int_{\mathbb{R}^{d'}} \|y\|^2 d\bar{\nu}(y) - 2 \sup_{\pi \in \Pi(\bar{\mu}, \bar{\nu})} \sup_{P \in \mathbb{V}_{d'}(\mathbb{R}^r)} \text{tr}(P^T P_1 K_\pi),
 \end{aligned}$$

where  $K_\pi = \int_{\mathbb{R}^d \times \mathbb{R}^{d'}} x y^T d\pi(x, y)$ . Applying Proposition 6, we get

$$\sup_{\pi \in \Pi(\bar{\mu}, \bar{\nu})} \sup_{P \in \mathbb{V}_{d'}(\mathbb{R}^r)} \text{tr}(P^T P_1 K_\pi) = \sup_{\pi \in \Pi(\bar{\mu}, \bar{\nu})} \|P_1 K_\pi\|_*.$$

Now observe that  $P_1 K_\pi$  has the same singular values as  $K_\pi$  since  $K_\pi^T P_1^T P_1 K_\pi = K_\pi^T K_\pi$ . Thus  $\|P_1 K_\pi\|_* = \|K_\pi\|_*$  and so  $EW_2(\psi_{\#}\mu, \nu) = EW_2(\mu, \nu)$ , which concludes the proof.  $\square$

## B.6 Proof of Lemma 9

*Proof of Lemma 9.* First note that in this proof, we denote  $\mathbb{R}^{d \times d'}$  the set of matrices of size  $d \times d'$  that we distinct of the set  $\mathbb{R}^{dd'}$  of vector with  $d \times d'$  coordinates. We set  $g : P \in \mathbb{R}^{d \times d'} \mapsto \Sigma_1^{\frac{1}{2}} P^T \Sigma_0 P \Sigma_1^{\frac{1}{2}}$  and  $h : Q \in \mathbb{S}_+^{d'} \mapsto Q^{\frac{1}{2}}$  such that for all matrix  $P$  of size  $d \times d'$ , we have

$$f(P) = \text{tr}(h(g(P))).$$

For any matrix  $A \in \mathbb{R}^{d \times d'}$ , we denote  $\text{vec}(A) \in \mathbb{R}^{dd'}$  the vector obtained by stacking the columns of  $A$ . Observe that, see (Magnus and Neudecker, 2019) for details, for any function  $\phi : \mathbb{R}^{d \times d'} \rightarrow \mathbb{R}^{r \times s}$ , the Jacobian matrix  $J[\phi]$  of  $\phi$  can be defined as, for all  $P \in \mathbb{R}^{d \times d'}$ ,

$$J[\phi](P) = \frac{\partial \text{vec}(f(P))}{\partial \text{vec}(P)}.$$

Moreover, observe that since  $f : \mathbb{R}^{d \times d'} \rightarrow \mathbb{R}$ ,  $J[f][P] \in \mathbb{R}^{dd'}$  and

$$\frac{\partial f(P)}{\partial P} = \text{vec}^{-1}(J^T[f](P)),$$

where  $\text{vec}^{-1}$  is the inverse vector operator, i.e. such that for any  $A \in \mathbb{R}^{d \times d'}$ ,  $\text{vec}^{-1}(\text{vec}(A)) = A$ . Applying the chain rule to derive  $f$ , we have

$$J[f](P) = J[\text{tr}((h \circ g)(P))]J[h](g(P))J[g](P).$$

- First, we compute  $J[g](P)$ . It follows, using formula provided by Petersen et al. (2008) and Magnus and Neudecker (2019),

$$\partial(\Sigma_1^{\frac{1}{2}} P^T \Sigma_0 P \Sigma_1^{\frac{1}{2}}) = \Sigma_1^{\frac{1}{2}} \partial P^T \Sigma_0 P \Sigma_1^{\frac{1}{2}} + \Sigma_1^{\frac{1}{2}} P^T \Sigma_0 \partial P \Sigma_1^{\frac{1}{2}},$$

and so

$$\begin{aligned}
 \partial \text{vec}(\Sigma_1^{\frac{1}{2}} P^T \Sigma_0 P \Sigma_1^{\frac{1}{2}}) &= (\Sigma_1^{\frac{1}{2}} P^T \Sigma_0 \otimes_K \Sigma_1^{\frac{1}{2}}) \partial \text{vec}(P^T) + (\Sigma_1^{\frac{1}{2}} \otimes_K \Sigma_1^{\frac{1}{2}} P^T \Sigma_0) \partial \text{vec}(P) \\
 &= (\Sigma_1^{\frac{1}{2}} P^T \Sigma_0 \otimes_K \Sigma_1^{\frac{1}{2}}) K_{dd'} \partial \text{vec}(P) + (\Sigma_1^{\frac{1}{2}} \otimes_K \Sigma_1^{\frac{1}{2}} P^T \Sigma_0) \partial \text{vec}(P) \\
 &= (I_{d^2} + K_{d^2})(\Sigma_1^{\frac{1}{2}} \otimes_K \Sigma_1^{\frac{1}{2}} P^T \Sigma_0) \partial \text{vec}(P),
 \end{aligned}$$

where  $\otimes_K$  denotes the Kronecker product and for any  $r$ ,  $K_r$  is the commutation matrix of size  $r \times r$ , see (Magnus and Neudecker, 2019) for details. Thus,

$$J[g](P) = (I_{d^2} + K_{d^2})(\Sigma_1^{\frac{1}{2}} \otimes_K \Sigma_1^{\frac{1}{2}} P^T \Sigma_0).$$

- Now we compute  $J[h](Q)$ . Observe that we have for any  $Q \in \mathbb{S}_+^{d'}$ ,

$$Q^{\frac{1}{2}} Q^{\frac{1}{2}} = Q.$$

Thus it follows, denoting  $s : Q \mapsto Q^{1/2}$ ,

$$\partial s(Q)Q^{\frac{1}{2}} + Q^{\frac{1}{2}}\partial s(Q) = \partial Q .$$

This latter equation is a Sylvester equation with variable  $\partial s(Q)$ , which is equivalent to the following linear system:

$$(Q^{\frac{1}{2}} \oplus_K Q^{T\frac{1}{2}})\partial \text{vec}(s(Q)) = \partial \text{vec}(Q) ,$$

where  $\oplus_K$  stands for the Kronecker sum. If  $Q$  is non-degenerate,  $Q^{\frac{1}{2}} \oplus_K Q^{T\frac{1}{2}}$  is also non-degenerate and so in that case

$$J[h](Q) = (Q^{\frac{1}{2}} \oplus_K Q^{T\frac{1}{2}})^{-1} .$$

- Finally, it is easy to see that for  $R \in \mathbb{R}^{d' \times d'}$  we have

$$J[\text{tr}](R) = \text{vec}^T(\text{Id}_{d'}) .$$

Thus, denoting  $A = \Sigma_1^{\frac{1}{2}} P^T \Sigma_0 P \Sigma_1^{\frac{1}{2}}$  and observing that  $A$  is symmetric and full-rank when  $P$  is full-rank (since we supposed that  $\Sigma_0$  and  $\Sigma_1$  are full rank), it follows that for all full-rank matrix  $P$  of size  $d \times d'$ ,

$$J^T[f](P) = (\Sigma_1^{\frac{1}{2}} \otimes_K \Sigma_0 P \Sigma_1^{\frac{1}{2}})(I_{d'^2} + K_{d'^2})(A^{\frac{1}{2}} \oplus_K A^{\frac{1}{2}})^{-1} \text{vec}(\text{Id}_{d'}) ,$$

where we used that  $K_{d'^2}$  and  $(A \oplus_K A)^{-1}$  were symmetric. Observe now that  $(A^{\frac{1}{2}} \oplus_K A^{\frac{1}{2}})^{-1} \text{vec}(\text{Id}_{d'}) = \text{vec}(X)$ , where  $X \in \mathbb{R}^{d' \times d'}$  is the unique solution of the following Sylvester equation

$$A^{\frac{1}{2}} X + X A^{\frac{1}{2}} = \text{Id}_{d'} .$$

Since  $A$  is symmetric, one can set  $A = QDQ^T$  where  $Q \in \mathbb{O}(\mathbb{R}^{d'})$  and  $D$  is a diagonal matrix of size  $d'$ . The Sylvester equation can be rewritten

$$D^{\frac{1}{2}} Y + Y D^{\frac{1}{2}} = \text{Id}_{d'} ,$$

where  $Y = Q^T X Q$ . Since  $A$  is full-rank,  $D$  is invertible and it is easy to see that the unique solution of this latter equation is  $Y = (1/2)D^{-\frac{1}{2}}$  and so  $X = (1/2)A^{-\frac{1}{2}}$  and thus

$$(A^{\frac{1}{2}} \oplus_K A^{\frac{1}{2}})^{-1} \text{vec}(\text{Id}_{d'}) = \frac{1}{2} \text{vec}(A^{-\frac{1}{2}}) .$$

Moreover, since  $A$  is symmetric, we have  $K_{d'^2} \text{vec}(A^{-\frac{1}{2}}) = \text{vec}(A^{-\frac{1}{2}})$  and so it follows that

$$\begin{aligned} J^T[f](P) &= (\Sigma_1^{\frac{1}{2}} \otimes_K \Sigma_0 P \Sigma_1^{\frac{1}{2}}) \text{vec}(A^{-\frac{1}{2}}) \\ &= \text{vec}(\Sigma_0 P \Sigma_1^{\frac{1}{2}} A^{-\frac{1}{2}} \Sigma_1^{\frac{1}{2}}) , \end{aligned}$$

which concludes the proof.  $\square$

## C Additional theoretical results on $EW_2$

In this section, we show some additional theoretical results on  $EW_2$ . First, we show that Problem ( $EW_2$ ) is always achieved.

### C.1 Metric properties of $EW_2$

In this section, we show that  $EW_2$  defines a pseudometric on  $\bigsqcup_{k \geq 1} \mathcal{W}_2(\mathbb{R}^k)$  that is invariant to isometries  $\phi : \mathbb{R}^{d'} \rightarrow \mathbb{R}^d$  for the Euclidean norm. More precisely, we show the following result.

**Theorem C1.** *In the following,  $\mu \in \mathcal{W}_2(\mathbb{R}^{d'})$  and  $\nu \in \mathcal{W}_2(\mathbb{R}^{d'})$ . Then,*

- (i)  $EW_2$  is symmetric, non-negative and satisfies the triangular inequality, i.e. for any  $\xi \in \mathcal{W}_2(\mathbb{R}^{d''})$ ,

$$EW_2(\mu, \nu) \leq EW_2(\mu, \xi) + EW_2(\xi, \nu) .$$

- (ii)  $EW_2(\mu, \nu) = 0$  if and only if there exists an isometry  $\phi : \mathbb{R}^{d'} \rightarrow \mathbb{R}^d$  such that  $\nu = \phi_{\#} \mu$ .

Thus  $EW_2$  defines a pseudometric on  $\bigsqcup_{k \geq 1} \mathcal{W}_2(\mathbb{R}^k)$ .

Before turning to the proof of Theorem C1, we will show the following intermediary result.

**Lemma C2.** *Let  $\mu \in \mathcal{W}_2(\mathbb{R}^d)$  and  $\nu \in \mathcal{W}_2(\mathbb{R}^{d'})$  and let suppose  $d \geq d'$ . Then there exists an optimal isometry  $\phi^* : \mathbb{R}^{d'} \rightarrow \mathbb{R}^d$  such that  $EW_2(\mu, \nu) = W_2(\mu, \phi^*_{\#}\nu)$ .*

*Proof.* Using Lemma A3 and Lemma A1, we have that

$$\begin{aligned} EW_2^2(\mu, \nu) &= \inf_{P \in \mathbb{V}_{d'}(\mathbb{R}^d)} \inf_{\pi \in \Pi(\bar{\mu}, \bar{\nu})} \int_{\mathbb{R}^d \times \mathbb{R}^{d'}} \|x - Py\|^2 d\pi(x, y) \\ &= \inf_{P \in \mathbb{V}_{d'}(\mathbb{R}^d)} W_2^2(\bar{\mu}, P_{\#}\bar{\nu}), \end{aligned}$$

where  $\bar{\mu}$  and  $\bar{\nu}$  are the centered measures associated with  $\mu$  and  $\nu$ . Let us denote  $J : P \mapsto W_2(\bar{\mu}, P_{\#}\bar{\nu})$  and let us show that  $J$  is continuous. For any  $P_0$  and  $P_1$  in  $\mathbb{V}_{d'}(\mathbb{R}^d)$ , we have,

$$|J(P_0) - J(P_1)| = |W_2(\bar{\mu}, P_{0\#}\bar{\nu}) - W_2(\bar{\mu}, P_{1\#}\bar{\nu})| \leq W_2(P_{0\#}\bar{\nu}, P_{1\#}\bar{\nu}),$$

where we used the triangular inequality property of  $W_2$ . Furthermore,

$$\begin{aligned} W_2^2(P_{0\#}\bar{\nu}, P_{1\#}\bar{\nu}) &= \inf_{\pi \in \Pi(P_{0\#}\bar{\nu}, P_{1\#}\bar{\nu})} \int_{\mathbb{R}^d \times \mathbb{R}^d} \|x - y\|^2 d\pi(x, y) \\ &= \inf_{\pi \in \Pi(\bar{\nu}, \bar{\nu})} \int_{\mathbb{R}^{d'} \times \mathbb{R}^{d'}} \|P_0x - P_1y\|^2 d\pi(x, y), \end{aligned}$$

where we used Lemma A1 twice. Now observe that the coupling  $(\text{Id}_{d'}, \text{Id}_{d'})_{\#}\bar{\nu}$  is in  $\Pi(\bar{\nu}, \bar{\nu})$ , so it follows

$$\inf_{\pi \in \Pi(\bar{\nu}, \bar{\nu})} \int_{\mathbb{R}^{d'} \times \mathbb{R}^{d'}} \|P_0x - P_1y\|^2 d\pi(x, y) \leq \int_{\mathbb{R}^{d'}} \|P_0x - P_1x\|^2 d\bar{\nu}(x).$$

Finally, for any  $x \in \mathbb{R}^{d'}$ , we have

$$\|P_0x - P_1x\|^2 \leq \|x\|^2 \sup_{\|z\|=1} \|(P_0 - P_1)z\|^2 \leq \|P_0 - P_1\|_{\mathcal{F}}^2 \|x\|^2,$$

and so it follows that

$$|J(P_0) - J(P_1)|^2 \leq \|P_0 - P_1\|_{\mathcal{F}}^2 \int_{\mathbb{R}^{d'}} \|x\|^2 d\bar{\nu}.$$

Since  $\nu$  is in  $\mathcal{W}_2(\mathbb{R}^{d'})$ ,  $\bar{\nu}$  is in  $\mathcal{W}_2(\mathbb{R}^{d'})$  and so  $\int_{\mathbb{R}^{d'}} \|x\|^2 d\bar{\nu} < +\infty$ . It follows that  $|J(P_0) - J(P_1)| \rightarrow 0$  when  $\|P_0 - P_1\|_{\mathcal{F}} \rightarrow 0$  and so  $J$  is continuous. Moreover, since  $\mathbb{V}_{d'}(\mathbb{R}^d)$  is compact (James, 1976),  $J$  has a minimum on  $\mathbb{V}_{d'}(\mathbb{R}^d)$  as a result of the classic Weierstrass theorem that states that any real-valued continuous function defined on a compact set achieves its infimum. Thus, there exists  $P^*$  such that  $EW_2(\mu, \nu) = W_2(\bar{\mu}, P_{\#}^*\bar{\nu})$  and setting  $b^* = \mathbb{E}_{X \sim \mu}[X] - P^* \mathbb{E}_{Y \sim \nu}[Y]$  and  $\phi^*(x) = P^*x + b^*$  for all  $x \in \mathbb{R}^d$ , we get that there exists  $\phi^* \in \text{Isom}_{d'}(\mathbb{R}^d)$  such that  $EW_2(\mu, \nu) = W_2(\mu, \phi^*_{\#}\nu)$ , which concludes the proof.  $\square$

Now we are ready to prove Theorem C1.

*Proof of Theorem C1.* First observe that non-negativity is straightforward. Furthermore, observe also that if  $d \neq d'$ , symmetry is also straightforward. Now suppose  $d = d'$  and observe that the set  $\mathbb{V}_{d'}(\mathbb{R}^d)$  coincides with the set of orthogonal matrices  $\mathbb{O}(\mathbb{R}^d)$ . Thus we have

$$\begin{aligned} \inf_{\phi \in \text{Isom}_d(\mathbb{R}^d)} W_2(\mu, \phi_{\#}\nu) &= \inf_{\pi \in \Pi(\mu, \nu)} \inf_{P \in \mathbb{O}(\mathbb{R}^d), b \in \mathbb{R}^d} \int_{\mathbb{R}^d \times \mathbb{R}^d} \|x - Py - b\|^2 d\pi(x, y) \\ &= \inf_{\pi \in \Pi(\mu, \nu)} \inf_{P \in \mathbb{O}(\mathbb{R}^d), b \in \mathbb{R}^d} \int_{\mathbb{R}^d \times \mathbb{R}^d} \|P^T x - y - P^T b\|^2 d\pi(x, y) \\ &= \inf_{\psi \in \text{Isom}_d(\mathbb{R}^d)} W_2(\psi_{\#}\mu, \nu), \end{aligned}$$

and so  $EW_2$  is also symmetric in that case. and so  $EW_2$  is also symmetric in that case. Before turning to the proof of the two other points, we recall that the infimum in  $\phi$  is always achieved, see Lemma C2.

- (i) Now we prove the triangle inequality. Let  $r \geq \max\{d, d', d''\}$ ,  $\phi_0 \in \text{Isom}_d(\mathbb{R}^r)$  and for  $\xi \in \mathcal{W}_\infty(\mathbb{R}^{d''})$ , let  $\phi_1 \in \arg \min_{\phi \in \text{Isom}_{d''}(\mathbb{R}^r)} W_2(\phi_0 \# \mu, \phi \# \xi)$ . We have, using first Proposition 7, then using the triangle inequality property of  $W_2$ ,

$$\begin{aligned} EW_2(\mu, \nu) &= EW_2(\phi_0 \# \mu, \nu) = \inf_{\phi \in \text{Isom}_{d'}(\mathbb{R}^r)} W_2(\phi_0 \# \mu, \phi \# \nu) \\ &\leq \inf_{\phi \in \text{Isom}_{d'}(\mathbb{R}^r)} [W_2(\phi_0 \# \mu, \phi_1 \# \xi) + W_2(\phi_1 \# \xi, \phi \# \nu)] \\ &\leq W_2(\phi_0 \# \mu, \phi_1 \# \xi) + \inf_{\phi \in \text{Isom}_{d'}(\mathbb{R}^r)} W_2(\phi_1 \# \xi, \phi \# \nu) \\ &\leq EW_2(\phi_0 \# \mu, \xi) + EW_2(\phi_1 \# \xi, \nu). \end{aligned}$$

We conclude then by applying Proposition 7 on both terms.

- (ii) Suppose without any loss of generality that  $d \geq d'$  and suppose  $EW_2(\mu, \nu) = 0$ . Since the infimum in  $\phi$  is achieved, there exists  $\phi \in \text{Isom}_{d'}(\mathbb{R}^d)$  such that  $W_2(\mu, \phi \# \nu) = 0$  and so  $\mu = \phi \# \nu$ . The reverse implication is obvious.

Finally, observe that if  $\mu$  and  $\nu$  have finite order 2 moments, then  $EW_2$  necessarily takes finite values, and so  $EW_2$  defines a pseudometric on  $\bigsqcup_{k \geq 1} \mathcal{W}_2(\mathbb{R}^k)$ .  $\square$

Note that similarly to  $EW_2$ , one can show that the infimum in  $\phi$  is always achieved and that  $MEW_2$  satisfies all the properties of a pseudometric on  $\mathcal{GMM}_\infty$  by simply replacing  $W_2$  by  $MW_2$  in the proofs above.

## C.2 $EW_2$ between Gaussian distributions

The following result shows that when  $\mu$  and  $\nu$  are Gaussian measures, Problems  $(EW_2)$  and  $(GW_2\text{-IP})$  share some common solutions.

**Proposition C3.** *Suppose without any loss of generality that  $d \geq d'$ . Let  $\mu = N(0, \Sigma_0)$  and  $\nu = N(0, \Sigma_1)$  be two centered Gaussian measures on  $\mathbb{R}^d$  and  $\mathbb{R}^{d'}$ . Let  $P_0, D_0$  and  $P_1, D_1$  be the respective diagonalizations of  $\Sigma_0 (= P_0 D_0 P_0^T)$  and  $\Sigma_1 (= P_1 D_1 P_1^T)$  that sort the eigenvalues in non-increasing order. We suppose that  $\mu$  is not degenerate, i.e.  $\Sigma_0$  is non-singular. Then the problem*

$$EW_2(\mu, \nu) = \inf_{P \in \mathbb{V}_{d'}(\mathbb{R}^d)} W_2(\mu, P \# \nu),$$

admits solutions of the form  $(\pi^*, P^*)$  with  $P^*$  of the form  $P^* = P_0 \tilde{\text{Id}}_{d'}^{[d, d']} P_1^T$  and  $\pi^* = (\text{Id}_d, T) \# \mu$  with  $T$  being any affine map such that for all  $x \in \mathbb{R}^d$ ,

$$T(x) = P_1 \left( \tilde{\text{Id}}_{d'} D_1^{\frac{1}{2}} D_0^{(d')^{-\frac{1}{2}}} \right)^{[d, d']} P_0^T x.$$

In other terms, the solutions of Problem  $(GW_p)$  with inner-product costs exhibited in [Salmona et al. \(2021\)](#) are also solutions of Problem  $(EW_2)$ . Furthermore,

$$EW_2^2(\mu, \nu) = \text{tr}(D_0) + \text{tr}(D_1) - 2\text{tr}(D_0^{(d')^{\frac{1}{2}}} D_1^{\frac{1}{2}}).$$

*Proof.* Using Proposition 6, we get that Problem  $(EW_2)$  is equivalent to

$$\sup_{\pi \in \Pi(\mu, \nu)} \sup_{P \in \mathbb{V}_{d'}(\mathbb{R}^d)} \langle P, K_\pi \rangle_{\mathcal{F}},$$

where  $K_\pi = \int xy^T d\pi(x, y)$ . As in [Salmona et al. \(2021\)](#), we use the necessary condition for  $\pi$  to be in  $\Pi(\mu, \nu)$  that is that the covariance matrix  $\Sigma_\pi$  of the law  $\pi$  is a PSD matrix, or equivalently that the Schur complement of  $\Sigma_\pi$ , i.e.  $\Sigma_1 - K_\pi^T \Sigma_0^{-1} K_\pi$  is also a PSD matrix. This gives the following inequality:

$$\sup_{\pi \in \Pi(\mu, \nu)} \sup_{P \in \mathbb{V}_{d'}(\mathbb{R}^d)} \langle P, K_\pi \rangle_{\mathcal{F}} \leq \max_{K : \Sigma_1 - K^T \Sigma_0^{-1} K \in \mathbb{S}_+^{d'}} \max_{P \in \mathbb{V}_{d'}(\mathbb{R}^d)} \langle P, K \rangle_{\mathcal{F}}.$$

The rest of the proof is inspired from the proof of the closed-form of the  $W_2$  between two Gaussians provided by [Givens et al. \(1984\)](#). We want to solve the following constrained optimization problem

$$\min_{\substack{\Sigma_1 - K^T \Sigma_0^{-1} K \in \mathbb{S}_+^{d'} \\ P \in \mathbb{V}_{d'}(\mathbb{R}^d)}} -2\text{tr}(P^T K) .$$

Using Lemma [A5](#), we can write  $\text{tr}(P^T K)$  as a function of  $B_r$ . This gives the following equivalent constrained optimization problem

$$\min_{B_r^T B_r = \text{Id}_r, P^T P = \text{Id}_{d'}} -2\text{tr}(P^T \Sigma_0^{\frac{1}{2}} B_r \Lambda_r U_r^T) .$$

The Lagrangian of this latter problem reads as

$$\mathcal{L}(B_r, P, C_0, C_1) = -2\text{tr}(P^T \Sigma_0^{\frac{1}{2}} B_r \Lambda_r U_r^T) + \text{tr}(C_0(B_r^T B_r - \text{Id}_r)) + \text{tr}(C_1(P^T P - \text{Id}_{d'})) ,$$

where  $C_0 \in \mathbb{S}^r$  and  $C_1 \in \mathbb{S}^{d'}$  are the Lagrange multipliers respectively associated with the constraints  $B_r^T B_r = \text{Id}_r$  and  $P^T P = \text{Id}_{d'}$ . The first order condition gives

$$\begin{cases} \Sigma_0^{\frac{1}{2}} P U_r \Lambda_r = B_r C_0 \\ \Sigma_0^{\frac{1}{2}} B_r \Lambda_r U_r^T = P C_1 . \end{cases}$$

Since  $\Sigma_0$ ,  $P$ ,  $U_r$ , and  $\Lambda_r$  are full rank,  $\Sigma_0^{\frac{1}{2}} P U_r \Lambda_r$  is of rank  $r$  and so  $C_0$  is also of rank  $r$ . Thus we get that

$$B_r = \Sigma_0^{\frac{1}{2}} P U_r \Lambda_r C_0^{-1} ,$$

and so

$$B_r^T B_r = \text{Id}_r = C_0^{-1} \Lambda_r U_r^T P^T \Sigma_0 P U_r \Lambda_r C_0^{-1} .$$

Thus,

$$C_0 = (\Lambda_r U_r^T P^T \Sigma_0 P U_r \Lambda_r)^{\frac{1}{2}} .$$

On the other hand, by reinjecting the expression of  $B_r$  in the other first order condition we get

$$P^T \Sigma_0 P U_r \Lambda_r (\Lambda_r U_r^T P^T \Sigma_0 P U_r \Lambda_r)^{-\frac{1}{2}} \Lambda_r U_r^T = C_1 .$$

By multiplying this equation by itself we get

$$P^T \Sigma_0 P U_r \Lambda_r^2 U_r^T = C_1^2 .$$

Since  $C_1^2$  is symmetric we get that  $P^T \Sigma_0 P$  commutes with  $U_r \Lambda_r^2 U_r^T$  and so  $\Sigma_1 - S$ . Moreover, as before we have

$$\begin{aligned} \text{tr}(P^T K) &= \text{tr}((\Sigma_1 - S)^{\frac{1}{2}} P^T \Sigma_0 P (\Sigma_1 - S)^{\frac{1}{2}})^{\frac{1}{2}} \\ &= \text{tr}((\Sigma_1 - S)^{\frac{1}{2}} (P^T \Sigma_0 P)^{\frac{1}{2}}) . \end{aligned}$$

Using the Courant-Fischer min-max theorem ([Courant, 1920](#); [Fischer, 1905](#)) to characterize the eigenvalues of  $\Sigma_1 - S$  - see ([Givens et al., 1984](#), Proposition 7) for details, we get that  $\text{tr}(P^T K)$  is maximized when  $S = 0$  and so the problem is equivalent to the following problem

$$\max_{\substack{P \in \mathbb{V}_{d'}(\mathbb{R}^d) \\ P^T \Sigma_0 P \Sigma_1 = \Sigma_1 P^T \Sigma_0 P}} \text{tr}(\hat{D}_1^{\frac{1}{2}} D_{0,P}^{\frac{1}{2}}) ,$$

where  $(\hat{P}_1, \hat{D}_1)$  is any diagonalization of  $\Sigma_1$  and  $D_{0,P} = \hat{P}_1^T P^T \Sigma_0 P \hat{P}_1$ . For all  $y \in \mathbb{R}^{d'}$  we have

$$\alpha_d \|y\|^2 \leq y^T P^T \Sigma_0 P y \leq \alpha_1 \|y\|^2 ,$$

where  $\alpha_1, \dots, \alpha_d$  are the eigenvalues of  $\Sigma_0$  ordered in non-increasing order. Thus, denoting  $\lambda_1, \dots, \lambda_{d'}$  the eigenvalues of  $P^T \Sigma_0 P$ , we get that for all  $k \leq d'$ ,

$$\alpha_d \leq \lambda_k \leq \alpha_1 .$$

Since we want to maximize  $\text{tr}(\hat{D}_1^{\frac{1}{2}} D_{0,P}^{\frac{1}{2}})$ , we set the largest eigenvalue  $\lambda_1$  of  $P^T \Sigma_0 P$  to  $\alpha_1$ . We denote  $y_1 \in \mathbb{R}^{d'}$  the eigenvector associated. We have  $y_1 P^T \Sigma_0 P y_1 = \alpha_1$  and  $\|P y_1\| = \|y_1\| = 1$  so using Lemma A4, we get that  $\|P y_1\|$  is an eigenvector of  $\Sigma_0$  associated with  $\alpha_1$ . Let  $\lambda_k$  and  $y_k$  be any other eigenvalue and its associated eigenvector in the orthonormal basis in which  $P^T \Sigma_0 P$  is diagonal. We have  $y_k^T y_1 = 0$  and so  $y_k^T P^T P y_1 = 0$ . Thus  $P y_k$  is orthogonal to  $P y_1$ . Since  $\|P y_k\| = 1$ , we get that  $P y_k$  is also an eigenvector of  $\Sigma_0$  and so it exists  $i \leq d - 1$  such that  $\lambda_k = y_k^T P^T \Sigma_0 P y_k = \alpha_i$ . Thus, we conclude that the eigenvalues of the optimal  $P^T \Sigma_0 P$  are the  $d'$  largest eigenvalues of  $\Sigma_0$ . Moreover,  $\text{tr}(\hat{D}_1^{\frac{1}{2}} D_{0,P}^{\frac{1}{2}})$  is clearly maximized when  $D_{0,P}$  and  $\hat{D}_1$  have their eigenvalues sorted in the same order. We conclude then that setting  $D_{0,P} = D_0^{(d')}$  and  $\hat{D}_1 = D_1$ , where  $D_0$  and  $D_1$  are the diagonal matrices associated with the diagonalizations that sort the eigenvalues in non-increasing, maximizes the problem and so it follows that

$$\max_{\substack{\Sigma_1 - K^T \Sigma_0^{-1} K \in \mathbb{S}_+^{d'} \\ P \in \mathbb{V}_{d'}(\mathbb{R}^d)}} 2\text{tr}(P^T K) = 2\text{tr}(D_0^{(d')\frac{1}{2}} D_1^{\frac{1}{2}}).$$

Finally, observe that when setting  $K^*$  of the form

$$K^* = P_0(\tilde{\text{Id}}_{d'} D_0^{(d')\frac{1}{2}} D_1^{\frac{1}{2}})^{[d,d']} P_1^T,$$

we have

$$\|K^*\|_* = \text{tr}((K^{*T} K^*)^{\frac{1}{2}}) = \text{tr}((D_0^{(d')} D_1)^{\frac{1}{2}}) = \text{tr}(D_0^{(d')\frac{1}{2}} D_1^{\frac{1}{2}}).$$

Moreover, observe that this is the solution of Equation ( $\mathcal{F}$ -COV) exhibited in (Salmona et al., 2021, Lemma 3.2). Thus  $K^*$  is clearly in the feasible set and so is optimal. By reinjecting the optimal value in the expression of  $EW_2(\mu, \nu)$ , we get

$$EW_2^2(\mu, \nu) = \text{tr}(D_0) + \text{tr}(D_1) - 2\text{tr}(D_0^{(d')\frac{1}{2}} D_1^{\frac{1}{2}}).$$

Furthermore, using the results of Salmona et al. (2021), we get directly that the optimal plans  $\pi^*$  are of the form  $(\text{Id}_d, T)_{\#} \mu$  with  $T$  linear of the form

$$T = P_1 \left( \tilde{\text{Id}}_{d'} D_1^{\frac{1}{2}} D_0^{(d')-\frac{1}{2}} \right)^{[d',d]} P_0^T$$

Finally, observe that  $K^*$  admits as SVD  $P_0(D_0^{(d')\frac{1}{2}} D_1^{\frac{1}{2}})^{[d,d']} \tilde{\text{Id}}_{d'} P_1^T$ . For a given fixed  $\tilde{\text{Id}}_{d'}$ , we get using Lemma B1, that the optimal  $P^*$  associated with  $K^*$  is  $P^* = P_0 \tilde{\text{Id}}_{d'}^{[d,d']} P_1^T$ , which concludes the proof.  $\square$

## D More details on Projection Wasserstein discrepancy

In this section, we give more details on the OT distance introduced in Cai and Lim (2022) that we call here *projection Wasserstein discrepancy*. We recall that for  $\mu \in \mathcal{W}_2(\mathbb{R}^d)$  and  $\nu \in \mathcal{W}_2(\mathbb{R}^{d'})$  with  $d \geq d'$ , this OT distance is defined as

$$PW_2(\mu, \nu) = \inf_{\phi \in \Gamma_d(\mathbb{R}^{d'})} W_2(\phi_{\#} \mu, \nu),$$

where  $\Gamma_d(\mathbb{R}^{d'})$  is the set of all affine mapping from  $\mathbb{R}^d$  to  $\mathbb{R}^{d'}$  of the form  $\varphi(x) = P^T(x - b)$  with  $P \in \mathbb{V}_{d'}(\mathbb{R}^d)$  and  $b \in \mathbb{R}^d$ . One key results of Cai and Lim (2022) is to show that  $PW_2$  has the following equivalent formulation

$$PW_2(\mu, \nu) = \inf_{\xi \in \mathcal{W}_2^{\nu}(\mathbb{R}^d)} W_2(\mu, \xi),$$

where  $\mathcal{W}_2^{\nu}(\mathbb{R}^d)$  is the subset of  $\mathcal{W}_2(\mathbb{R}^d)$  defined as

$$\mathcal{W}_2^{\nu}(\mathbb{R}^d) = \{\xi \in \mathcal{W}_2(\mathbb{R}^d) : \text{there exists } \phi(x) = P^T(x - b) \text{ with } P \in \mathbb{V}_{d'}(\mathbb{R}^d) \text{ and } b \in \mathbb{R}^d \text{ such that } \phi_{\#} \xi = \nu\}.$$

Observe that this latter formulation is structurally different of  $EW_2$  since for any isometry  $\phi : \mathbb{R}^{d'} \rightarrow \mathbb{R}^d$ , the distribution  $\phi_{\#} \nu$  is necessarily degenerate, whereas this is not the case for the distribution  $\xi$ . The difference between  $EW_2$  and  $PW_2$  is illustrated in Figure D1.

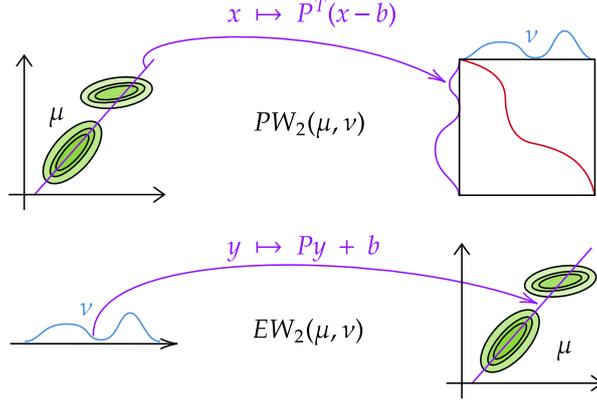


Figure D1: Link between  $PW_2$  and  $EW_2$  for two distributions  $\mu$  and  $\nu$  respectively on  $\mathbb{R}^2$  and  $\mathbb{R}$ . In  $PW_2$ ,  $\mu$  is projected into  $\mathbb{R}$  by a mapping of the form  $x \mapsto P^T(x - b)$ . In  $EW_2$ ,  $\nu$  is transformed into a degenerate measure (lying on the purple line) on  $\mathbb{R}^2$  with an isometric mapping of the form  $y \mapsto Py + b$ .

## D.1 Equivalent formulation

To highlight the difference between  $(EW_2)$  and  $(PW_2)$ , we derive an equivalent problem for  $(PW_2)$  similarly to Proposition 6. Observe that in that case, the mapping  $\phi$  in  $(PW_2)$  is not an isometry since it is not injective. As a result, the term that previously depended only on the marginal  $\mu$  in the development of the square of the Euclidean distance will now depend on  $P$ . More precisely, this gives the following result.

**Proposition D1.** *Let  $\mu \in \mathcal{W}_2(\mathbb{R}^d)$  and  $\nu \in \mathcal{W}_2(\mathbb{R}^{d'})$  and let suppose  $d \geq d'$ . Problem  $(PW_2)$  is equivalent to*

$$\inf_{\pi \in \Pi(\bar{\mu}, \bar{\nu})} \inf_{P \in \mathbb{V}_{d'}(\mathbb{R}^d)} \left( \text{tr}(P^T \Sigma_x P) - 2 \text{tr}(P^T K_\pi) \right),$$

where  $\Sigma_x = \int_{\mathbb{R}^d \times \mathbb{R}^d} xx^T d\bar{\mu}(x)$ ,  $K_\pi = \int_{\mathbb{R}^d \times \mathbb{R}^{d'}} xy^T d\pi(x, y)$ , and where  $\bar{\mu}$  and  $\bar{\nu}$  are the centered measures associated with  $\mu$  and  $\nu$ .

*Proof of Proposition D1.* First observe that using Lemma A3, we can consider without any loss generality that  $\mu$  and  $\nu$  are centered and omit  $b$ . Using Lemma A1, it follows

$$\begin{aligned} PW_2^2(\mu, \nu) &= \inf_{P \in \mathbb{V}_{d'}(\mathbb{R}^d)} \inf_{\pi' \in \Pi(P_{\#}^T \mu, \nu)} \int_{\mathbb{R}^{d'} \times \mathbb{R}^{d'}} \|z - y\|^2 d\pi'(z, y) \\ &= \inf_{P \in \mathbb{V}_{d'}(\mathbb{R}^d)} \inf_{\pi \in \Pi(\mu, \nu)} \int_{\mathbb{R}^d \times \mathbb{R}^{d'}} \|P^T x - y\|^2 d\pi(x, y) \\ &= \inf_{P \in \mathbb{V}_{d'}(\mathbb{R}^d)} \left( \int_{\mathbb{R}^d} \|P^T x\|^2 d\mu(x) + \int_{\mathbb{R}^{d'}} \|y\|^2 d\nu(y) - 2 \sup_{\pi \in \Pi(\mu, \nu)} \int_{\mathbb{R}^d \times \mathbb{R}^{d'}} (P^T x)^T y d\pi(x, y) \right), \end{aligned}$$

and so the problem is equivalent to

$$\inf_{P \in \mathbb{V}_{d'}(\mathbb{R}^d)} \left( \int_{\mathbb{R}^d} \|P^T x\|^2 d\mu(x) - 2 \sup_{\pi \in \Pi(\mu, \nu)} \int_{\mathbb{R}^{d'} \times \mathbb{R}^{d'}} (P^T x)^T y d\pi(x, y) \right),$$

which is itself equivalent to (7), which concludes the proof.  $\square$

Observe that Problem (7) can be interpreted as a regularization in  $P$  of Problem (5). It can also be interpreted as a  $W_2$  problem between  $\nu$  and a measure  $\mu'$  which has a different second-order moment than  $\mu$ .

## D.2 $PW_2$ between Gaussian distributions

Finally, we study the behavior of Problem  $(PW_2)$ , initially introduced by Cai and Lim (2022), when  $\mu$  and  $\nu$  are Gaussian distribution. In the following,  $\mu = \mathcal{N}(m_0, \Sigma_0)$  and  $\nu = \mathcal{N}(m_1, \Sigma_1)$  and we suppose  $d \geq d'$  and that  $\Sigma_0$  is non-singular. Let  $(\alpha_1, \dots, \alpha_d)^T \in \mathbb{R}^d$  and  $(\beta_1, \dots, \beta_{d'})^T \in \mathbb{R}^{d'}$  be the respective eigenvalues

of  $\Sigma_0$  and  $\Sigma_1$  ordered in non-increasing order and let us now denote by  $(P_{0\downarrow}, D_{0\downarrow})$  and  $(P_{1\downarrow}, D_{1\downarrow})$  the respective diagonalizations of  $\Sigma_0 (= P_{0\downarrow} D_{0\downarrow} P_{0\downarrow}^T)$  and  $\Sigma_1 (= P_{1\downarrow} D_{1\downarrow} P_{1\downarrow}^T)$  which sort the eigenvalues in non-increasing order, i.e.  $D_{0\downarrow} = \text{diag}(\alpha_1, \dots, \alpha_d)$  and  $D_{1\downarrow} = \text{diag}(\beta_1, \dots, \beta_{d'})$ . Let  $(P_{0\uparrow}, D_{0\uparrow})$  and  $(P_{1\uparrow}, D_{1\uparrow})$  denote the respective diagonalizations of  $\Sigma_0$  and  $\Sigma_1$  which sort the eigenvalues in non-decreasing order, i.e.  $D_{0\uparrow} = \text{diag}(\alpha_d, \dots, \alpha_1)$  and  $D_{1\uparrow} = \text{diag}(\beta_{d'}, \dots, \beta_1)$ . We show the following result.

**Proposition D2.** *Suppose  $d \geq d'$ . Let  $\mu = N(0, \Sigma_0)$  and  $\nu = N(0, \Sigma_1)$  with  $\Sigma_0 \in \mathbb{S}_{++}^d$  and  $\Sigma_1 \in \mathbb{S}_{++}^{d'}$ . Then,*

$$PW_2(\mu, \nu) = \inf_{P \in \mathbb{V}_{d'}(\mathbb{R}^d)} W_2(P_{\#}^T \mu, \nu) = \inf_{P : P^T \Sigma_0 P \Sigma_1 = \Sigma_1 P^T \Sigma_0 P} \|(P^T \Sigma_0 P)^{\frac{1}{2}} - \Sigma_1^{\frac{1}{2}}\|_{\mathcal{F}},$$

Furthermore,

(i) if  $\alpha_d > \beta_1$ , then

$$PW_2(\mu, \nu) = \|D_{0\uparrow}^{(d')}^{\frac{1}{2}} - D_{1\uparrow}^{\frac{1}{2}}\|_{\mathcal{F}}.$$

It is achieved at any  $(\pi^*, P^*)$  of the form  $P^* = P_{0\uparrow} \tilde{\text{Id}}_{d'}^{[d, d']} P_{1\uparrow}^T$  and  $\pi^* = (\text{Id}_d, T)_{\#} \mu$  with  $T$  being any linear mapping of the form,

$$T = P_{1\uparrow} \left( \tilde{\text{Id}}_{d'} D_{1\uparrow}^{\frac{1}{2}} D_{0\uparrow}^{(d')^{-\frac{1}{2}}} \right)^{[d', d]} P_{0\uparrow}^T.$$

(ii) if  $\alpha_1 < \beta_{d'}$ , then

$$PW_2(\mu, \nu) = \|D_{0\downarrow}^{(d')}^{\frac{1}{2}} - D_{1\downarrow}^{\frac{1}{2}}\|_{\mathcal{F}}.$$

It is achieved at any  $(\pi^*, P^*)$  of the form  $P^* = P_{0\downarrow} \tilde{\text{Id}}_{d'}^{[d, d']} P_{1\downarrow}^T$  and  $\pi^* = (\text{Id}_d, T)_{\#} \mu$  with  $T$  being any linear mapping of the form,

$$T = P_{1\downarrow} \left( \tilde{\text{Id}}_{d'} D_{1\downarrow}^{\frac{1}{2}} D_{0\downarrow}^{(d')^{-\frac{1}{2}}} \right)^{[d', d]} P_{0\downarrow}^T.$$

*Proof.* As before, the proof is inspired from the proof of the closed-form of the  $W_2$  between two Gaussians provided by Givens et al. (1984). This time, we want to solve the following constrained optimization problem

$$\min_{\substack{\Sigma_1 - K^T \Sigma_0^{-1} K \in \mathbb{S}_{++}^{d'} \\ P \in \mathbb{V}_{d'}(\mathbb{R}^d)}} \text{tr}(P^T \Sigma_0 P) - 2\text{tr}(P^T K).$$

Again, one can, using Lemma A5, write  $\text{tr}(P^T K)$  as a function of  $B_r$ . This gives the following problem

$$\min_{\substack{B_r^T B_r = \text{Id}_r \\ P^T P = \text{Id}_{d'}}} \text{tr}(P^T \Sigma_0 P) - 2\text{tr}(P^T \Sigma_0^{\frac{1}{2}} B_r \Lambda_r U_r^T).$$

The Lagrangian of this latter problem reads as

$$\mathcal{L}(B_r, P, C_0, C_1) = \text{tr}(P^T \Sigma_0 P) - 2\text{tr}(P^T \Sigma_0^{\frac{1}{2}} B_r \Lambda_r U_r^T) + \text{tr}(C_0 (B_r^T B_r - \text{Id}_r)) + \text{tr}(C_1 (P^T P - \text{Id}_{d'})),$$

where  $C_0 \in \mathbb{S}^r$  and  $C_1 \in \mathbb{S}^{d'}$  are the Lagrange multipliers respectively associated with the constraints on  $B_r$  and  $P$ . The first order condition gives

$$\begin{cases} \Sigma_0^{\frac{1}{2}} P U_r \Lambda_r = B_r C_0 \\ \Sigma_0^{\frac{1}{2}} B_r \Lambda_r U_r^T = P C_1 + \Sigma_0 P. \end{cases}$$

Since  $\Sigma_0$ ,  $P$ ,  $U_r$ , and  $\Lambda_r$  are full rank,  $\Sigma_0^{\frac{1}{2}} P U_r \Lambda_r$  is of rank  $r$  and so  $C_0$  is also of rank  $r$ . Thus we get that

$$B_r = \Sigma_0^{\frac{1}{2}} P U_r \Lambda_r C_0^{-1},$$

and so

$$B_r^T B_r = \text{Id}_r = C_0^{-1} \Lambda_r U_r^T P^T \Sigma_0 P U_r \Lambda_r C_0^{-1}.$$

Thus

$$C_0 = (\Lambda_r U_r^T P^T \Sigma_0 P U_r \Lambda_r)^{\frac{1}{2}}.$$

On the other hand, by reinjecting the expression of  $B_r$  in the other first order condition we get

$$P^T \Sigma_0 P U_r \Lambda_r (\Lambda_r U_r^T P^T \Sigma_0 P U_r \Lambda_r)^{-\frac{1}{2}} \Lambda_r U_r^T = C_1 + P^T \Sigma_0 P.$$

By multiplying this equation by itself, we get

$$P^T \Sigma_0 P U_r \Lambda_r^2 U_r^T = (C_1 + P^T \Sigma_0 P)^2.$$

Since  $(C_1 + P^T \Sigma_0 P)^2$  is symmetric, we get that  $P^T \Sigma_0 P$  commutes with  $U_r \Lambda_r^2 U_r^T$  and thus with  $\Sigma_1 - S$ . Moreover,

$$\begin{aligned} \text{tr}(P^T K) &= \text{tr}(C_0) = \text{tr}((\Lambda_r U_r^T P^T \Sigma_0 P U_r \Lambda_r)^{\frac{1}{2}}) \\ &= \text{tr}(U_r^T U_r (\Lambda_r U_r^T P^T \Sigma_0 P U_r \Lambda_r)^{\frac{1}{2}}) \\ &= \text{tr}(U_r (\Lambda_r U_r^T P^T \Sigma_0 P U_r \Lambda_r)^{\frac{1}{2}} U_r^T) \\ &= \text{tr}((U_r \Lambda_r U_r^T P^T \Sigma_0 P U_r \Lambda_r U_r^T)^{\frac{1}{2}}) \\ &= \text{tr}((\Sigma_1 - S)^{\frac{1}{2}} P^T \Sigma_0 P (\Sigma_1 - S)^{\frac{1}{2}})^{\frac{1}{2}}. \end{aligned}$$

As before, using the Courant-Fischer min-max theorem (Courant, 1920; Fischer, 1905) to characterize the eigenvalues of  $\Sigma_1 - S$ , we get that  $\text{tr}(P^T K)$  is maximized when  $S = 0$ . Thus we get that

$$PW_2^2(\mu, \nu) = \min_{P^T \Sigma_0 P \Sigma_1 = \Sigma_1 P^T \Sigma_0 P} \text{tr}(P^T \Sigma_0 P) + \text{tr}(\Sigma_1) - \text{tr}((\Sigma_1^{\frac{1}{2}} P^T \Sigma_0 P \Sigma_1^{\frac{1}{2}})^{\frac{1}{2}}).$$

Since  $P^T \Sigma_0 P$  and  $\Sigma_1$  commute, this expression can be reduced to

$$\begin{aligned} PW_2^2(\mu, \nu) &= \min_{P^T \Sigma_0 P \Sigma_1 = \Sigma_1 P^T \Sigma_0 P} \text{tr} \left( \left( (P^T \Sigma_0 P)^{\frac{1}{2}} - \Sigma_1^{\frac{1}{2}} \right)^2 \right) \\ &= \min_{P^T \Sigma_0 P \Sigma_1 = \Sigma_1 P^T \Sigma_0 P} \|D_{0,P}^{\frac{1}{2}} - D_1^{\frac{1}{2}}\|_{\mathcal{F}}^2, \end{aligned} \quad (12)$$

where  $(P_1, D_1)$  is any diagonalization of  $\Sigma_1 (= P_1 D_1 P_1^T)$ , and where  $D_{0,P} = P_1^T P^T \Sigma_0 P P_1$ . Thus, the problem is reduced to find the  $P \in \mathbb{V}_{d'}(\mathbb{R}^d)$  such that the eigenvalues of  $(P^T \Sigma_0 P)^{\frac{1}{2}}$  are the closest possible (in term of  $l_2$  distance) to the eigenvalues of  $\Sigma_1^{\frac{1}{2}}$ . Let  $(\alpha_1, \dots, \alpha_d)^T$  and  $(\beta_1, \dots, \beta_{d'})^T$  denotes the respective eigenvalues of  $\Sigma_0$  and  $\Sigma_1$  sorted in decreasing order. Observe that for all  $P \in \mathbb{V}_{d'}(\mathbb{R}^d)$  and for all  $y \in \mathbb{R}^{d'}$ , we have

$$\alpha_d \|y\|^2 = \alpha_d \|Py\|^2 \leq y^T P^T \Sigma_0 P y \leq \alpha_1 \|Py\|^2 = \alpha_1 \|y\|^2,$$

and so, for  $k \leq d'$ , if  $\lambda_k$  is an eigenvalue of  $P^T \Sigma_0 P$ , then

$$\alpha_d \leq \lambda_k \leq \alpha_1.$$

- (i) Suppose  $\alpha_d > \beta_1$ : since the eigenvalues of  $P^T \Sigma_0 P$  are necessarily greater than  $\alpha_d$ , we set the minimum eigenvalue of  $P^T \Sigma_0 P$  to  $\lambda_{d'} = \alpha_d$  in order to minimize (12). We denote  $y_{d'} \in \mathbb{R}^{d'}$  the eigenvector associated. We have  $y_{d'}^T P^T \Sigma_0 P y_{d'} = \alpha_d$  and  $\|P y_{d'}\| = \|y_{d'}\| = 1$  so using Lemma A4, we get that  $\|P y_{d'}\|$  is an eigenvector of  $\Sigma_0$  associated with  $\alpha_d$ . Let  $\lambda_k$  and  $y_k$  be any other eigenvalue and its associated eigenvector in the orthonormal basis in which  $P^T \Sigma_0 P$  is diagonal. We have  $y_k^T y_{d'} = 0$  and so  $y_k^T P^T P y_{d'} = 0$ . Thus  $P y_k$  is orthogonal to  $P y_{d'}$ . Since  $\|P y_k\| = 1$ , we get that  $P y_k$  is also an eigenvector of  $\Sigma_0$  and so it exists  $i \leq d-1$  such that  $\lambda_k = y_k^T P^T \Sigma_0 P y_k = \alpha_i$ . Thus, we conclude that the eigenvalues of the optimal  $P^T \Sigma_0 P$  are the  $d'$  smallest eigenvalues of  $\Sigma_0$ . Now we determine their order. We have

$$\|D_{0,P}^{\frac{1}{2}} - D_1^{\frac{1}{2}}\|_{\mathcal{F}}^2 = \text{tr}(D_{0,P}) + \text{tr}(D_1) - 2\text{tr}(D_{0,P}^{\frac{1}{2}} D_1^{\frac{1}{2}}).$$

Since only  $\text{tr}(D_{0,P}^{\frac{1}{2}} D_1^{\frac{1}{2}})$  depends of the order of the eigenvalues, one can observe that setting  $D_{0,P} = D_{0\uparrow}^{(d')}$  and  $D_1 = D_{1\uparrow}$  minimizes the expression. The optimal value is achieved for any  $P$  of the form

$$P^* = P_{0\uparrow} \tilde{\text{Id}}_{d'}^{[d,d']} P_{1\uparrow}^T,$$

Since for a given  $P$ , the expression of the optimal map which minimizes  $W_2(P_{\#}^T \mu, \nu)$  is given by, for all  $x \in \mathbb{R}^{d'}$ ,

$$T_{W_2}(x) = (P^T \Sigma_0 P)^{-1} (P^T \Sigma_0 P \Sigma_1)^{\frac{1}{2}} x .$$

Re-injecting  $P^*$  in the above gives the expression of  $T$  in that case.

- (ii) Suppose that  $\alpha_1 < \beta_d$ : since the eigenvalues of  $P^T \Sigma_0 P$  are necessarily smaller than  $\alpha_1$ , we set  $\lambda_1 = \alpha_1$  in order to minimize (12). We denote  $y_1 \in \mathbb{R}^{d'}$  the eigenvector associated. We have  $y_1 P^T \Sigma_0 P y_1 = \alpha_1$  and  $\|P y_1\| = \|y_1\| = 1$  so using Lemma A4, we get that  $\|P y_1\|$  is an eigenvector of  $\Sigma_0$  associated with  $\alpha_1$ . Applying the same reasoning as before, we get that the eigenvalues of the optimal  $P^T \Sigma_0 P$  are the  $d'$  largest eigenvalues of  $\Sigma_0$ . Thus, setting  $D_{0,P} = D_{0\downarrow}^{(d')}$  and  $D_1 = D_{1\downarrow}$  minimizes (12). This is achieved for any  $P$  of the form

$$P^* = P_{0\downarrow} \tilde{\text{Id}}_{d'}^{[d,d']} P_{1\downarrow}^T .$$

By re-injecting this in the expression of  $T_{W_2}$ , we get the expression of  $T$  in that case, which concludes the proof. □

Note that this result generalizes Cai and Lim (2022, Example VI.1) that derived the expression of the  $PW_2$  discrepancy between a  $d$ -dimensional Gaussian and a one-dimensional Gaussian distributions. The  $PW_2$  problem between Gaussian distributions is thus equivalent to minimize the Hellinger distance between  $P^T \Sigma_0 P$  and  $\Sigma_1$  on the subset of  $\mathbb{V}_{d'}(\mathbb{R}^d)$  of matrices  $P$  such that  $P^T \Sigma_0 P$  and  $\Sigma_1$  commute. Observe that  $PW_2$  has a different behavior in the case where the eigenvalues of  $\Sigma_0$  are all greater than the eigenvalues of  $\Sigma_1$  and in the case where the eigenvalues of  $\Sigma_0$  are all smaller than the eigenvalues of  $\Sigma_1$ . In the case where the eigenvalues of  $\Sigma_0$  and  $\Sigma_1$  are entangled,  $PW_2$  vanishes as soon as there exists a projection  $P \in \mathbb{V}_{d'}(\mathbb{R}^d)$  such that  $P^T \Sigma_0 P$  has the same eigenvalues than  $\Sigma_1$ . Geometrically speaking, this corresponds to finding a  $d'$ -dimensional plan in  $\mathbb{R}^d$  encoded by  $P$  on which the *projection* of  $\mu$  has the same structure than  $\nu$  has on  $\mathbb{R}^{d'}$ . This is a really different behavior from the previously studied OT distances that vanish only when there exists a  $d'$ -dimensional plan *that contains entirely* the support of  $\mu$  and such that  $\mu$  has the same structure on that plan than  $\nu$  has on  $\mathbb{R}^{d'}$ . In other words,  $P^T$  is not an *isometric* operator but a projection operator, and so it can transform  $\mu$  while pushing it into a distributions  $\mu'$  on  $\mathbb{R}^{d'}$  that will have a similar structure to  $\nu$  whereas in  $\mathbb{R}^d$ , the embedded measure  $P_{\#} \nu$  will be different from  $\mu$ . The following example illustrates the difference between  $PW_2$  and the previously studied OT distances: let  $\mu = \text{N}(0, \Sigma_0)$  and  $\nu = \text{N}(0, \sigma_1^2)$  with

$$\Sigma_0 = \begin{pmatrix} 2 & 0 \\ 0 & 1 \end{pmatrix} \quad \text{and} \quad \sigma_1^2 = \frac{3}{2} .$$

Then we have  $PW_2(\mu, \nu) = 0$  but  $EW_2(\mu, \nu) > 0$ . Observe indeed that when setting  $p^* = \left(\frac{1}{\sqrt{2}} \frac{1}{\sqrt{2}}\right)^T$ , we have

$$\left(\frac{1}{\sqrt{2}} \frac{1}{\sqrt{2}}\right) \begin{pmatrix} 2 & 0 \\ 0 & 1 \end{pmatrix} \begin{pmatrix} \frac{1}{\sqrt{2}} \\ \frac{1}{\sqrt{2}} \end{pmatrix} = \frac{3}{2} ,$$

and so  $p^{*T} \Sigma_0 p^* = \sigma_1^2$ . Since  $p^*$  is clearly in  $\mathbb{V}_1(\mathbb{R}^2)$  and  $p^{*T} \Sigma_0 p^*$  commutes clearly with  $\sigma_1^2$  (since there both are scalars), we have

$$PW_2^2(\mu, \nu) \leq |(p^{*T} \Sigma_0 p^*)^{\frac{1}{2}} - \sigma_1|^2 = 0 ,$$

and so  $PW_2(\mu, \nu) = 0$ . On the other hand,

$$EW_2^2(\mu, \nu) = \text{tr}(\Sigma_0) + \sigma_1 - 2\text{tr}(\Sigma_0^{(1)\frac{1}{2}} \sigma_1) = \frac{9}{2} - 2\sqrt{3} > 0 .$$